UNIVERSIDADE DE LISBOA
FACULDADE DE CIÊNCIAS
DEPARTAMENTO DE BIOLOGIA VEGETAL

Identification of Arl13b GTPase-activating proteins towards the impairment of tumor progression

Inês Margarida Castro Ferreira

Mestrado em Biologia Molecular e Genética

Dissertação orientada por:
Professor Doutor Duarte Barral
Professora Doutora Rita Zilhão

2018

«But once again always remember that not all the men who work at science are scientists. So few! […] It is born in you. Sometimes I think you have a little of it born in you. If you have it, there is only one thing […] you must do: work twice as hard as you can.»

Sinclair Lewis, Arrowsmith (1925)

Agradecimentos

Não posso deixar de agradecer o apoio e a confiança de inúmeras pessoas sem cujo contributo esta investigação e dissertação não teriam sido, de todo, possíveis concretizar.

Em primeiro lugar, gostaria de agradecer ao Doutor Duarte Barral por me ter aceite no seu laboratório, tendo-me dado, assim, a oportunidade de fazer parte de um grupo de investigação. Queria agradecer, sobretudo, pelo excelente papel que desempenhou como orientador, pelos ensinamentos e conselhos que me transmitiu, bem como pelo incentivo constante ao desenvolvimento de um pensamento crítico, não apenas fundamentais para a realização deste trabalho, como também para o meu futuro em Ciência. Agradeço, ainda, a sua disponibilidade e apoio constantes, o cuidado e atenção com que sempre me acompanhou, e o esforço que sempre empenhou para manter a união do grupo, tanto dentro como fora do laboratório.

Gostaria de deixar um agradecimento muito especial à Cristina Casalou, por ter acompanhado, de mais perto, esta importante fase da minha formação. Um obrigada sincero pela sua presença constante durante este ano, por tudo o que me ensinou, desde as bases mais fundamentais até aos pequenos detalhes, pela disponibilidade e apoio que sempre demonstrou em me ouvir e esclarecer as minhas dúvidas, pela preocupação e cuidado que me ofereceu incessantemente, pela compreensão e paciência incansáveis com que me orientou, acompanhando, também, as minhas falhas, e ainda pela dedicação e tempo dispensados a cada momento.

Quero agradecer, também, a cada um dos meus colegas de laboratório:

À Xana, por tudo o que me ensinou, por sempre se mostrar disponível para me ouvir e ajudar quando precisei, não esquecendo, claro, os momentos de bom humor que trouxe ao laboratório e o facto de ter sido a minha salvação das muitas vezes em que algo ficava esquecido na bancada.

À Liliana, por desde o início me ter feito sentir integrada no grupo, com a sua boa disposição e simpatia, por me ter ouvido e aconselhado sempre que necessitei, e pela preocupação, apoio e amizade que me ofereceu constantemente.

Ao Hugo, pelo papel de "irmão mais velho"; pela amizade, conselhos e ajuda que sempre me dispôs, bem como pela animação que transmitiu ao grupo.

À Matilde, pelo companheirismo, amizade e prontidão com que sempre se ofereceu em ajudar.

À Cecília, pela preocupação, sugestões e amizade que sempre me ofereceu.

À Cristina Escrevente, pelos conselhos que se revelaram bastante úteis, bem como a amizade e boa disposição que trouxe ao laboratório.

À Daniela, que apesar de não ter trabalhado comigo na bancada, deu-me vários conselhos importantes.

A este grupo fantástico na qual tive oportunidade de trabalhar, que me acolheu durante este ano e que me fez sentir realmente integrada, valorizando sempre a minha contribuição.

Um agradecimento a todos os colaboradores do ITQB e iBET que participaram neste projeto, não só sua pela contribuição direta na purificação das proteínas, como também pelas reuniões regulares para a discussão de resultados, das quais resultaram diversas sugestões que contribuíram para o avanço do meu trabalho, nomeadamente em relação aos ensaios de medição de hidrólise de GTP *in vitro*:

À Andreia, que se juntou, mais tarde, ao nosso grupo, não só pela purificação da ACAP1 e da Arl13b em células de mamífero, como também por toda a ajuda que me ofereceu, pela sua disponibilidade, prontidão, simpatia e boa disposição incansáveis, bem como pelas sugestões relativas à escrita da tese.

À Doutora Margarida Archer e respetivo grupo, em especial ao Diogo, pela purificação da Arl13b em *E. coli*. Ao Diogo agradeço também a orientação e apoio durante as semanas em que estive no ITQB a acompanhar o seu trabalho, a ajuda que sempre me ofereceu ao longo deste ano e a sua simpatia, disponibilidade e prontidão constantes.

À Lígia e à Sofia, com a orientação da Doutora Ana Barbas, pela purificação das Arf GAPs ASAP1 e ASAP3. Gostaria também de agradecer a contribuição da Sandra Monteiro, Cátia Peres e da Khrystyna Kucheryava neste processo.

Ao Doutor Tiago Bandeiras, pela partilha de conhecimento e conselhos que se revelaram importantes nos ensaios com as proteínas purificadas.

Gostaria, ainda, de deixar um agradecimento a algumas pessoas que, apesar de não fazerem parte do nosso grupo de investigação, trabalharam de perto connosco, quer no laboratório, quer participando em reuniões e encontros fora do mesmo:

Ao Pedro, pela partilha de vários momentos no laboratório onde a sua ajuda se revelou importante.

Ao João Charneca, pela disponibilidade que sempre ofereceu em ajudar e pela animação que trouxe ao laboratório.

À Teresa, pela simpatia e interesse que sempre demonstrou.

Às alunas de rotação Rakhi, Anna e Oriana por terem partilhado a bancada comigo.

Não posso deixar de agradecer, também, a algumas pessoas do CEDOC, nomeadamente:

Ao Doutor Michel Kranendonk, da ToxOmics, por me ter dado permissão para utilizar o leitor de placas do seu grupo, essencial neste projeto. Ao Francisco, à Diana e à Marisa por estarem sempre disponíveis para me ajudar na sua utilização quando necessitei, mesmo estando ocupados com o seu próprio trabalho.

Ao José Inácio, por me ter ajudado com o protocolo de transfecção por electroporação das minhas tão difíceis células, também me disponibilizando o material necessário para tal, o que acabou por salvar as minhas experiências de imunofluorescência nas quais já começava a depositar muito pouca esperança.

Ao José Ramalho, por nos ter emprestado vários anticorpos e materiais necessários ao trabalho laboratorial desenvolvido no âmbito deste projeto, mesmo cujos resultados não exponha na presente

dissertação. Foram experiências importantes para que conseguisse decidir qual a melhor abordagem a seguir em algumas situações, até definir a que eventualmente me levaria aos resultados definitivos.

A todos os membros que fizeram parte do laboratório 2.7 durante este ano, contribuindo para um ótimo ambiente de trabalho, de companheirismo e entreajuda, proporcionado, também, momentos de diversão. Ainda, a todas as pessoas do CEDOC por me terem acolhido e por todos os momentos que lá passei.

Ainda, aos investigadores Paul Randazzo e Victor Hsu, por terem fornecido ao nosso grupo de investigação alguns dos vetores de expressão das Arf GAPs, fundamentais para o desenvolvimento deste projeto.

À Professora Doutora Rita Zilhão, por ter aceite orientar a minha tese, pela preocupação, disponibilidade e atenção que sempre me dispôs, sem qualquer hesitação, e por sempre depositar em mim a sua confiança.

Ao Doutor Paulo Matos, pela disponibilidade e simpatia em nos receber para a discussão relativa aos ensaios de medição de hidrólise de GTP *in vitro* e pelas sugestões que se revelaram essenciais nessa componente do trabalho.

À minha família, em especial aos meus pais, por todo o apoio, incentivo e alegria que me transmitem a cada instante. Um agradecimento sincero à minha irmã pela sua orientação e conselhos nesta caminhada que já iniciou há muito, sendo uma importante referência para mim; pela amizade, segurança e encorajamento que sempre me transmitiu em todos os momentos. A eles agradeço por tornarem as minhas aspirações possíveis.

A todos os meus amigos, por partilharem comigo o desejo de aqui chegar. Ao Kevin, em especial, por ter vivido comigo, de mais perto, esta experiência.

Por último, mas não menos importante, um agradecimento muito especial ao Marco, pela sua presença constante nesta jornada, pelo seu apoio, motivação e ânimo incondicionais, e por sempre saber me confortar em fases de maior dificuldade. Por ser, acima de tudo, o meu melhor amigo.

Enfim, estou muito grata a todos aqueles que, de um modo ou de outro, deram o seu contributo para que a realização da presente dissertação fosse possível, constituindo uma meta fundamental na minha vida académica e profissional. Agradeço não só por terem possibilitado a materialização destas folhas, mas também pelo ano repleto de trabalho, aprendizagem e crescimento, sem dúvida constituindo importantes alicerces para a minha carreira científica.

A todos, o meu sincero **muito obrigada**!

Abstract

Cancer metastasis relies on cancer cell migration and invasion of tissues surrounding the primary tumor and is the leading cause of cancer-related deaths. Our group previously showed that the small GTPase Arl13b positively regulates breast cancer cell migration, invasion and metastasis. In fact, this protein is widely expressed in most normal human tissues and its expression is enhanced in several tumorigenic tissues. Therefore, Arl13b inactivation represents a promising therapeutic strategy to control cancer progression. However, any GTPase-activating proteins (GAPs), which inactivate small GTPases, are known for Arl13b. Thus, my aim was to identify GAPs that promote the inactive conformation of Arl13b, contributing to unravel regulators of the activity of this protein. I found that Arl13b co-immunoprecipitates with the Arf GAPs ASAP1, ASAP3 and ACAP1, but not with GIT1, using total protein extracts obtained from MDA-MB-231 breast cancer cells. Moreover, the co-immunoprecipitation was enhanced in the presence of GTPγS, compared to excess GDP, indicating that the interactions occur in a GTP-dependent manner. Additionally, I observed that ASAP1, ASAP3 and ACAP1 co-localize with Arl13b in MDA-MB-231 cells in structures associated with the plasma membrane and in actin-rich structures involved in cell migration or invasion. To assess if these Arf GAPs can induce the GTP hydrolysis activity of Arl13b, an *in vitro* GTPase activity assay was performed using recombinant purified proteins. I observed that ASAP1 and ASAP3 do not promote Arl13b GTP hydrolysis, while the result obtained for ACAP1 was not conclusive. Previous studies indicate that ASAP3 silencing leads to decreased cancer cell migration and invasion, similar to the Arl13b silencing, but the effect of ASAP1 silencing on these processes has been contradictory. On the other hand, ACAP1 has not been directly implicated in cancer. I found that *ASAP1* and *ASAP3* are upregulated in highly invasive breast cancer cell lines, similar to *ARL13B*. Furthermore, the results obtained show that ACAP1 silencing leads to the enhancement of breast cancer cell migration and invasion. These findings correlate with the downregulation of *ACAP1* in more invasive breast cancer cell lines, contrary to what occurs with *ARL13B*. Altogether, these results provide new insights into the regulation and molecular mechanisms of Arl13b in cancer progression, suggesting that ASAP1 and ASAP3 act as Arl13b effectors, while ACAP1 emerge as a promising candidate with GAP activity on Arl13b.

Keywords: Arl13b, Arf GAPs, cell migration, cell invasion, cancer progression.

Resumo

O processo de metastização depende da migração e invasão de células cancerígenas para os tecidos circundantes ao tumor primário e é a principal causa das mortes relacionadas com cancro. O nosso grupo descobriu que a pequena GTPase Arl13b regula positivamente a migração, invasão e metastização de células de cancro de mama. De facto, esta proteína é amplamente expressa na maioria dos tecidos normais humanos, tendo a sua expressão aumentada em diversos tecidos tumorais. Desta forma, a inativação da Arl13b representa uma estratégia terapêutica promissora para controlar a progressão tumoral. Contudo, não são conhecidas proteínas indutoras da atividade GTPásica (GAPs), que inativam proteínas deste tipo, para a Arl13b. Assim, o meu objetivo foi identificar GAPs que promovessem a conformação inativa da Arl13b, contribuindo para a descoberta de fatores que regulam a atividade desta proteína. Os resultados obtidos indicam que a Arl13b co-imunoprecipita com as Arf GAPs ASAP1, ASAP3 e ACAP1, mas não com a GIT1, usando extratos de proteína total de células de cancro de mama MDA-MB-231. Além disso, os resultados mostram que a co-imunoprecipitação aumenta na presença de GTPγS, comparando com excesso de GDP, indicando que as interações ocorrem de uma forma dependente de GTP. Adicionalmente, observei que a ASAP1, ASAP3 e ACAP1 co-localizam com a Arl13b nas células MDA-MB-231 em estruturas associadas à membrana plasmática e em estruturas ricas em actina envolvidas na migração ou invasão celulares. Para identificar quais destas Arf GAPs poderiam induzir a atividade de hidrólise de GTP da Arl13b, utilizou-se um ensaio *in vitro* de atividade GTPásica, recorrendo a proteínas recombinantes purificadas. Verifiquei que a ASAP1 e a ASAP3 não promovem a hidrólise de GTP pela Arl13b, enquanto que o resultado obtido para a ACAP1 não foi conclusivo. Estudos anteriores indicam que o silenciamento da ASAP3 resulta na diminuição da migração e invasão de células tumorais, tal como o silenciamento da Arl13b, enquanto que o efeito do silenciamento da ASAP1 nestes processos tem sido contraditório. Por outro lado, não há estudos que demonstrem um papel direto da ACAP1 no cancro. Descobri que os genes *ASAP1* e *ASAP3* são sobreexpressos em linhas celulares de cancro de mama altamente invasivas, de forma análoga ao gene *ARL13B*. Além disso, os resultados obtidos demonstram que o silenciamento da ACAP1 leva a um aumento da migração e invasão de células de cancro de mama. Isto correlaciona-se com a reduzida expressão do gene *ACAP1* em linhas celulares de cancro de mama mais invasivas, contrariamente ao que foi verificado para o gene *ARL13B*. Em conjunto, estes resultados contribuem para o conhecimento da regulação e dos mecanismos moleculares da Arl13b na progressão tumoral, sugerindo que a ASAP1 e a ASAP3 atuam como efetores da Arl13b, enquanto que a ACAP1 surge como um candidato promissor a GAP da Arl13b.

Palavras-chave: Arl13b, Arf GAPs, migração celular, invasão celular, progressão tumoral.

Resumo extenso

O processo de metastização depende da migração e invasão de células cancerígenas para os tecidos circundantes ao tumor primário e é a principal causa das mortes relacionadas com cancro. O nosso grupo descobriu que a pequena GTPase Arl13b regula positivamente a migração, invasão e metastização de células de cancro de mama. Para além disso, foi descrito recentemente que algumas destas funções se estendem, igualmente, a células de tumores gástricos e meduloblastomas. De facto, esta proteína é amplamente expressa na maioria dos tecidos normais humanos, tendo a sua expressão aumentada em diversos tecidos tumorais. Desta forma, a inativação da Arl13b representa uma estratégia terapêutica promissora para controlar a progressão tumoral em vários tipos de cancro. Contudo, não são conhecidas proteínas que regulem a atividade da Arl13b, tais como fatores de troca de nucleótidos de guanina (GEFs), que ativam as pequenas GTPases, ou proteínas indutoras da atividade GTPásica (GAPs), que as inativam. Especificamente, o meu objetivo foi identificar GAPs que promovessem a conformação inativa da Arl13b, contribuindo, também, para compreender de que forma esta proteína é regulada.

Para verificar se a Arl13b interage com Arf GAPs que poderiam mediar a sua inativação, recorri a ensaios de imunoprecipitação usando extratos de proteína total de células de cancro da mama MDA-MB-231. Para tal, transfectei células MDA-MB-231 a expressar de forma estável Arl13b-mCherry ou mCherry, usado como controlo negativo, com plasmídeos que expressavam as diferentes Arf GAPs em fusão com a *tag* FLAG. Os lisados celulares foram incubados com um análogo de GTP não hidrolisável (GTPγS) ou excesso de GDP. Os resultados obtidos mostram que a Arl13b co-imunoprecipita com as Arf GAPs ASAP1, ASAP3 e ACAP1, mas não com a GIT1, e que a interação aumenta na presença da conformação ativa Arl13b-GTP, comparando com a conformação inativa Arl13b-GDP. Estes resultados indicam que a interação da Arl13b com a ASAP1, ASAP3 e ACAP1 ocorre de uma forma dependente de GTP. Para determinar se a presença de atividade GAP poderia influenciar a ligação à Arl13b, testei ainda a interação desta proteína com uma forma mutada da ASAP1, [R497K]ASAP1. Este mutante não possui atividade GAP devido a uma alteração numa posição conservada do seu domínio Arf GAP. Tal como a forma *wildtype*, verifiquei que o mutante [R497K]ASAP1 interage com a Arl13b de uma forma dependente de GTP.

Resultados anteriores do nosso grupo mostraram que a Arl13b se localiza em regiões ricas em actina perto da membrana plasmática, em filamentos de actina, em lamelipódia, filopódia, *ruffles* circulares dorsais e em invadopódia. Uma vez que a interação da Arl13b com a ASAP1, ASAP3 e ACAP1 foi confirmada, determinei a co-localização destas Arf GAPs com a actina e a Arl13b através de microscopia confocal. Para tal, foram usadas células MDA-MB-231 a sobreexpressar transientemente as proteínas ASAP1, ASAP3 ou ACAP1 com a *tag* FLAG. A co-localização entre as Arf GAPs e a Arl13b foi determinada em células MDA-MB-231 co-transfectadas com um plasmídeo que expressava a Arl13b em fusão com a *tag* GFP. Concordando com a informação descrita na literatura, observei que a ASAP1, ASAP3 e ACAP1 co-localizam com estruturas ricas em actina filamentosa. Especificamente, a ASAP1 co-localiza com a actina em estruturas protuberantes próximas da membrana plasmática e em estruturas que se assemelham a invadopódia, a ASAP3 interage com a actina na membrana plasmática e em filamentos de actina na periferia da célula, e a ACAP1, por sua vez, associa-se com a actina também em filamentos de actina localizados na proximidade da membrana plasmática. Para além disso, observei que a ASAP1, ASAP3 e ACAP1 co-localizam com a Arl13b sobretudo em estruturas localizadas na membrana plasmática. A interação com a ASAP1 verificou-se em *ruffles* periféricas e em estruturas que se assemelham a invadopódia, com a ASAP3 em *ruffles* periféricas e circulares dorsais, e com a ACAP1 em filopódia e *ruffles* periféricas. Todas estas estruturas de remodelação do citoesqueleto de actina estão associadas à migração ou invasão celulares, indicando que estas Arf GAPs atuam conjuntamente com a Arl13b na regulação destes processos. Para confirmar se a ausência de atividade GAP da ASAP1 afetaria

a sua localização, investiguei a co-localização do mutante [R497K]ASAP1 com a actina e a Arl13b. Tal como a forma *wildtype*, a forma mutante interage com a actina em estruturas protuberantes perto da membrana plasmática, neste caso, em lamelipódia, e em estruturas que se assemelham a invadopódia. A interação com a Arl13b também se verificou na membrana plasmática e em *ruffles* periféricas. Assim, a ausência de atividade GAP da ASAP1 não só não condiciona a interação com a Arl13b de uma forma dependente de GTP, como também não interfere com a sua co-localização. Estes resultados apoiam a hipótese descrita na literatura de que a atividade GAP da ASAP1 não é necessária para algumas das suas funções, podendo atuar não só como GAP, mas também como efetora das proteínas da família Arf. Neste contexto, estes dados sugerem que a ação conjunta da Arl13b e da ASAP1 não requer a atividade GAP da ASAP1. Por fim, não foi detetada a co-localização da GIT1 com a Arl13b, suportando os resultados obtidos nos ensaios de co-imunoprecipitação.

A identificação da ASAP1, ASAP3 e ACAP1 como proteínas que interagem com a Arl13b e a sua co-localização em estruturas ricas em actina envolvidas na migração ou invasão das células tumorais levantou a hipótese destas proteínas poderem atuar como GAPs da Arl13b. Por esse motivo, investiguei se a ASAP1, ASAP3 e/ou a ACAP1 poderiam induzir a atividade de hidrólise de GTP da Arl13b. Para tal, recorri a um ensaio *in vitro* de atividade GTPásica e a proteínas recombinantes purificadas. Verifiquei que a ASAP1 e a ASAP3 não promovem a hidrólise de GTP pela Arl13b. O resultado obtido para a ACAP1 não foi conclusivo, uma vez que a hidrólise de GTP aumentou significativamente na presença única desta proteína e de GTP. Isto deveu-se, possivelmente, à presença de uma proteína contaminante na sequência de um processo de purificação ineficiente. Desta forma, é necessário proceder a uma nova purificação da ACAP1, de modo a garantir a ausência de proteínas contaminantes que interferiram na hidrólise de GTP.

O nosso grupo demonstrou previamente que o silenciamento do gene *ARL13B* resulta na diminuição da migração e invasão de fibroblastos e das células de cancro de mama MCF7 e MDA-MB-231. O papel da ASAP1 e da ASAP3 nestes processos celulares está descrito na literatura: enquanto que o silenciamento do gene *ASAP3* leva a uma redução na migração e invasão das células MDA-MB-231, o efeito do silenciamento do gene *ASAP1* nestes processos é contraditório. Adicionalmente, verifiquei que os genes *ASAP1* e *ASAP3* são sobreexpressos em linhas celulares de cancro de mama mais invasivas, tal como o gene *ARL13B*. Os resultados obtidos confirmam que estas Arf GAPs, tal com a Arl13b, estão associadas à progressão tumoral.

Para a ACAP1, não existem estudos que descrevam o seu papel direto na migração e invasão das células tumorais. Desta forma, determinei qual o efeito do silenciamento do gene *ACAP1* nestes processos, recorrendo a ensaios de migração e invasão em *transwells* com células MDA-MB-231 silenciadas para o respetivo gene. Os resultados mostram que o silenciamento do gene *ACAP1* leva a um aumento da migração e invasão das células tumorais. Para além disso, este resultado correlaciona-se com a reduzida expressão do mesmo gene em linhas celulares de cancro de mama mais invasivas, inversamente ao que se verifica para a expressão do gene *ARL13B*. Estes dados não só suportam o envolvimento direto da ACAP1 na progressão tumoral, não descrito até aqui, como também indicam a existência de um efeito oposto entre esta Arf GAP e a Arl13b na migração e invasão das células tumorais.

Conjuntamente, os resultados aqui apresentados sugerem que a ASAP1 e a ASAP3 atuam como efetores da Arl13b. Estas duas Arf GAPs ligam-se à Arl13b de uma forma GTP-dependente e, ao mesmo tempo, não são capazes de promover a sua atividade GTPásica. Para além disso, os níveis de expressão da Arl13b, ASAP1 e ASAP3 estão aumentados em células de cancro de mama mais invasivas, indicando que atuam no mesmo sentido. Embora o efeito da ASAP1 na migração e invasão de células tumorais não seja consistente na literatura, o efeito da ASAP3 nestes processos é idêntico ao que o nosso grupo verificou para a Arl13b. Relativamente à ACAP1, os resultados não permitem afirmar que esta proteína atua como GAP da Arl13b. Contudo, o facto desta Arf GAP se ligar à Arl13b de uma forma GTP-dependente, de ter efeitos opostos à Arl13b na migração e invasão de células tumorais, e de ter uma

expressão inversa à da Arl13b em células de cancro de mama progressivamente mais invasivas, sugere a ACAP1 como um candidato promissor a atuar como GAP da Arl13b.

Este estudo propõe, assim, uma hipótese de como é que a Arl13b poderá ser inativada, contribuindo, também, para a compreensão dos mecanismos através dos quais esta proteína regula a progressão tumoral. Estudos futuros deverão focar-se não só nas proteínas já identificadas, mas também na procura de outros candidatos reguladores da Arl13b, podendo contribuir, desta forma, para o desenvolvimento de terapias anti-tumorais.

Index of contents

Index of figures

Index of tables

List of abbreviations, acronyms and symbols

≈	Approximately equal to
ø	Diameter
[α-^{32}P]GTP	Guanosine triphosphate labeled on the alpha phosphate group with ^{32}P
aa	Amino acids
ACAP	Arf GAP with coiled-coil domain, ANK repeats and PH domain
ADAP	Arf GAP with dual PH domains
ADP	Adenosine diphosphate
AGAP	Arf GAP with GTPase domain, ANK repeats and PH domain
AGFG	Arf GAP with phenylalanine (F) and glycine (G) repeats
ANK	Ankyrin
ANOVA	Analysis of variance
ARAP	Arf GAP with Rho GAP domain, ANK repeats and PH domain
Arf	ADP-ribosylation factor
Arg	Arginine
Arl	Arf-like
Arl13b$^{1-225}$	Arl13b truncated form comprising residues 1-225
Arl13b^{hnn}	Arl13b^{hennin}
Arp	Arf-related protein
Arp2/3	Actin-related protein 2/3
ASAP	Arf GAP with SH3 domain, ANK repeats and PH domain
BAR	Bin/Amphiphysin/Rvs
BLAST	Basic Local Alignment Search Tool
BM	Basement membrane
bp	Base pairs
BSA	Bovine serum albumin
CCD	Coiled-coil domain
cDNA	Complementary deoxyribonucleic acid
CDR	Circular dorsal ruffle

CMV	Cytomegalovirus
CO_2	Carbon dioxide
CV	Column volume
Cy3	Cyanine 3
DAPI	4',6-diamidino-2-phenylindole
DMEM	Dulbecco's Modified Eagle medium
DNA	Deoxyribonucleic acid
dNTP	Deoxyribonucleotide triphosphate
DTT	Dithiothreitol
E. coli	*Escherichia coli*
ECL	Enhanced chemiluminescence
ECM	Extracellular matrix
EDTA	Ethylenediaminetetraacetic acid
EGFP	Enhanced green fluorescent protein
EGTA	Ethylene glycol-bis(β-aminoethyl ether)-*N*,*N*,*N*',*N*'-tetraacetic acid
ELMOD2	ELMO domain-containing protein 2
EMT	Epithelial-mesenchymal transition
FA	Focal adhesion
F-actin	Filamentous-actin
FBS	Fetal bovine serum
FLAG	DYKDDDDK peptide sequence
GAP	GTPase-activating protein
GAPDH	Glyceraldehyde-3-phosphate dehydrogenase
GDI	Guanine nucleotide dissociation inhibitor
G-domain	Nucleotide-binding domain
GDP	Guanosine diphosphate
GEF	Guanine nucleotide exchange factor
GFP	Green fluorescent protein
GIT	G-protein-coupled receptor kinase interactor
GLUT4	Glucose transporter type 4

G-protein	Guanine nucleotide-binding protein
GST	Glutathione S-transferase
GTP	Guanosine-5'-triphosphate
GTPase	Guanosine triphosphatase
GTPɣS	Guanosine-5'-O-(ɣ-thio)triphosphate
HEK	Human embryonic kidney
HEPES	4-(2-hydroxyethyl)-1-piperazineethanesulfonic acid
HRP	Horseradish peroxidase
IPTG	Isopropyl β-D-1-thiogalactopyranoside
kDa	Kilodalton
LB	Lysogeny broth
Lys	Lysine
M2	Clone M2
MEF	Mouse embryonic fibroblast
miR	Micro ribonucleic acid
mRNA	Messenger ribonucleic acid
MWCO	Molecular weight cut-off
NCBI	National Center for Biotechnology Information
NMII	Non-muscle myosin II
NMIIA	Non-muscle myosin IIA
NT control shRNA	Non-targeting control shRNA
$p(dN)_6$	Deoxyribonucleotide hexamer random primer sequence
PAK	p21-activated kinase
PBR	Paxillin-binding region
PBS	Phosphate-buffered saline
PCR	Polymerase chain reaction
PH	Pleckstrin homology
Pi	Inorganic phosphate
PIX	PAK-interacting exchange factor
PR	Peripheral ruffle

PRR	Proline-rich region
Rab	Ras-related protein in brain
Ran	Ras-related nuclear protein
Ras	Rat sarcoma
RB	Reaction buffer
Rho	Ras homologous
RNA	Ribonucleic acid
RT-qPCR	Real-time quantitative polymerase chain reaction
Sar	Secretion-associated and Ras-related
SD	Standard deviation
SDS	Sodium dodecyl sulfate
SDS-PAGE	SDS-polyacrylamide gel electrophoresis
SH3	Src homology 3
SHD	Spa-homology domain
Shh	Sonic hedgehog
shRNA	Short hairpin ribonucleic acid
SMAP	Small Arf GAP
TAE	Tris-acetate-EDTA
Tks5	SH3 and PX domain-containing protein 2A
Tris	Tris(hydroxymethyl)aminomethane
Triton X-100	4-(1,1,3,3-Tetramethylbutyl)phenyl-polyethylene glycol
Tween 20	Polyethylene glycol sorbitan monolaurate
UV	Ultraviolet
VSV-G	Vesicular stomatitis virus glycoprotein
XRP2	Protein encoded by *RP2* gene

1. Introduction

1.1. Metastatic dissemination of cancer cells

Cancer encompasses a large group of diseases involving abnormal cell growth with the potential to spread to other organs. To evolve to a neoplastic state, normal cells acquire a series of specific traits in a multistep process, enabling them to become tumorigenic. These features comprise sustained proliferative signaling, evasion of growth suppressors, resistance to cell death, replicative immortality, induction of angiogenesis and activation of invasion and metastasis (Hanahan and Weinberg, 2011).

Most cancer-related deaths are caused by metastasis, involving cancer cell migration and invasion of tissues surrounding the primary tumor (Bravo-Cordero *et al.*, 2012). Polarized epithelial cells acquire a migratory phenotype in a process known as epithelial-mesenchymal transition (EMT). EMT involves important changes that include the loss of cell-cell and cell-extracellular matrix (ECM) adhesions, which allow them to disseminate and locally invade the adjacent tissues (Thiery, 2002; Taylor *et al.*, 2010).

The first barrier that tumor cells must overcome is the basement membrane (BM) of the native epithelium (Figure 1.1), followed by migration through the ECM of the tumor stroma (Bravo-Cordero *et al.*, 2012). Then, cancer cells enter the circulation by intravasation, by penetrating the BM of the vascular endothelium of nearby blood and lymphatic vessels and moving through the space between adjacent endothelial cells (Eddy *et al.*, 2017). In the bloodstream, circulating cells must adhere to endothelial cells, leave the vessels' lumen by extravasation and enter the stroma of competent metastatic organs (Reymond *et al.*, 2013). Here, cells start to proliferate, which leads to colonization (Van Zijl *et al.*, 2011) and formation of a new mass of cancer cells that can eventually evolve into a macroscopic tumor which is clinically detectable (Reymond *et al.*, 2013).

The metastatic dissemination is a complex process that requires a critical spatial and temporal coordination of the trafficking of vesicles carrying cargo involved in cell adhesion and signaling, as well as the remodeling of the actin cytoskeleton (Fife *et al.*, 2014). Membrane trafficking and actin cytoskeleton remodeling represent, indeed, key regulators of cell polarity, migration, invasion and growth, and are often disrupted in and by metastatic tumor cells (Yamaguchi and Condeelis, 2007).

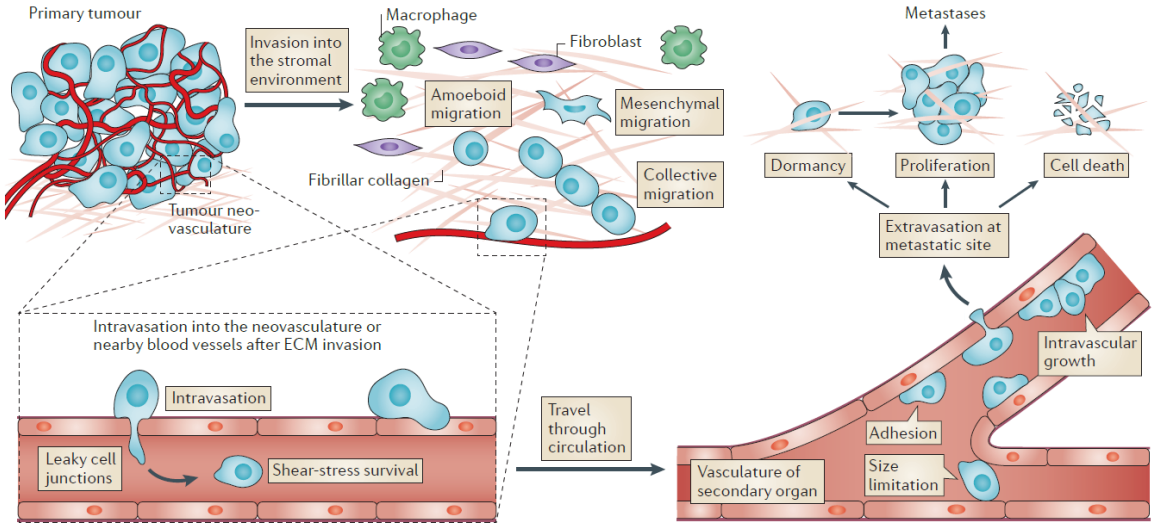

Figure 1.1. Mechanisms of metastatic dissemination. Cancer cells leave the primary tumor by invading through the basement membrane of the native epithelium and the tumor stroma. Then, they penetrate the surrounding tissues and move towards the neighboring blood vasculature using different types of migration. Here, invading cancer cells enter the bloodstream by intravasation, spreading through the circulation until they transmigrate into potential secondary tumor sites. In the new microenvironment, tumor cells enter a state of dormancy or undergo proliferation, potentially giving rise to micrometastases and eventual macrometastases. However, most cancer cells will not be able to colonize the new tissues, undergoing cell death, instead. ECM, extracellular matrix. Taken from Reymond *et al.*, 2013.

1.2. Dynamic organization of the actin cytoskeleton during cancer cell migration and invasion

The study of the fundamental mechanisms of cell migration and invasion is essential for the understanding of tumor cell metastatic dissemination. Migrating and invading cells acquire a polarized morphology, allowing the formation of structures with protrusive and adhesive functions that differ on their architecture (Le Clainche and Carlier, 2008). These changes require highly coordinated rearrangements of the actin cytoskeleton and a regulated interaction with ECM (Gardel *et al.*, 2010).

The formation of adhesion structures by migrating cells is critical for cell migration. Focal adhesions (FAs) are dynamic adhesive structures that provide the link between antiparallel contractile bundles of actin, named stress fibers (Figure 1.2), and ECM proteins, such as fibronectin (Kuo, 2013). This interaction occurs mainly through integrins, a family of heterodimeric transmembrane proteins that transduce both mechanical and chemical signals, leading to cytoskeletal rearrangements and morphological polarization that drive cell migration (Mayor and Etienne-Manneville, 2016). The intracellular ligands that anchor these adhesions include vinculin and paxillin, which play an important role in FA dynamics (Geiger *et al.*, 2001).

At the cell front, actin assembly extends sheet-like membrane protrusions called lamellipodia (Figure 1.2), where actin is organized in dense arrays of branched and crosslinked filaments (Small *et al.*, 2002). When the actin bundles extend beyond the edge of lamellipodia, they form filopodia (Figure 1.2), which are thin finger-like projections composed by tightly packed parallel filaments (Mattila and Lappalainen, 2008). Filopodia are believed to act as environmental sensors, influencing the direction of cell movement (Letort *et al.*, 2015). Both lamellipodia and filopodia are maintained by localized actin polymerization at the barbed ends of the filaments, towards the leading edge of the cell and simultaneous depolymerization at the rear end. This process is known as “actin treadmilling” and is responsible for the generation of protrusive forces in lamellipodia and filopodia that are essential for cell migration (Wang, 1985). The lamella (Figure 1.2), a loose array of unbranched actin filaments, is positioned immediately behind the lamellipodia and has a slower actin turnover (Le Clainche and Carlier, 2008).

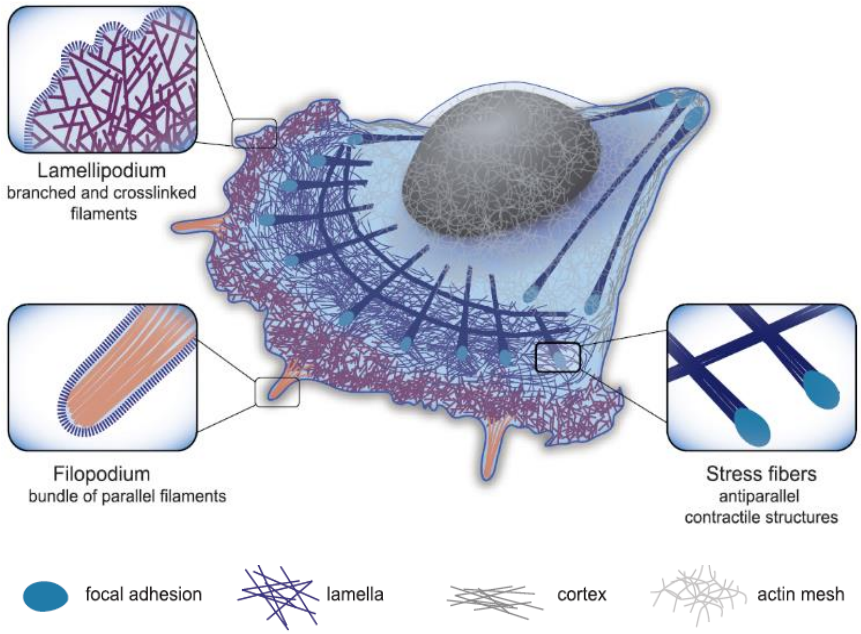

Figure 1.2. Subcellular organization of the actin cytoskeleton during cell migration. Migrating cells acquire a polarized morphology, allowing the formation of structures with protrusive and adhesive functions that differ on their architecture, upon the dynamic organization of the actin cytoskeleton. At the leading edge of the cell, in lamellipodia, actin is organized in dense arrays of branched and crosslinked filaments, while in filopodia, actin forms projections composed by parallel and crosslinked filaments that are tightly packed. Contractile stress fibers can be found as antiparallel filaments in the cytoplasm. Lamella, a loose array of unbranched actin filaments, is located immediately behind lamellipodia. Taken from Letort *et al.*, 2015.

Migrating cells also form peripheral ruffles (PRs) and circular dorsal ruffles (CDRs), that are membrane sheet-like and non-adhesive protrusions that extend vertically from the peripheral or the dorsal cell surface, respectively (Abercrombie *et al.*, 1970). Both structures have been associated with cell motility, as they provide a structural basis for force generation (Buccione *et al.*, 2004). PRs are active and persistent structures that assemble at the leading edge of migrating cells, folding and moving backwards, while CDRs are more dynamic and transient structures that are induced upon stimulation by growth factors (Hoon *et al.*, 2012). After the extension of the ruffle edges at the dorsal surface, CDRs constrict towards their center in a coordinated manner, creating a characteristic circular shape (Itoh and Hasegawa, 2013). Besides their role in cell migration, CDRs are also implicated in receptor internalization and macropinocytosis (Hoon *et al.*, 2012). Indeed, it has been described that, upon FA disassembly, integrin internalization occurs by macropinocytosis through CDRs, followed by its recycling back to the emerging focal adhesions at the leading edge of the cell (Gu *et al.*, 2011).

To cross the dense cross-linked networks of ECM and form metastases, tumor cells need to develop invadopodia (Linder, 2007). Invadopodia are specialized ventral membrane extensions that degrade and remodel the ECM through the exocytosis of proteolytic enzymes, namely matrix metalloproteases, which leads to the breaching of epithelia and endothelia BMs (Buccione *et al.*, 2004; Monteiro *et al.*, 2013). Moreover, they are composed of an actin-rich core that is surrounded by adhesion and scaffolding proteins (Murphy and Courtneidge, 2011). Invadopodia appear as small dot-like clusters with a core of actin near the nucleus and in the vicinity of the Golgi complex (Gimona *et al.*, 2008).

Cancer cells stimulate the formation of lamellipodia, filopodia, PRs, CDRs and invadopodia, and control their turnover through a variety of signaling molecules, their activity regulators and downstream effectors (Yamaguchi and Condeelis, 2007). One of the most prominent groups of proteins that regulate these mechanisms are the small guanosine triphosphatases (GTPases) of the Ras superfamily (Gardel *et al.*, 2010; Fife *et al.*, 2014). These proteins are responsible for the dynamic spatiotemporal regulation of several processes required for cancer cell migration and invasion, namely cell-cell and cell-ECM adhesions, actin cytoskeleton remodeling and vesicular trafficking (Goitre *et al.*, 2014).

1.3. Small GTPases and their regulators in cancer

The human Ras superfamily of small GTPases includes more than 150 members that are grouped in five main families, based on sequence and function similarities: Ras, Rho, Rab, Ran and Arf (Wennerberg *et al.*, 2005). The members of this superfamily are membrane-associated proteins, generally with a low molecular weight, that are capable of binding GTP and hydrolyze it, due to the existence of a nucleotide-binding domain (G-domain) (Goitre *et al.*, 2014). They share a common functional mechanism of cycling between an inactive GDP-bound state and an active GTP-bound state, serving as binary molecular switches (Vetter and Wittinghofer, 2001). For this reason, small GTPases are also known as guanine nucleotide-binding proteins (G-proteins). The Mg^{2+} ion plays a critical role in the high-affinity binding of the guanine nucleotide to the G-domain (Vetter and Wittinghofer, 2001).

Because GDP is usually tightly bound to small GTPases and their GTP hydrolysis activity is intrinsically slow, their activation requires the dissociation of GDP and its exchange for GTP catalyzed by guanine nucleotide exchange factors (GEFs) and the stimulation of GTP hydrolysis by GTPase-activating proteins (GAPs) to promote their inactivation (Bos *et al.*, 2007). GEFs induce the dissociation of GDP in part through destabilizing bound Mg^{2+} from GTPase active site, consequently allowing the nucleotide exchange by GTP (Sprang and Coleman, 1998). The GDP-dissociation is also dependent on the concentration of GTP in the cytosol (Zhang *et al.*, 2005). Binding to GTP leads to a conformational change that allows the interaction with effectors (Herrmann, 2003) and the stable binding to membranes (Goitre *et al.*, 2014). Additionally, small GTPases that carry a farnesyl or geranylgeranyl group in their C-terminal region are also regulated by guanine nucleotide dissociation inhibitors (GDIs). GDIs shield the hydrophobic lipid groups of GTPases in their GDP-bound form, preventing the guanine nucleotide

exchange and consequently their attachment to membranes and interaction with regulators and effectors (Cherfils and Zeghouf, 2013).

The complex regulation of Ras superfamily small GTPases enables their involvement in a diverse spectrum of biochemical and biological processes, determined by variations in their structure, post-translational modifications and the action of their regulators and downstream effectors (Wennerberg *et al.*, 2005). Indeed, they act as signaling operators in response to diverse extracellular stimuli, influencing cell proliferation, morphology, polarity, adhesion and migration, mainly by controlling the cytoskeletal rearrangement and the directional transport of vesicles (Goitre *et al.*, 2014).

Due to the crucial functions in fundamental cellular processes, dysregulation of the expression or activity of many small GTPases and their regulatory proteins has been associated with several human diseases, like developmental abnormalities, neurological syndromes (Seixas *et al.*, 2013; Simanshu *et al.*, 2017; Messina, 2018) and several types of cancer (Porter *et al.*, 2016; Wang *et al.*, 2017; Sheng *et al.*, 2018; Shaughnessy and Echard, 2018; Earp *et al.*, 2018). Namely, proteins from the Arf family and their activity regulators, Arf GEFs and Arf GAPs, have been found to be abnormally expressed in different types of human cancers (Casalou *et al.*, 2016).

1.3.1. Arf family

The Arf (ADP-ribosylation factor) family comprises six Arf proteins (Arf1-Arf6) and 22 Arl (Arf-like) proteins, as well as Arp (Arf-related proteins) and Sar (Secretion-associated and Ras-related) proteins (Pasqualato *et al.*, 2002). Arfs are key regulators of membrane trafficking, organelle structure and actin cytoskeleton remodeling, being critical for several cellular functions, including cell spreading and migration (D'Souza-Schorey and Chavrier, 2006; Donaldson and Jackson, 2011; Kjos *et al.*, 2018). They are activated by Arf GEFs and inactivated by Arf GAPs (Figure 1.3), sharing a much larger GDP/GTP conformational change than the one occurring in other members of the Ras superfamily (Goitre *et al.*, 2014). However, it remains unclear if Arf GEFs and Arf GAPs can also function on Arl proteins. Also, unlike Rab and Rho small GTPases, no GDI proteins have been identified for Arf or Arl proteins (Donaldson and Jackson, 2011).

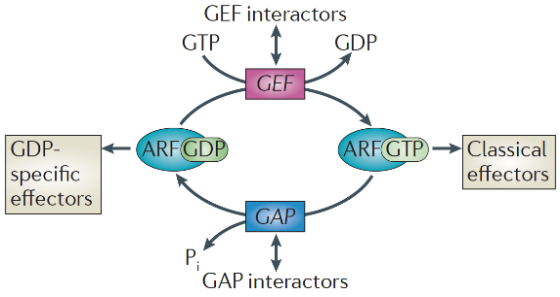

Figure 1.3. The GTP/GDP cycle of Arf proteins. Arf proteins cycle between an inactive GDP-bound conformation and an active GTP-bound conformation. GTP hydrolysis is catalyzed by Arf GAPs that hydrolyze GTP to GDP with a concomitant release of inorganic phosphate (Pi). GDP remains bound to the Arf proteins until exchanged for GTP by Arf GEFs. In the GTP-bound form, the interaction with "classical effectors" allows Arf proteins to carry out their functions. Notably, several proteins that interact with Arf GEFs and Arf GAPs and effectors that associate specifically with the GDP-bound form of Arf proteins have been found. Taken from Donaldson and Jackson, 2011.

Similar to other small GTPases, a complex of Arf-GTP with an effector protein mediates Arf function (Nie *et al.*, 2003). Increased attention has been given to networks of proteins that interact with Arf GEFs and Arf GAPs themselves, as well as distinct effectors that bind specifically to the GDP-bound conformation of Arf proteins (Figure 1.3). In fact, several studies over the last few years have provided evidence that the activity of Arf GEFs and Arf GAPs is more extended and complex than initially thought, since they can be recruited to assemble protein complexes at specific sites independently of their catalytic activity. Thus, it is possible that Arf GEFs and Arf GAPs can initiate

their own cellular responses, acting not only as activity modulators but also as downstream effectors (Donaldson and Jackson, 2011).

Due to the key roles of Arf proteins on several cellular processes that are relevant to tumorigenesis (Hashimoto *et al.*, 2004; Ha *et al.*, 2008; Morishige *et al.*, 2008; Hongu *et al.*, 2016; Rafiq *et al.*, 2017), Arf GEFs and Arf GAPs have emerged as candidate regulators of cancer progression (Casalou *et al.*, 2016) and suggested as potential targets of anti-cancer therapies (Vigil *et al.*, 2010).

1.3.2. Arf GEFs

Arf GEFs contain a conserved Sec7 domain that catalyzes the release of GDP and the binding of GTP to the Arf protein (Gillingham and Munro, 2007). In humans, there are 15 Arf GEFs, divided in six subfamilies (Donaldson and Jackson, 2011). So far, only Arl13b has been described as a specific GEF of Arl proteins, in this case of Arl3 (Ivanova *et al*., 2017).

A role for several GEFs in cancer has been suggested by their aberrant activation as a consequence of upregulated gene expression, presence of missense mutations or abnormal signal-mediated GTPase activation by growth factors (Vigil *et al.*, 2010). Indeed, several Arf GEFs have emerged as candidate regulators of cancer progression (Vigil *et al.*, 2010; Casalou *et al.*, 2016), as in the case of Arf6 activation which promotes the invasive behavior of breast cancer cells (Morishige *et al.*, 2008).

1.3.3. Arf GAPs

The human Arf GAP family is composed by 31 members, which are divided in ten major subtypes, based on their respective domain structure: Arf GAP1, Arf GAP2/3, ADAPs, SMAPs, AGFGs, GITs, ASAPs, ACAPs, ARAPs and AGAPs (Kahn *et al.*, 2008). Arf GAPs are characterized by the presence of a conserved zinc-finger GAP catalytic domain, responsible for stimulating Arf GTPase activity (Gillingham and Munro, 2007). So far, only two Arl-specific GAPs have been identified: XRP2 in the case of Arl3 and ELMOD2 in the case of Arl2 and Arl3 (Donaldson and Jackson, 2011).

A role for Arf GAPs in cancer progression has also been proposed (Casalou *et al.*, 2016), although whether it is through their GAP activity on Arf GTPases is not known (Vigil *et al.*, 2010). In fact, ASAP, GIT, SMAP and AGAP proteins have been shown to contribute directly to oncogenesis. ARAPs and ACAPs regulate processes related to cell migration, like signaling responses, membrane ruffling and cell adhesion, but have not been directly implicated in cancer (Ha *et al.*, 2008).

1.3.3.1. ASAP subfamily

The ASAP subfamily includes ASAP1 (≈ 126 kDa), ASAP2 (≈ 112 kDa) and ASAP3 (≈ 99 kDa), which differ in their C-terminal region (Figure 1.4). The acronym refers to the initial nomenclature Arf GAPs with a SH3 domain, Ankyrin (ANK) repeats and a PH domain. However, later studies indicated that ASAP3 lacks a SH3 domain (Randazzo and Hirsch, 2004). Common domains of this subfamily also include the BAR domain, as well as proline-rich motifs. Additionally, ASAP1 contains E/DLPPKKP tandem repeats (Ha *et al.*, 2008). These proteins interact with many signaling molecules, regulating several aspects of endocytic traffic and actin remodeling (Kahn *et al.*, 2008).

ASAP1 and ASAP2 present GAP activity towards Arf1, Arf5 and to some extent also Arf6 (Brown *et al.*, 1998; Andreev *et al.*, 1999). ASAP1 stabilizes FAs (Liu *et al.*, 2002), regulates integrin-mediated adhesion (Randazzo *et al.*, 2000), controls and promotes invadopodia formation (Bharti *et al.*, 2007), inhibits CDRs assembly (Randazzo *et al.*, 2000) and binds to regulators of the endocytic pathway (Inoue *et al.*, 2008). A protein interactor whose activity is regulated by ASAP1 is the non-muscle myosin IIA (NMIIA) (Chen *et al.*, 2016). The interaction between both proteins could explain the role of ASAP1 in cell migration and adhesion, since NMIIA is known to regulate these processes (Vicente-Manzanares *et al.*, 2009). Thus, ASAP1 has an essential role in actin remodeling by integrating different signals that

ensure the coordination between membrane traffic and cytoskeletal rearrangements at each step of cycling events that result in cell movement (Randazzo *et al.*, 2000). Some studies raised the possibility that the ASAP1 GAP activity might not be necessary for some of this Arf GAP specific functions (Donaldson and Jackson, 2011), like the formation of invadopodia, supporting the hypothesis that ASAP1 could also function as an Arf effector (Ha *et al.*, 2008).

ASAP2 localizes at the Golgi apparatus and plasma membrane, being involved in the regulation of vesicular trafficking and cell migration (Andreev *et al.*, 1999; Kondo *et al.*, 2000).

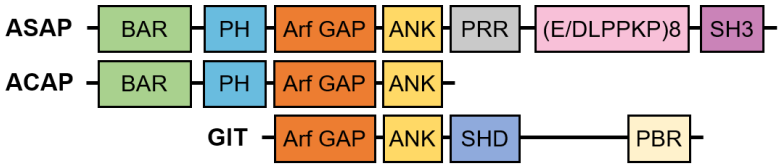

Figure 1.4. Domain architecture of ASAP, ACAP and GIT. Arf GAPs share a conserved Arf GAP domain. The other domains are: ANK, ankyrin repeats; BAR, Bin/Amphiphysin/Rvs; PBR, paxillin-binding region; PH, pleckstrin homology domain; PRR, proline-rich region; SH3, Src homology 3; SHD, Spa-homology domain. Adapted from Ha *et al.*, 2008.

ASAP3 acts as an Arf GAP for Arf1, Arf5 and Arf6 (Fang *et al.*, 2006; Ha *et al.*, 2008). It associates with FAs and CDRs and also plays a role in actin stress fiber formation. However, unlike ASAP1, it is not detected in invadopodia (Ha *et al.*, 2008). A recent work suggests that ASAP3 could promote NMII activation by phosphorylation, whose activity is critical for cell migration (Luo *et al.*, 2017).

Among the members of the ASAP subfamily, only ASAP1 and ASAP3 have been directly implicated in oncogenesis (Ha *et al.*, 2008). While ASAP1 has been found to be upregulated in uveal melanoma (Ehlers *et al.*, 2005), as well as in breast (Onodera *et al.*, 2005), colorectal (Buffart *et al.*, 2005) and prostate cancers (Lin *et al.*, 2008), ASAP3 is highly expressed in hepatocellular carcinoma (Okabe *et al.*, 2004) and in non-small cell lung (Fan *et al.*, 2014), colorectal (Tian *et al.*, 2017) and breast cancers (Mao *et al.*, 2017). These studies indicate that the upregulation of ASAP1 and ASAP3 correlates with increased tumor cell invasion and metastasis.

Previous studies showed that ASAP3 silencing impairs cell migration of HeLa cervical cancer cells and MDA-MB-231 breast cancer cells (Fang *et al.*, 2006; Ha *et al.*, 2008), as well as invasion of MDA-MB-231 (Ha *et al.*, 2008) and lung carcinoma cell lines (Fan *et al.*, 2014). Although the molecular mechanisms for these effects are not known, a model has been proposed based on the regulation of FA composition by ASAP3 (Ha *et al.*, 2008). Lastly, the reported consequences of ASAP3 on cancer cell proliferation have not been consistent (Ha *et al.*, 2008).

It has been described that the C-terminal region of ASAP1 binds to several oncogenes that influence cell migration, invasion and metastasis (Luo *et al.*, 2007). However, the effects of this protein on cancer cell migration and invasion are contradictory. Silencing of ASAP1 has no effect on migration of MDA-MB-231 cells (Ha *et al.*, 2008), but its depletion in fibroblasts (Furman *et al.*, 2002) and prostate cancer cells (Lin *et al.*, 2008) impairs cell migration. Although ASAP1 has been reported to be required for the formation of invadopodia (Bharti *et al.*, 2007), its silencing has no effect on the invasion capacity of MDA-MB-231 cells. However, another study described the opposite (Ha *et al.*, 2008).

Overall, the role of ASAP1 and ASAP3 in cancer is not completely understood and the molecular bases for these mechanisms still need to be determined.

1.3.3.2. ACAP subfamily

ACAP is the acronym for Arf GAPs with a Coiled-coil domain, later identified as a BAR domain, ANK repeats and a PH domain (Kahn *et al.*, 2008) (Figure 1.4). ACAP1 (≈ 81 kDa), ACAP2 (≈ 88 kDa) and ACAP3 (≈ 93 kDa) function as Arf GAPs of Arf6 (Jackson *et al.*, 2000; Miura *et al.*, 2016), being required for Arf6-mediated membrane recycling regulation (De Curtis, 2001). ACAP1 facilitates the

interaction between clathrin and cargo in the recycling of GLUT4, a glucose transporter, acting as both Arf6 GAP and effector in the same pathway (Li *et al.*, 2007). These observations support the dual role of Arf GAPs, serving as terminators of Arf signaling, as well as Arf effectors (East and Kahn, 2011). Besides the function on membrane recycling, ACAPs regulate Arf6-dependent actin remodeling and cell movement (Inoue and Randazzo, 2007). Indeed, ACAP1 or ACAP2 overexpression inhibits Arf6-induced formation of actin-rich structures, like membrane ruffles and membrane protrusions (Jackson *et al.*, 2000). ACAP1 silencing interferes with integrin recycling and cell migration (Randazzo *et al.*, 2007) and its overexpression reduces the size of FAs (Chen *et al.*, 2014). In fact, it has been suggested that ACAP1 regulates β1 integrin trafficking (Li *et al.*, 2005). An additional function described for ACAP1 is the downregulation of NF-κB signaling activation (Yamamoto-Furusho *et al.*, 2006).

ACAP1 has not been directly implicated in cancer, but it has been shown to potentially play a role in breast cancer progression, since the continued cycling of Arf6 is necessary for the invasion of breast cancer cells (Hashimoto *et al.*, 2004). Furthermore, Arf6 expression has been described to be higher in highly invasive breast cancer cells comparing to poorly invasive or non-invasive breast cancer and normal mammary epithelial cells (Hashimoto *et al.*, 2004). Additionally, nonsynonymous somatic mutations in *ACAP1* were identified in human breast tumors and the authors suggest a link to its involvement in NF-κB pathway (Jiao *et al.*, 2012). Moreover, a recent genome-wide association study suggested that higher expression levels of *ACAP1* in whole blood samples are associated with an increased risk of developing breast cancer (Hoffman *et al.*, 2017). The authors suggest a different model for how ACAP1 may be involved in breast cancer progression, since it interacts with GLUT4, whose silencing diminishes cell proliferation and cell viability (Garrido *et al.*, 2015). ACAP2 shows a pro-apoptotic role in cancer cells and it is downregulated in different types of cancer (Sullivan *et al.*, 2015). Finally, a role for ACAP3 in cancer has not been described.

1.3.3.3. GIT subfamily

GIT stands for G-protein-coupled receptor kinase interactor. Mammals express two GIT proteins, GIT1 (≈ 84 kDa) and GIT2 (≈ 85 kDa), which share a conserved domain architecture, including the Arf GAP catalytic domain, three ANK repeats, an SHD domain and a unique binding site for the FA adaptor protein paxillin (Ha *et al.*, 2008) (Figure 1.4). GIT proteins are Arf GAPs of Arf6 (Vitale *et al.*, 2000) and GIT1 specifically has a role in Arf6-mediated membrane recycling (De Curtis, 2001).

Over 100 GIT-associated proteins and several direct partners have been described (Zhou *et al.*, 2016). The most prominent partner is the PAK-interacting exchange factor (PIX), which binds GIT proteins to form oligomeric complexes (Premont *et al.*, 2004). The best described role for GIT-PIX complexes is in cell adhesion and migration, where they regulate cytoskeletal remodeling by binding to paxillin (Zhou *et al.*, 2016) to stabilize FAs (Randazzo *et al.*, 2007). GIT1 associates with paxillin in what has been described as supramolecular complexes that appear like punctate cytoplasmic structures that mediate the relocation of paxillin to sites of protrusion at the cell's edge (Manabe *et al.*, 2002) in an Arf6-dependent manner (De Curtis, 2001).

GIT and PIX proteins are important regulators of essential processes that are often disrupted in cancer cells (Zhou *et al.*, 2016). Indeed, GIT1 is upregulated in several cancer types, including liver, colon (Peng *et al.*, 2013; Chen *et al.*, 2015), lung (Chang *et al.*, 2015) and kidney (Lu *et al.*, 2015), as well as in melanoma (Huang *et al.*, 2014). GIT2 is downregulated in breast cancer (Sirirattanakul *et al.*, 2015). More recently, GIT1 has been described as a direct target of four distinct microRNAs (miR) in different types of cancer: miR-491-5p (Huang *et al.*, 2014), miR-149 (Chan *et al.*, 2014; Dong *et al.*, 2017), miR-138 (Li *et al.*, 2015) and miR-34c (Tao *et al.*, 2016). The downregulation of these microRNAs results in the upregulation of GIT1, which in turn enhances cancer cell proliferation, migration, invasion and *in vivo* metastasis.

1.3.4. Arl13b

Arl13b is an atypical member of the Arl subfamily with a molecular weight of 48 kDa. This subfamily comprises over 20 members, which seem to have broader roles than Arf proteins (Donaldson and Jackson, 2011). Unlike the other Arf family members that have a single conserved G-domain at the N-terminal region with approximately 20 kDa, Arl13b has an additional extended domain with 24 kDa of unknown function at the C-terminal region that contains coiled-coil domains and a proline-rich region (Hori *et al.*, 2008) (Figure 1.5). Furthermore, its G -domain contains a modification at a highly conserved glutamine residue (Ivanova *et al.*, 2017). The consequence of this change is currently unknown. However, since this residue is directly involved in GTP hydrolysis, it might be predicted to change Arl13b constitute level of activation, its mechanisms of GTP hydrolysis or both (Ivanova *et al.*, 2017). Moreover, palmitoylation of Arl13b has been described to be a post-translational modification essential for its localization and function, as well as its stability and half-life extension (Roy *et al.*, 2017).

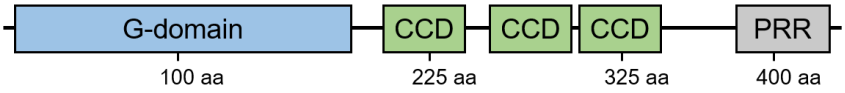

Figure 1.5. Domain architecture of Arl13b. This atypical small GTPase contains a N-terminal G-domain, central coiled-coil domains (CCD) and flexible C-terminal region containing a proline-rich region (PRR). aa, amino acids. Adapted from Hanke-Gogokhiaa *et al.*, 2017.

Arl13b is known to be involved in intraflagellar transport (Li *et al.*, 2010) and ciliogenesis, acting together with the exocyst, identified as an Arl13b effector (Seixas *et al.*, 2016). Different missense mutations in *ARL13B* have been associated with Joubert syndrome, an autosomal recessive disorder characterized by abnormal cilia function, leading to neurological and other developmental deficiencies (Cantagrel *et al.*, 2008; Thomas *et al.*, 2015; Rafiullah *et al.*, 2017). Arl13b$^{hennin\ (hnn)}$ mutant mouse embryos, which carry a null allele of Arl13b, show defects in cilia structure and Sonic hedgehog (Shh) signaling coupled with severe and lethal developmental defects (Caspary *et al.*, 2007). Arl13b^{hnn} mouse embryonic fibroblasts (MEFs) have shorter cilia with defective axoneme architecture and altered dynamic of Shh signaling (Larkins *et al.*, 2011).

In addition to the functions in primary cilia and Shh signaling, our group has demonstrated a role for Arl13b in endocytic recycling traffic and that Arl13b co-localizes with the actin cytoskeleton and interacts with it (Barral *et al.*, 2012; Casalou *et al.*, 2014). Indeed, our laboratory has shown that this protein is needed for *in vitro* cell migration of MEFs and *in vivo* migration of neural crest cells in zebrafish embryos (Casalou *et al.*, 2014). The mechanism by which Arl13b regulates cell migration is not fully understood (Casalou *et al.*, 2014). However, our group also identified NMIIA as an Arl13b effector and both proteins have been demonstrated to be required for CDR formation, where they colocalize with actin (Casalou *et al.*, 2014).

More recently, other studies have demonstrated a role of Arl13b in different types of cancer. This protein stimulates proliferation, migration and invasion both *in vitro* and *in vivo* in gastric tumor cells (Shao *et al.*, 2017) and medulloblastoma cell lines (Bay *et al.*, 2018). Our group also found that Arl13b regulates migration and invasion of MCF7 and MDA-MB-231 breast cancer cells (Casalou, Faustino *et al.*, unpublished results). Moreover, *ARL13B* depletion in highly invasive cancer cells impairs both primary breast tumor and lung metastases formation in orthotopic mouse models (Casalou, Faustino *et al.*, unpublished results). Remarkably, the analysis of cancer samples shows that Arl13b expression levels are highly correlated with tumor size and the late stages of invasion in gastric (Shao *et al.*, 2017) and breast cancers (Casalou, Faustino *et al.*, unpublished results). Together, these observations suggest that Arl13b plays an important role in tumor progression by positively regulating cancer cell migration and invasion and that it could be targeted to prevent cancer cell metastatic dissemination. Notably, any GEFs or GAPs are known for Arl13b.

2. Objectives

Previous results from our laboratory have uncovered a novel role for Arl13b in breast cancer, mainly by positively regulating cancer cell migration, invasion, and ultimately metastatic dissemination. This suggest that Arl13b could serve as a novel molecular target in anti-cancer therapies to prevent breast cancer progression. Considering this evidence, the main goal of this work was **to identify Arf GAPs that promote the inactive conformation of Arl13b** by screening known Arf GAPs for their capacity in catalyzing Arl13b GTP hydrolysis, thus contributing to unravel factors that regulate Arl13b function in cancer cell migration and invasion.

I started the screen by testing the Arf GAPs ASAP1, ASAP3, ACAP1 and GIT1, since they are known to regulate the actin cytoskeleton remodeling and membrane traffic (Randazzo *et al.*, 2007), cellular functions in which Arl13b is also involved (Barral *et al.*, 2012; Casalou *et al.*, 2014). Moreover, they have a role on cell adhesion, migration and invasion (Liu *et al.*, 2002; Li *et al.*, 2005; Bharti *et al.*, 2007; Randazzo *et al.*, 2007; Ha *et al.*, 2008) and ASAP1, ASAP3 and GIT1 have been directly implicated in oncogenesis (Ha *et al.*, 2008). In contrast, ACAP1 has been associated with actin remodeling and cell movement (Inoue and Randazzo, 2007), but a direct function in cancer has not been described. Furthermore, these Arf GAPs were the first to be studied in this project due to the availability of tools required for cell transfection, protein purification and lentivirus production.

Specific aim 1: **Assess the interaction of Arf GAPs with Arl13b and co-localization with actin and Arl13b in breast cancer cells**.

Since the main goal of this project was to identify Arf GAPs for Arl13b, I started by verifying which of the four Arf GAPs interacts with Arl13b by co-immunoprecipitation. Additionally, I aimed to determine the subcellular co-localization of Arl13b and the Arf GAPs in breast cancer cells.

Specific aim 2: **Identify Arf GAPs that induce Arl13b GTP hydrolysis.**

After the identification of the Arf GAPs that bind to Arl13b, I aimed to identify the ones that could stimulate the GTP hydrolysis activity of Arl13b, using an *in vitro* GTPase activity assay and recombinant purified proteins.

Specific aim 3: **Determine if ACAP1 regulates migration and invasion of breast cancer cells.**

Since Arl13b silencing leads to a decrease in migration and invasion of breast cancer cells, I aimed to assess if the inverse phenotype is obtained upon ACAP1 silencing, since the effects of ASAP1, ASAP3 and GIT1 on cancer cell migration and invasion are already described in the literature.

Specific aim 4: **Evaluate the expression of Arl13b and Arf GAPs in non-tumorigenic and tumorigenic breast cell lines and the correlation with tumor invasiveness.**

As described above, Arl13b expression levels are highly correlated with tumor size and the late stage of invasion of breast cancers. Therefore, I analyzed Arl13b and Arf GAPs gene expression in non-tumorigenic and tumorigenic breast cell lines to assess a possible correlation with breast cancer progression.

3. Material and methods

3.1. Cell culture

Cell culture reagents were obtained from Gibco. MDA-MB-231 breast cancer cells and HeLa cervical cancer cells were maintained at 37ºC and 5% CO_2 in Dulbecco's Modified Eagle medium (DMEM) supplemented with 10% heat-inactivated fetal bovine serum (FBS), 100 U/mL penicillin-streptomycin, 2 mM GlutaMAX and 15 mM HEPES (DMEM Complete medium).

3.2. Constructs and cell transfection

pEGFP-C-CMV5-Arl13b (Hori *et al.*, 2008) was a kind gift from Kenji Kontani (University of Tokyo, Japan). pCI-ASAP1-FLAG (Brown *et al.*, 1998), pCI-[R497K]ASAP1-FLAG (Randazzo *et al.*, 2000) and pCI-ASAP3-FLAG (Ha *et al.*, 2008) plasmids were kindly provided by Paul Randazzo (National Cancer Institute, Bethesda, Maryland, USA) and were verified by restriction enzyme digestion. pEGFP-N1-GIT1-FLAG and pFLAG-CMV2-ACAP1 constructs were obtained from Addgene (plasmids #15697 and #15225, respectively). All genes were cloned in mammalian expression vectors. The constructs used are listed and described in Table 3.1. All expression vectors were produced and purified from transformed *Escherichia coli* (DH5-alpha) glycerol stocks using QIAfilter Plasmid Midi Kit for DNA purification (QIAGEN), according to the manufacturer's instructions. After purification, DNA plasmids were quantified by measuring absorbance at 260 nm using NanoDrop 2000c (Thermo Scientific).

Table 3.1. DNA expression plasmids used for transient transfections.

Gene	Vector backbone	Bacterial resistance	Tag	Backbone size (bp)	Insert size (bp)
ARL13B	pEGFP-C-CMV5	Ampicillin	EGFP	4682	1900
ASAP1	pCI-FLAG	Ampicillin	FLAG	≈ 4000*	≈ 3500*
[R497K]ASAP1	pCI-FLAG	Ampicillin	FLAG	≈ 4000*	≈ 3500*
ASAP3	pCI-FLAG	Ampicillin	FLAG	≈ 4000*	≈ 2000*
ACAP1	pFLAG-CMV2	Ampicillin	FLAG	4679	2223
GIT1	pEGFP-N1	Kanamycin	FLAG/EGFP	4000	2200

* verified by restriction enzyme digestion.

3.2.1. Restriction enzyme digestion

pCI-ASAP1-FLAG, pCI-[R497K]ASAP1-FLAG and pCI-ASAP3-FLAG constructs were verified by restriction enzyme digestion using the Fast Digestion of DNA kit (Thermo Scientific), according to the manufacturer's instructions. Each plasmid was digested with *Eco*RI (0.2 U/µg DNA) and *Not*I (0.1 U/µg DNA) restriction enzymes, or with each one separately. Reaction mixtures were prepared at room temperature and contained 2 µL of 10× FastDigest buffer, 1 µg of each DNA plasmid and 1 µL of restriction enzymes (0.5 µL of each enzyme for double digestion). Nuclease free-water was added to 20 µL of total reaction volume. The reaction mixtures were mixed, spun down and incubated at 37ºC for 5 minutes, with agitation. Finally, the restriction enzymes were inactivated at 80ºC for 2 minutes. An 1% agarose gel in 1× TAE (Tris-acetate-EDTA) buffer was prepared and supplemented with GreenSafe Premium (NZYTech) to detect the nucleic acids. The digestion products were then run along with NZYDNA Ladder III (NZYTech) at 120 V during approximately 30 minutes. Fluorescence was detected using the ChemiDoc Touch Imaging System (Bio-Rad).

3.2.2. Reagent-based transfection

MDA-MB-231 or HeLa cells were seeded 24 hours before transfection on 24-well culture plates at 7×10^4 cells/well on glass coverslips (ø 13 mm) for immunofluorescence analysis or on 100 mm culture dishes at 2.5×10^6 cells/dish for immunoprecipitation assays. Immediately before transfection, the medium was replaced by antibiotic-free growth medium (DMEM supplemented with 10% FBS, 2 mM GlutaMAX and 15 mM HEPES). Plasmid transfections were performed using Lipofectamine 2000 (Invitrogen) according to the manufacturer's instructions. In the case of 24-well culture plates, cells were transfected with 1 µg of DNA and 1 µL of Lipofectamine in 100 µL (final volume) of Opti-MEM (Gibco). In the case of 10 cm culture dishes, cells were transfected with 10 µg of DNA and 15 µL of Lipofectamine in 1 mL (final volume) of Opti-MEM. Four hours after transfection, the medium was replaced by DMEM Complete medium and cells were incubated at 37ºC and 5% CO_2. Experiments were performed approximately 24 hours after transfection.

3.2.3. Electroporation-based transfection

The electroporation-based transfection was performed using the Neon Transfection System (Invitrogen), according to the manufacturer's instructions. MDA-MB-231 cells in suspension (1×10^6 cells) were transfected with 3 µg of total DNA (1.5 µg of each DNA for double transfections) in 100 µL (final volume) of Resuspension Buffer R provided in the kit. Each transfection mixture was loaded in a 100 µL Neon Tip, which contains a gold-plated electrode and placed into the Neon Tube containing an electrode completely immersed in Electrolytic Buffer E2. Four pulses of 1400 V and 10 ms were applied. Transfected MDA-MB-231 cells were seeded on 24-well culture plates at 1.5×10^5 cells/well on glass coverslips (ø 13 mm) in DMEM Complete medium and experiments were performed 48 hours after.

3.3. Cell transduction

Protocols to produce lentiviral particles from pLenti6/V5-DEST Gateway or pLKO.1 vectors and for lentiviral infection to achieve stable overexpression or stable shRNA-mediated target gene knockdown, respectively, were adapted from The RNAi Consortium Library Database of the Broad Institute. These protocols were performed to overexpress mCherry-tagged Arl13b or to silence ACAP1 in MDA-MB-231 cells.

3.3.1. Lentivirus production

HEK293T cells were seeded at 1.5×10^5 cells/mL (6 mL per dish) in antibiotic-free growth medium on 60 mm culture dishes. After 24 hours of incubation at 37ºC and 5% CO_2, cells were transfected with a transfection mixture containing 900 ng of 2nd generation psPAX2 or pCMV-dR8.91 packaging plasmids, 100 ng of envelope plasmid (CMV-VSV-G) and 1 µg of target expression vector, pLKO.1 or pLenti6 vectors, in 30 µL (final volume) of Opti-MEM using FuGENE (Promega). Twenty hours after transfection, the medium was replaced by high serum growth medium (DMEM Complete supplemented with 30% FBS) and cells were incubated at 37ºC and 5% CO_2. The medium containing lentiviruses was harvested 40 and 64 hours post-transfection, and stored in aliquots at -80ºC until use. The DNA constructs used are listed and described in Table 3.2.

3.3.2. Lentiviral infection

MDA-MB-231 cells were seeded at 2×10^5 cells/well on 6-well culture plates in antibiotic-free growth medium (2 mL per well) and infected with lentiviruses on the next day. For this, the medium was replaced by 1.4 mL of fresh DMEM medium without antibiotics containing 8 µg/mL polybrene

Table 3.2. DNA plasmids used for stable cell transduction.

DNA	Vector backbone	Resistance
mCherry	pLenti6	Blasticidine
Arl13b-mCherry	pLenti6	Blasticidine
NT* control shRNA	pLKO.1	Puromycin
ACAP1 shRNA #1	pLKO.1	Puromycin
ACAP1 shRNA #2	pLKO.1	Puromycin
ACAP1 shRNA #3	pLKO.1	Puromycin

* NT - non-targeting.

(hexadimethrine bromide, Sigma-Aldrich) and 400 µL of lentiviruses were added to each well. Two wells were left without lentivirus in the case of non-transduced controls. After 24 hours, medium containing 10 µg/mL blasticidine S hydrochloride (Gibco) or 1.5 µg/mL puromycin (Gibco) was added to select for stably transduced cells. Non-transduced cells treated with antibiotic were used as a control of transduction efficiency. Cells were passed to 10 cm culture dishes in selection conditions and incubated at 37ºC and 5% CO_2 for at least 5 days before being assayed. The medium was changed every two days to maintain the blasticidine or puromycin selection. shRNA target sequences used are listed in Table 3.3.

Table 3.3. shRNA target sequences used for ACAP1 silencing.

shRNA	Target sequence (5'-3')
NT* control shRNA	CAACAAGATGAAGAGCACCAA
ACAP1 shRNA #1	TCACGCTAAATACGTGGAGAA
ACAP1 shRNA #2	GCTGATGTCAACTGGGTCAAT
ACAP1 shRNA #3	CTGGTTCACCATTCAGAGCAA

* NT - non-targeting.

3.4. Transwell migration and invasion assays

Migration and invasion were assessed in 8 µm pore size polycarbonate membrane transwells (Corning Costar) not coated or coated with Matrigel (Corning BioCoat), respectively, according to the manufacturer's instructions. Before cell seeding, the bottom of transwells was pre-coated with 10 µg/mL fibronectin (Gibco) and maintained at 4ºC overnight, in the case of migration assays, or pre-hydrated with DMEM serum-free medium for 2 hours, in the case of invasion assays. Fifty thousand cells in 100 µL of DMEM serum-free medium were seeded into the upper chamber of each transwell and DMEM Complete medium was added to the lower chamber of the plate to act as chemoattractant. After 6 or 21 hours (for migration or invasion assays, respectively), the cells remaining in the upper chamber of the transwells were scraped off with a cotton swab, while cells that had migrated/invaded through the membrane were fixed with 4% paraformaldehyde (Alfa Aesar) in PBS for 15 minutes and stained with 0.2% crystal violet in 20% methanol for extra 15 minutes. The excess dye was removed by successive washes with Mili-Q water and the inserts were allowed to dry at room temperature. Images of the cells that migrated/invaded through the membranes were taken with an inverted microscope (ZEISS Axiovert 40 CFL) equipped with a digital camera (AxioCam MRc) and ZEN 2 software (blue edition). The

number of cells that migrated or invaded from at least 10 randomly chosen fields were counted and represented as the % of migration or invasion, respectively, relative to control cells. Each experiment was performed three times independently with duplicate transwells.

3.5. RNA extraction, cDNA production and real-time quantitative PCR

Total RNA was extracted using the RNeasy Mini Kit (QIAGEN), according to the manufacturer's instructions. RNA was quantified with a NanoDrop 2000c (Thermo Scientific). Complementary DNA (cDNA) production was performed in a MyCycler Thermal Cycler System (Bio-Rad). Total RNA (1 µg) was transcribed into cDNA by incubation with 0.8 mM dNTP mix (Thermo Scientific) and 0.25 µg/µL Primer Random $p(dN)_6$ (Roche) at 65ºC for 5 minutes. After cooling the samples on ice, they were incubated with 5× First-Strand Buffer (Invitrogen), 10 mM DTT (Invitrogen) and 2 U/µL RNaseOUT Recombinant Ribonuclease Inhibitor (Invitrogen) at 25ºC for 2 minutes. Finally, 2.5 U/µL SuperScript II Reverse Transcriptase (Invitrogen) were added and samples were incubated at 25ºC for 15 minutes, at 42ºC for 50 minutes and at 70ºC for 15 minutes, sequentially. The cDNAs produced were diluted 1:10 in nuclease-free water.

Real-time quantitative PCR (RT-qPCR) was performed on clear LightCycler 480 Multiwell Plates 96 (Roche) using the FastStart Essential DNA Green Master kit (Roche) in a Real-Time PCR LightCycler 96 System (Roche) according to the manufacturer's instructions. Amplification of the *GAPDH* housekeeping gene was performed as an endogenous control for normalization of the expression level of each gene analyzed. The primers were designed using Primer-BLAST online platform from NCBI (National Center for Biotechnology Information, U.S. National Library of Medicine) and purchased from STAB VIDA. The primer sequences specific for the human genes are listed in Table 3.4. RT-qPCR data was analyzed using the Roche LightCycler 96 software (version 1.1).

Table 3.4. Primer sequences used for RT-qPCR.

Gene	Primer sequence (5'-3')	Orientation
ARL13B	GAATCCAAGGAGAATACCCTG	forward
ARL13B	CCAACACCAATATAGGCTTTC	reverse
ASAP1	TCTATCCCCAAATGTGCAGTC	forward
ASAP1	GTCTTCACTCGCCTCACTTT	reverse
ASAP3	GGTTGGCACAGTAAATGAAGC	forward
ASAP3	CATGTAGAGGGAAGGCAAAGG	reverse
ACAP1	TCTCAAGGACTCACCCCGTT	forward
ACAP1	CCAGACGGGTCTCCAATTCT	reverse
GAPDH	CATTTCCTGGTATGACAACGA	forward
GAPDH	GTCTACATGGCAACTGTGAG	reverse

3.6. Immunofluorescence staining and confocal microscopy

MDA-MB-231 (1.5×10^5 cells/well) or HeLa (7×10^4 cells/well) cells were seeded on glass coverslips (ø 13 mm) in 24-well culture plates and transfected as described in sections 3.2.3. or 3.2.2, respectively. Forty-eight or 24 hours after transfection, cells were fixed with 4% paraformaldehyde (Alfa Aesar) in PBS for 15 minutes at room temperature. After washing three times with PBS, cells were blocked and permeabilized with 0.5% BSA and 0.1% saponin in PBS (blocking/permeabilization solution) for 1 hour at room temperature. Mouse monoclonal anti-FLAG M2-Cy3 antibody (Sigma-

Aldrich) at 10 µg/ml was added in the same solution for 1 hour at room temperature in a humidified chamber. Alexa Fluor 568-conjugated phalloidin (Invitrogen) at 1 U/mL was used to label filamentous (F)-actin. After incubation, coverslips were washed three times with blocking/permeabilization solution and incubated with 1 µg/mL DAPI in PBS for 5 minutes. Finally, coverslips were mounted in mounting medium containing 10% Mowiol 4-88 (Sigma-Aldrich) in 100 mM Tris-HCl (pH 8.5) and 25% glycerol. Images were analyzed in a ZEISS LSM 710 confocal laser scanning microscope with a Plan-Apochromat 63×/1.4 NA oil-immersion objective and ZEN 2010B software. Images were processed with ImageJ software (version 1.52e).

3.7. Protein extraction

Overexpressing Arl13b-mCherry or mCherry MDA-MB-231 cells transfected with FLAG-tagged Arf GAPs were washed with PBS to remove the remaining medium and lysed with ice-cold lysis buffer (50 mM Tris-HCl pH 7.5, 1 mM EDTA, 1 mM EGTA, 150 mM NaCl, 2 mM $MgCl_2$, 1 mM DTT and 0.1% Triton X-100) for total protein extraction. Immediately before use, 1× cOmplete EDTA-free protease inhibitor cocktail (Roche) and 1 µM sodium orthovanadate (Sigma-Aldrich) phosphatase inhibitor were added to the lysis buffer. Cells were resuspended in the lysis buffer and incubated on ice for 30 minutes. After centrifugation at 18,900 × *g* for 30 minutes at 4ºC, supernatants were collected. Protein concentration was determined using the DC Protein Assay kit (Bio-Rad) according to the manufacturer's instructions and the absorbance was read at 750 nm on a NanoPhotometer (Implen).

3.8. Immunoprecipitation

To immunoprecipitate FLAG-tagged Arf GAPs, 850 µg of total protein extracts were pre-cleared with Protein G Sepharose 4 Fast Flow beads (GE Healthcare) for 1 hour at 4ºC with rotation. Before the incubation with the antibody, 0.5 mM GTPγS (Sigma-Aldrich) or 5 mM GDP (Sigma-Aldrich) were added to the pre-cleared lysates for 15 minutes at room temperature with agitation. Immunoprecipitation was performed using 1 µg of mouse monoclonal anti-FLAG M2 antibody (Sigma-Aldrich) for 16 hours at 4ºC under constant mixing. Protein G Sepharose beads were then added and samples were maintained under constant mixing for 4 hours at 4ºC. Samples were centrifuged at 18,900 × *g* for 5 minutes at 4ºC and the supernatants were discarded. Recovered beads were washed once with lysis buffer with high salt concentration (500 mM NaCl) and three times with lysis buffer. Finally, samples were resuspended in 2× Laemmli Sample Buffer (20 mM sodium phosphate, 2% SDS, 0.001% bromophenol blue, 0.2 M DTT and 2% glycerol) with 10% β-mercaptoethanol (loading buffer). After boiling at 95ºC for 5 minutes, samples were centrifuged at 18,900 × *g* for 5 minutes and the supernatants containing immunoprecipitated proteins were collected and maintained at -80ºC until further analysis.

3.9. SDS-polyacrylamide gel electrophoresis

Sodium dodecyl sulfate (SDS)-polyacrylamide gels, composed of 8 or 10% polyacrylamide resolving gel (pH 8.8) and 5% polyacrylamide stacking gel (pH 6.8), were prepared according to a well-established standard protocol (Sambrook and Russell, 2006) in a Mini Vertical Electrophoresis System (GE Healthcare). After gel immersion in running buffer (25 mM Tris base, 192 mM glycine and 0.1% SDS), the samples diluted in 2× loading buffer 1:1 were loaded on the gel along with 8 µL of Precision Plus Protein All Blue Standards (Bio-Rad). Electrophoresis was performed at 20 mA per running gel for 1 to 2 hours, depending on proteins' molecular weight.

3.10. Immunoblot analysis

Immunoprecipitated samples separated on 10% SDS-polyacrylamide gels were transferred onto nitrocellulose blotting membranes (0.45 µm pore; GE Healthcare) in transfer buffer (25 mM Tris base,

192 mM glycine, 0.25% SDS and 20% ethanol) for 75 minutes at 100 V and processed for immunoblotting. Membranes were then blocked using blocking buffer (5% non-fat dried milk, 0.1% Tween 20 in PBS) for 1 hour at room temperature. The antibodies were incubated in the same buffer. Goat polyclonal anti-mCherry antibody (SICGEN) diluted 1:1000 was used as the primary antibody in a humidified chamber for 1 hour at room temperature. Membranes were then washed three times for 5 minutes with 0.1% Tween 20 in PBS and incubated with anti-goat HRP-conjugated secondary antibody (Jackson ImmunoResearch) diluted 1:5000 for 1 hour at room temperature under continuous agitation. Finally, membranes were washed three times for 5 minutes with 0.1% Tween 20 in PBS and the antibodies detected using Amersham ECL Select reagents (GE Healthcare), according to the manufacturer's instructions. Chemiluminescence was detected using a ChemiDoc Touch Imaging System (Bio-Rad). The same blotting membranes where then incubated with mouse monoclonal antibody anti-FLAG M2 (Sigma-Aldrich) at 1 µg/mL and subsequently with anti-mouse HRP-conjugated secondary antibody (GE Healthcare) diluted 1:5000 to confirm immunoprecipitated FLAG-tagged proteins. Band intensities were quantified using ImageJ software (version 1.52e).

3.11. Protein expression and purification

Expression and purification of Arf GAPs was carried out by Lígia Nobre, Andreia Ferreira, Sofia Silva, Sandra Monteiro, Cátia Peres and Khrystyna Kucheryava with the coordination of Ana Barbas from Bayer Healthcare Satellite Laboratory, Animal Cell Technology Unit, Health & Pharma Division, iBET (Instituto de Biologia Experimental e Tecnológica). Arl13b production in bacterial expression system and subsequent purification were performed by Diogo Athayde under the supervision of Margarida Archer from Membrane Protein Crystallography Laboratory, Macromolecular Crystallography Unit, ITQB NOVA (Instituto de Tecnologia Química e Biológica da Universidade NOVA de Lisboa). Arl13b production in mammalian expression system and subsequent purification were performed by Andreia Ferreira from our group. The work also had the contribution of Tiago Bandeiras from Merck Healthcare Lab, Structural Biology for Drug Discovery Unit, Health & Pharma Division, iBET. Purified Arf6 was purchased from tebu-bio.

3.11.1. Recombinant Arf GAPs expression and purification

After selecting the optimal expression conditions through small-scale expression tests, Arf GAPs production was performed in 200-400 mL HEK293-E6 cell cultures transfected with 1 mg/L of each DNA plasmid (Table 3.1). Five days after transfection, cells were harvested and resuspended in lysis buffer (50 mM Tris-HCl pH 7.4, 150 mM NaCl, 1 mM EDTA and 1% Triton X-100). Lysates were then loaded on an anti-FLAG M2 Affinity Gel (Sigma-Aldrich), pre-equilibrated in equilibration buffer (50 mM Tris-HCl pH 7.5 and 150 mM NaCl). Proteins were eluted with FLAG peptide (Sigma-Aldrich) at 0.2 mg/mL and then concentrated with 30 kDa MWCO Vivaspins (Sartorius). Additional size exclusion chromatography was performed using a Superdex 200 Increase 10/300 GL column (GE Healthcare) with a buffer containing 100 mM Tris-HCl pH 7.5, 100 mM NaCl and 1.5 mM $MgCl_2$. Arf GAPs purity was assessed by SDS-PAGE and Western Blot and protein concentration was determined by Bradford method, using the Pierce Coomassie Plus Assay Reagent (Thermo Scientific), and relative quantification comparing with standard BSA band signal in SDS-polyacrylamide gel using ImageJ software (version 1.8.0_66). Finally, proteins were snap-frozen in liquid nitrogen and stored in small aliquots at -80ºC.

3.11.2. Recombinant Arl13b expression and purification

GST-tagged Arl13b truncated form ($Arl13b^{1-225}$) was cloned in pGEX-4T-3 vector. In order to optimize recombinant expression, several attempts were carried out altering the *E. coli* strains, growth medium, IPTG concentration, induction time and induction temperature. In subsequent medium-scale

cultures, recombinant proteins were expressed in BL21(DE3) competent *E. coli* in 500 mL LB medium cultures (at 37ºC, with 3 hours of induction with 0.5 mM IPTG and under constant agitation). Cell lysis was performed using a French Press at 10,000 Psi three times (Thermo IEC) with the following lysis buffer: 100 mM Tris-HCl pH 7.5, 100 mM NaCl, 20 mM $MgSO_4$, 20% glycerol and 1% Triton X-100. After spinning at 7,000 × *g* for 20 minutes at 4ºC to remove cell debris, supernatants were collected. Purification was performed with GSTrap FF affinity column (CV=1 mL, GE Healthcare) and eluted in lysis buffer with 20 mM reduced L-Glutathione (Sigma-Aldrich). Proteins were concentrated using Amicon Stirred Cell 50 mL (Merck) with 30 kDa MWCO Ultrafiltration Discs (Merck) down to 500 µL. Additional size exclusion chromatography was performed in a HiLoad 16/600 Superdex 200 pg column (GE Healthcare) using a buffer without detergent (100 mM Tris-HCl pH 7.5, 100 mM NaCl and 1.5 mM $MgCl_2$). In each step of the purification, samples were collected to evaluate protein purity by SDS-PAGE and Western Blot. Protein concentration was measured by UV absorbance using NanoDrop 2000c spectrophotometer (Thermo Scientific) and relative quantification comparing with standard BSA band signal in SDS-polyacrylamide gel using ImageJ software (version 1.8.0_66). Proteins were snap-frozen and stored in small aliquots at -80ºC.

Full-length FLAG-tagged Arl13b was cloned in pcDNA3.1(+) vector and expressed in HEK293-E6 cells. Purification was performed following the protocol described in section 3.11.1, except that all the buffers used contained 5% glycerol to enhance protein stability.

3.12. Coomassie gel staining

One µg of each purified protein was resuspended in 5 µL of 2× loading buffer, boiled at 95ºC for 5 minutes and analyzed on an 8% SDS-polyacrylamide gel by SDS-PAGE. The gel was stained with a staining solution (0.12% Coomassie Brilliant Blue G-250, 10% orthophosphoric acid, 10% ammonium sulfate and 20% anhydrous methanol) for 15 minutes at room temperature. Two de-staining solutions were used to wash the gel, the first one with 10% acetic acid and 50% methanol and the second with 7% acetic acid and 10% methanol, until the background of the gel was clear. Staining and destaining procedures were performed under constant agitation.

3.13. *In vitro* GTPase activity assay

In vitro GTPase activity assays were performed using CytoPhos Phosphate Assay Biochem Kit (Cytoskeleton, Inc.), according to the manufacturer's instructions. The reactions were conducted on clear flat 96-well tissue culture plates (Sigma-Aldrich). A standard curve was performed using increasing concentrations of a phosphate standard solution. Purified Arf6 or Arl13b (4.5 µg) were pre-loaded with GTP (200 µM) at room temperature for 40 minutes in reaction buffer (50 mM Tris-HCl pH 7.5, 50 mM NaCl, 20 mM EDTA and 5 mM $MgCl_2$), under continuous agitation. Each reaction contained 4.5 µg of GTP-loaded Arf6 or Arl13b and 8 µg of Arf GAP to a final reaction volume of 50 µL. The plates were incubated at 37ºC for 20 minutes and the phosphate generated by hydrolysis of GTP was measured by the addition of 120 µL of CytoPhos reagent for 10 minutes at room temperature. The absorbance was read at 650 nm in a microplate absorbance reader SpectraMax i3X (Molecular Devices) and the data obtained using the SoftMax Pro Software (version 7.0).

3.14. Statistical analysis

Data are presented as mean ± SD (standard deviation) for GTPase activity assays, migration and invasion assays and RT-qPCR. One-way ANOVA with Dunnett's multiple comparison test was used to analyze the migration and invasion assays data sets relative to non-targeting (NT) control shRNA. One-way ANOVA with Tukey's multiple comparison test was used to analyze the RT-qPCR data. Statistical analysis was performed using GraphPad Prism software (version 6.01).

4. Results

4.1. ASAP1, ASAP3 and ACAP1 but not GIT1 interact with Arl13b in a GTP-dependent manner

Arf GAPs function by directly binding to the active GTP-bound conformation of Arf proteins (Cherfils and Zeghouf, 2013). Therefore, to assess if Arl13b interacts with Arf GAPs that could mediate its inactivation, I performed co-immunoprecipitation assays with total protein extracts obtained from MDA-MB-231 breast cancer cells. For that, MDA-MB-231 cells stably overexpressing Arl13b-mCherry, or mCherry as a negative control, were transfected with plasmids encoding the FLAG-tagged Arf GAPs ASAP1, ASAP3, ACAP1 or GIT1. Cell lysates were incubated with either a non-hydrolysable analog of GTP (GTPγS) or excess GDP. The interaction between Arl13b and Arf GAPs was analyzed by immunoblotting using an anti-mCherry antibody. Noteworthy, despite having a predicted size of 48 kDa, Arl13b is normally detected as a 60 kDa protein in SDS-PAGE. Since the protein used had an mCherry tag with 28.8 kDa, the band corresponding to Arl13b-mCherry is detected as a 90 kDa protein. This observation is in agreement with previous reports of aberrant migration of Arl13b in SDS-PAGE (Caspary *et al.*, 2007; Ivanova *et al.*, 2017). The immunoprecipitation of the Arf GAPs was confirmed by subsequently incubating the same blotting membranes with an anti-FLAG antibody.

I observed that Arl13b co-immunoprecipitates with ASAP1 (Figure 4.1A), ASAP3 (Figure 4.1C) and ACAP1 (Figure 4.1E), since a band corresponding to Arl13b-mCherry was detected specifically in the protein extracts obtained from MDA-MB-231 cells overexpressing Arl13b-mCherry. After quantification of bands intensity corresponding to Arl13b and the Arf GAPs, the ratios between the values obtained were calculated in order to normalize the results to the amount of immunoprecipitated proteins. For ASAP1 (Figure 4.1B), ASAP3 (Figure 4.1D) and ACAP1 (Figure 4.1F), the co-immunoprecipitation was enhanced in the presence of GTP-bound Arl13b, compared to GDP-loaded Arl13b. Thus, these results suggest that ASAP1, ASAP3 and ACAP1 could serve as Arf GAPs for Arl13b, promoting its inactive state, since the interaction occurs in a GTP-dependent manner. In contrast, I did not observe any specific interaction between Arl13b and GIT1, since an unspecific band was also detected in control mCherry protein extracts (Figure 4.1G).

Finally, to verify if the presence of GAP activity could influence the binding to Arl13b, I tested the interaction between Arl13b and a mutant form of ASAP1. [R497K]ASAP1 is an ASAP1 mutant lacking GAP activity due to an Arg→Lys mutation at a conserved position in the Arf GAP domain (Luo *et al.*, 2007). Similar to the wildtype form, I observed that [R497K]ASAP1 co-immunoprecipitates with Arl13b (Supplementary Figure 1A) and that the interaction is enhanced in the presence of GTPγS (Supplementary Figure 1B). Thus, this result shows that ASAP1 GAP activity in not required for the GTP-dependent interaction between ASAP1 and Arl13b.

4.2. ASAP1, ASAP3 and ACAP1 co-localize with F-actin and Arl13b

Previous results from our group have shown that Arl13b localizes to actin-rich regions at the plasma membrane and actin stress fibers in HeLa cells (Barral *et al.*, 2012), to lamellipodia, filopodia and CDRs in mouse fibroblasts (Casalou *et al.*, 2014) and to invadopodia in breast cancer cells (Casalou, Faustino *et al.*, unpublished results). Since I verified that Arl13b associates with ASAP1, ASAP3 and ACAP1, intracellular co-localization of Arf GAPs with actin and Arl13b was assessed. For this, MDA-MB-231 cells transiently overexpressing FLAG-tagged ASAP1, ASAP3 or ACAP1 were used and immunocytochemistry was performed with an anti-FLAG antibody to visualize the transfected Arf GAPs by confocal microscopy. To visualize F-actin, cells were also stained with phalloidin. Lastly, to assess the localization of Arl13b, MDA-MB-231 cells were transiently co-transfected with a plasmid

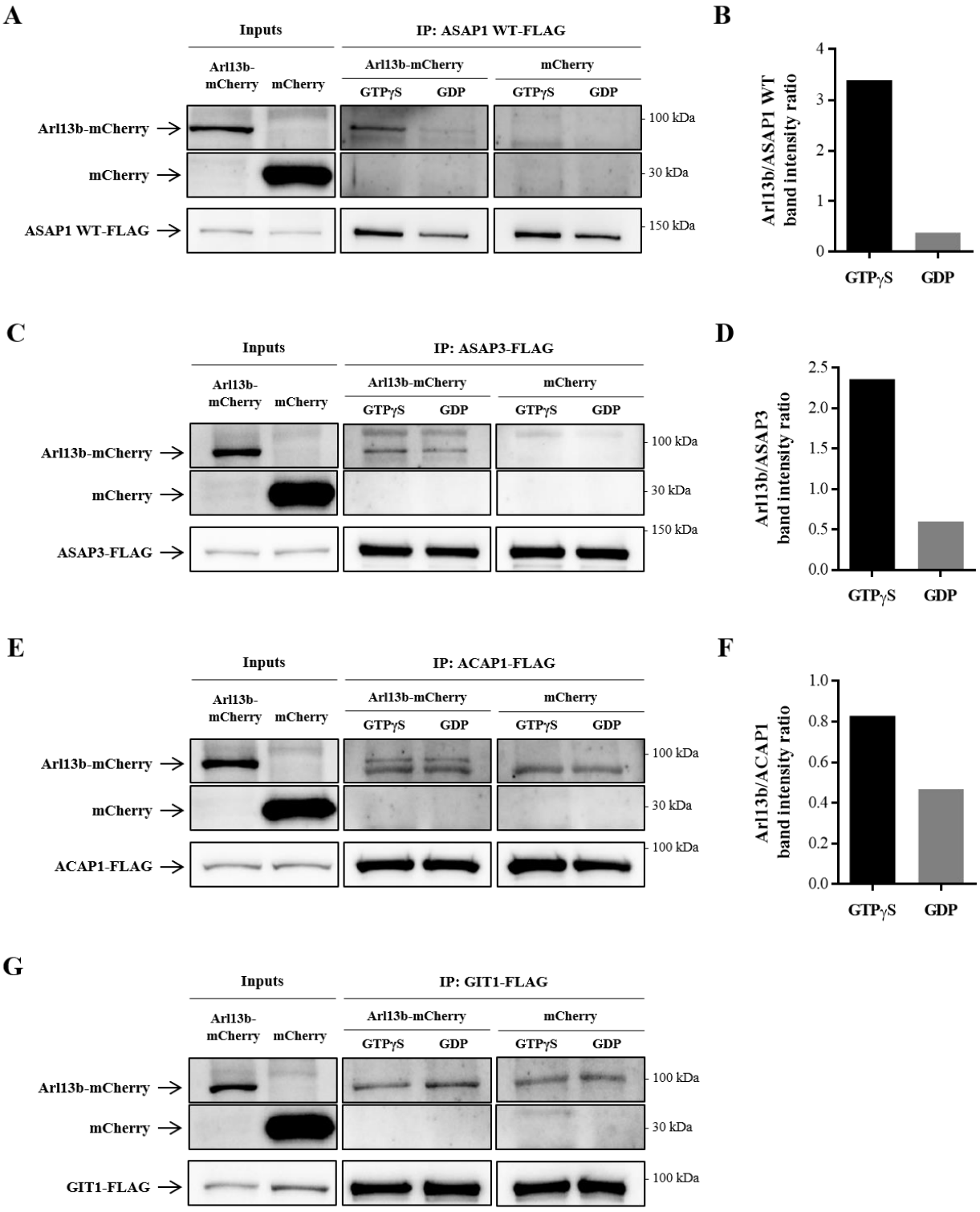

Figure 4.1. Co-immunoprecipitation of ASAP1, ASAP3, ACAP1 or GIT1 with Arl13b in MDA-MB-231 breast cancer cells. MDA-MB-231 cells stably overexpressing Arl13b-mCherry, or mCherry as a negative control, were transiently transfected with plasmids encoding FLAG-tagged Arf GAPs **(A)** ASAP1, **(C)** ASAP3, **(E)** ACAP1 or **(G)** GIT1. Protein extracts were incubated with an anti-FLAG antibody before immunoprecipitation with protein G sepharose beads in the presence of GTPγS or an excess of GDP. The immunoprecipitated products and total cell extracts were separated by SDS-PAGE. Immunoblotting was performed with an anti-mCherry antibody. Arf GAPs immunoprecipitation was confirmed by subsequently incubating the same blotting membranes with an anti-FLAG antibody. **(B, D, F)** Quantification of bands intensity corresponding to Arl13b and the Arf GAPs was performed using Image J. The ratios between the values obtained were calculated and the results normalized to the amount of immunoprecipitated proteins.

encoding GFP-tagged Arl13b. In agreement with previous data described in the literature, I observed that ASAP1, ASAP3 and ACAP1 co-localize with F-actin (Figure 4.2). ASAP1 co-localizes with actin in protrusive structures near the plasma membrane (Figure 4.2A and B) and in structures that resemble invadopodia (Figure 4.2C and D), since they appear as small dot-like clusters with a core of actin localized near the nucleus (Gimona *et al.*, 2008), confirming what was already described (Bharti *et al.*, 2007). ASAP3 (Figure 4.2E and F) interacts with actin at the plasma membrane and in structures near

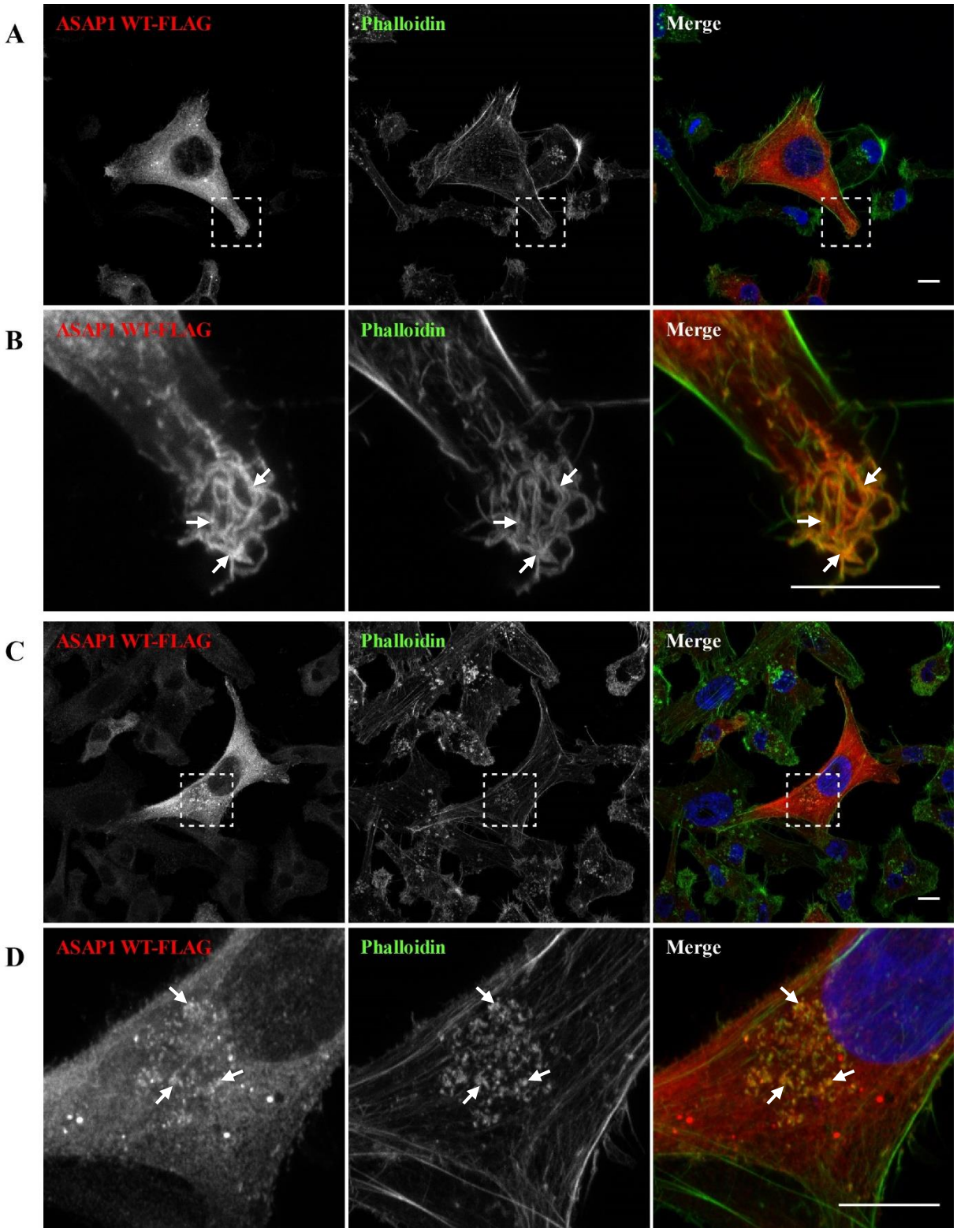

Continues in the next page.

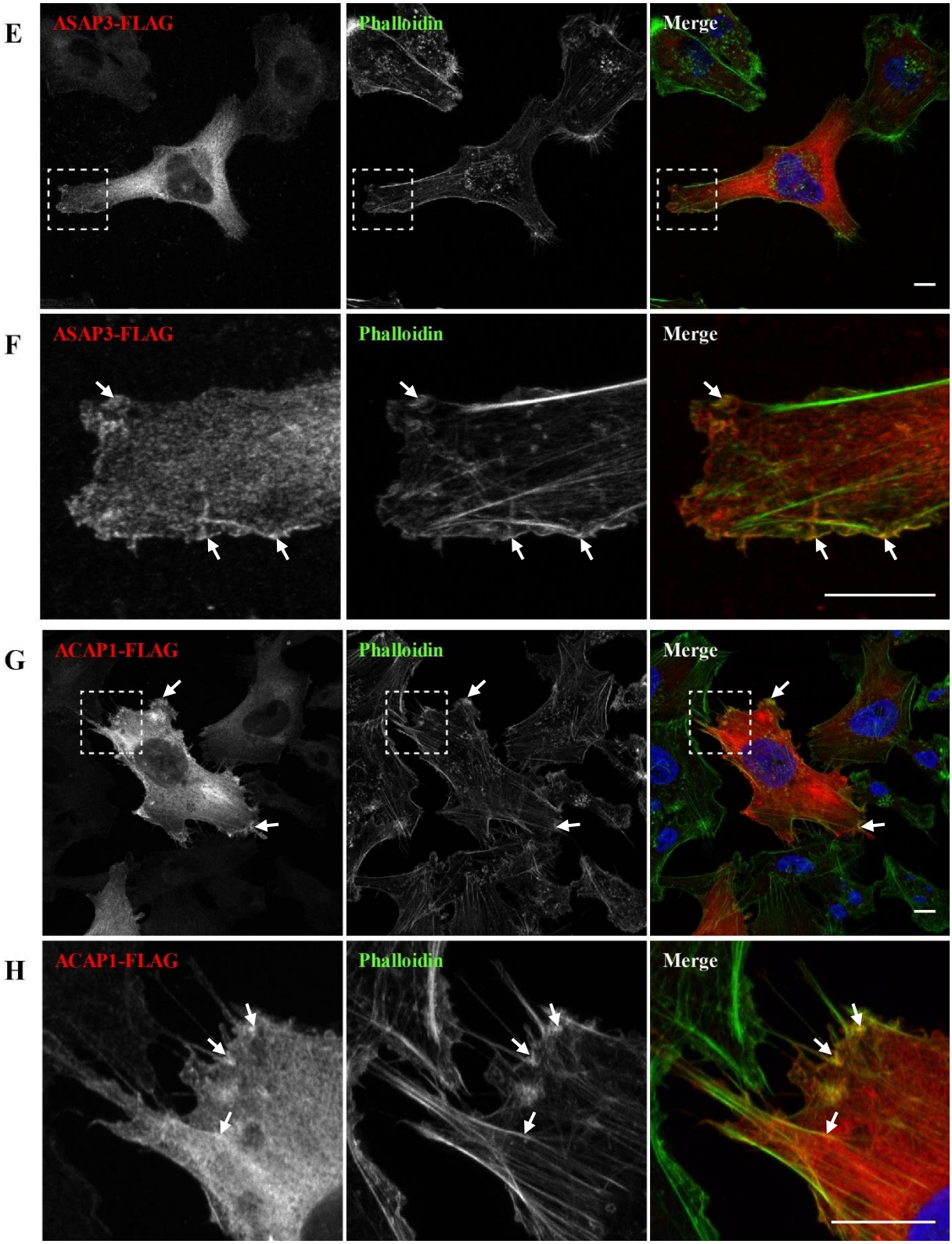

Figure 4.2. Co-localization of ASAP1, ASAP3 and ACAP1 with F-actin in MDA-MB-231 breast cancer cells. MDA-MB-231 cells transiently overexpressing FLAG-tagged Arf GAPs were fixed and stained with anti-FLAG Cy3 and Alexa Fluor 568-conjugated phalloidin to label F-actin. DAPI was used to stain nuclei. **(A, B)** ASAP1 co-localizes with actin in protrusive structures near the plasma membrane **(C, D)** and in structures that resemble invadopodia. **(E, F)** ASAP3 interacts with actin at the plasma membrane and in structures near the cell periphery like actin stress fibers. **(G, H)** ACAP1 associates with actin at stress fibers near the plasma membrane. **(B)**, **(D)**, **(F)** and **(H)** correspond to zoomed images of the areas indicated by the boxes in **(A)**, **(C)**, **(E)** and **(G)**, respectively. All images correspond to representative Z stacks obtained by confocal microscopy. Scale bars: 10 µm.

the cell periphery that are consistent with actin stress fibers, also in agreement with previous results (Ha *et al.*, 2008). ACAP1 (Figure 4.2G and H) associates with actin at stress fibers, near the plasma membrane. Furthermore, I observed that ASAP1, ASAP3 and ACAP1 co-localize with Arl13b namely in structures localized at the plasma membrane (Figure 4.3). It is possible to observe the overlap of Arl13b with ASAP1 in both PRs (Figure 4.3A and B) and in structures resembling invadopodia (Figure 4.3A), with ASAP3 in both CDRs and PRs (Figure 4.3C and D) and with ACAP1 in both filopodia and

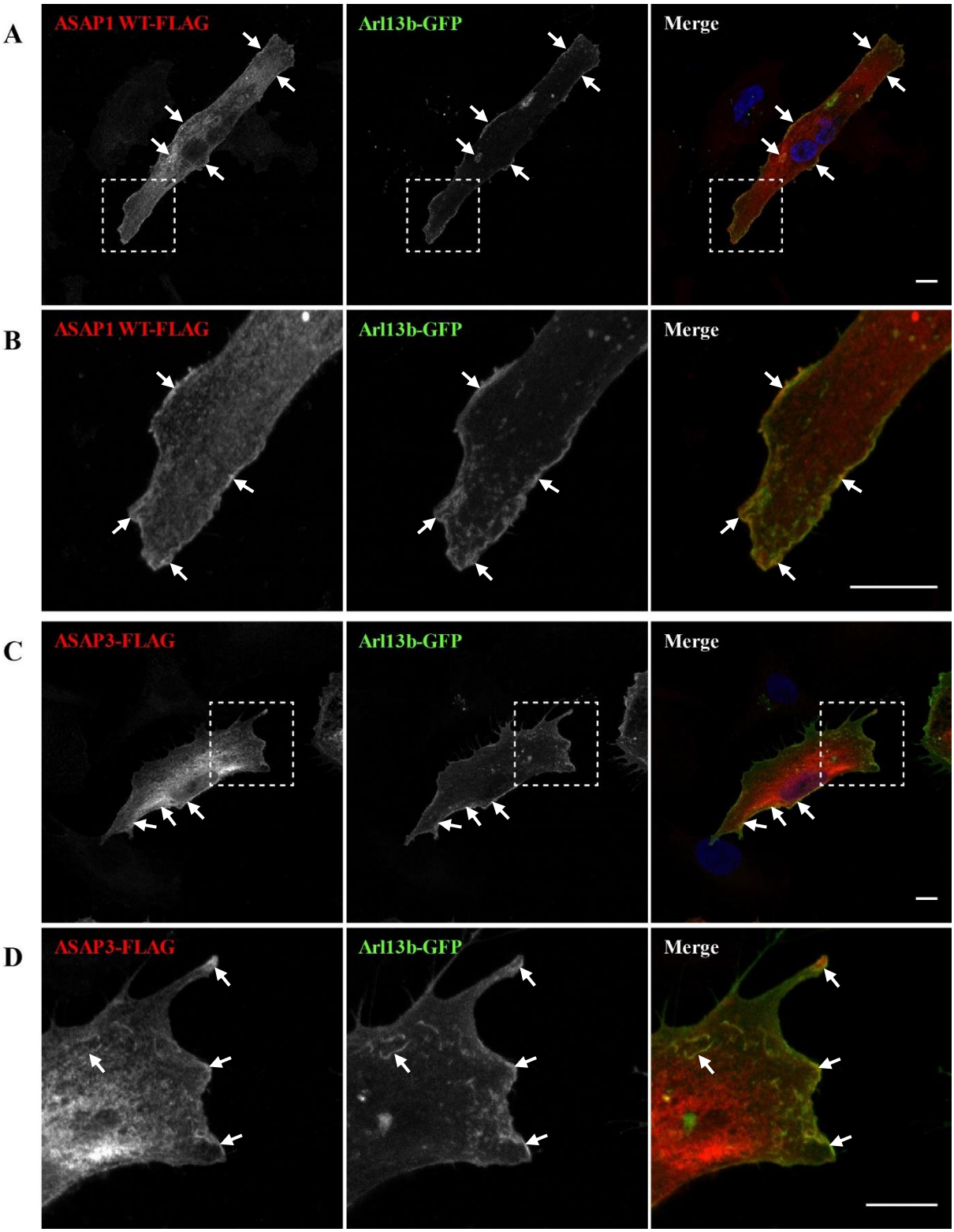

Continues in the next page.

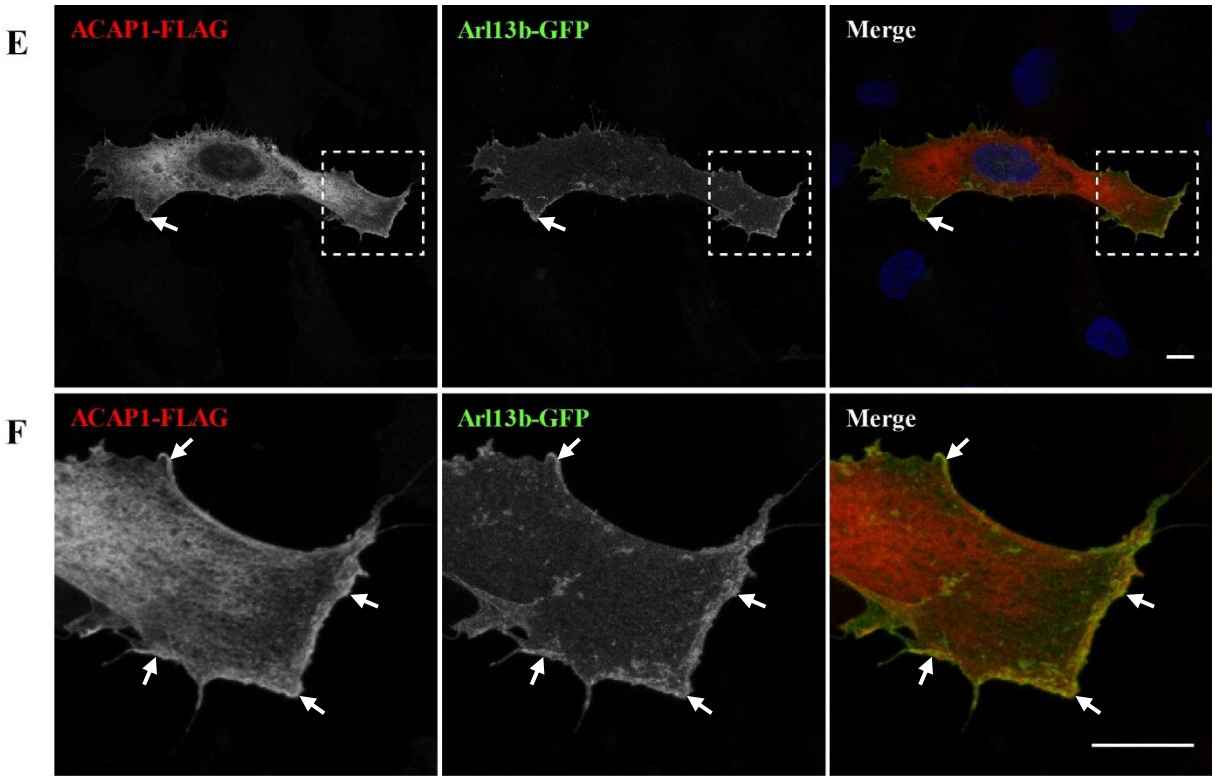

Figure 4.3. Co-localization of ASAP1, ASAP3 and ACAP1 with Arl13b in MDA-MB-231 breast cancer cells. MDA-MB-231 cells transiently overexpressing FLAG-tagged Arf GAPs and GFP-tagged Arl13b were fixed and stained with anti-FLAG Cy3. DAPI was used to stain nuclei. **(A, B)** ASAP1 co-localizes with Arl13b in PRs **(A)** and in structures resembling invadopodia, **(C, D)** ASAP3 in CDRs and PRs **(E, F)** and ACAP1 in filopodia and PRs. **(B)**, **(D)** and **(F)** correspond to zoomed images of the areas indicated by the boxes in **(A)**, **(C)** and **(E)**, respectively. All images correspond to representative Z stacks obtained by confocal microscopy. Scale bars: 10 µm.

PRs (Figure 4.3F and E). All these actin remodel structures are associated with cell migration or invasion, indicating that Arf GAPs and Arl13b could act together in the regulation of these processes.

To verify if GAP activity deficient ASAP1 mutant was localized differently than the wildtype, the co-localization with actin and Arl13b was assessed. Like the wildtype, the mutant form interacts with actin in protrusive structures near the plasma membrane, in this case, in lamellipodia (Supplementary Figure 2A and B), as well as in structures resembling invadopodia (Supplementary Figure 2C and D). The interaction of ASAP1[R497K] mutant with Arl13b also occurs at the plasma membrane and in PRs (Supplementary Figure 3). Thus, this result indicates that ASAP1 GAP activity is not required for the subcellular co-localization between Arl13b and ASAP1.

Lastly, to further explore the co-immunoprecipitation data described above, GIT1 intracellular localization was assessed in HeLa cells. I verified that GIT1 is localized in punctate cytoplasmic structures (Supplementary Figure 4), as described before (Manabe *et al.*, 2002). Furthermore, GIT1 did not co-localize with F-actin (Supplementary Figure 4A) and no detectable co-localization between Arl13b and GIT1 was observed (Supplementary Figure 4B). These results support the co-immunoprecipitation data and both indicate that Arl13b is not associated with GIT1. Hence, GIT1 was excluded from the subsequent experiments.

4.3. ASAP1 and ASAP3 do not promote Arl13b GTPase activity

The identification of ASAP1, ASAP3 and ACAP1 as Arl13b interactors and their co-localization in actin-rich structures raised the possibility that these proteins could function as Arl13b GAPs. Thus, I next aimed to assess if ASAP1, ASAP3 and/or ACAP1 could induce the GTP hydrolysis activity of Arl13b, using an *in vitro* GTPase activity assay and recombinant purified proteins. Recombinant FLAG-

tagged Arf GAPs and full-length Arl13b were expressed in HEK293-E6 mammalian cells, while GST-tagged Arl13b truncated form, Arl13b$^{1-225}$, was expressed in *E. coli*. The purification was performed using appropriate affinity columns and protein purity was evaluated by SDS-PAGE (Supplementary Figure 5). As can be observed, all the proteins were successfully produced and purified, although in some of them was detected protein degradation and/or the presence of contaminant proteins that together overestimated the protein concentration.

To measure Arl13b GTPase activity in the absence and presence of ASAP1, ASAP3 or ACAP1, I used an *in vitro* assay that detects Pi through an absorbance-based detection method. Therefore, before starting the reactions, I had to verify that all samples and buffers used were completely free of phosphate to avoid high background levels. Upon GTPase reaction completion, CytoPhos reagent was added to detect the generated Pi colorimetrically, by measuring absorbance the reaction at 650 nm. Concerning the reaction buffer used, $MgCl_2$ was included due to the essential role of Mg^{2+} ion in the high-affinity binding of the guanine nucleotide to GTPases (Vetter and Wittinghofer, 2001). Furthermore, it has been described that the divalent metal ion chelator EDTA mimics the role of GEFs, chemically inducing the nucleotide exchange by chelating Mg^{2+} at the GTPase active site (Mondal *et al.*, 2015). Thus, a previously optimized reaction buffer with an effective low Mg^{2+} concentration and EDTA was used to allow the continuous progression of intrinsic and GAP-stimulated GTPase activities without the requirement for GEFs (Mondal *et al.*, 2015).

In order to test the kit, I performed calibration curves using a phosphate standard solution. Then, the average curve obtained (Supplementary Figure 6) was used to calculate the GTP hydrolysis rate through the absorbance value read in each reaction.

As a positive control, Arf6 and ACAP1 were used (Supplementary Figure 7). The reaction buffer and the purified proteins did not show high backgrounds levels, indicating that all buffers and samples used were free of phosphate. The slight increment observed in the reaction buffer and in the purified

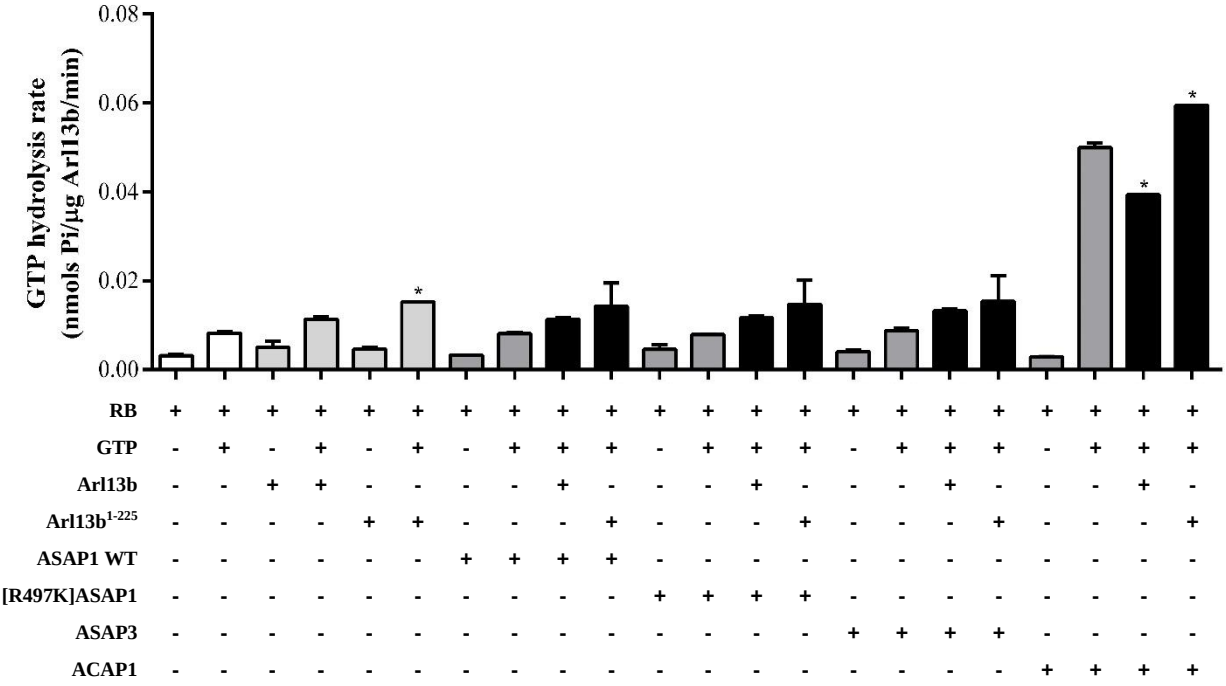

Figure 4.4. Measurement of intrinsic and GAP-stimulated Arl13b GTPase activity *in vitro*. Each reaction (in black) contained 4.5 µg of GTP-loaded Arl13b and 8 µg of the corresponding Arf GAP. Control reactions (in white or gray) contained only reaction buffer (RB), purified Arl13b in RB or purified Arf GAPs in RB in the same amount used in reactions, with or without GTP. All reactions were incubated at 37ºC for 20 minutes followed by the addition of CytoPhos reagent for 10 minutes at room temperature. The absorbance was read at 650 nm and the values were converted to GTP hydrolysis rate in nmols Pi/µg Arl13b/min. Results are displayed as mean ± SD of at least two independent experiments except for the cases marked with the asterisks (*), in which only one experiment was performed.

Arf6 in the presence of GTP is assumed to be a consequence of GTP spontaneous hydrolysis, with some possible but reduced contribution of the intrinsic GTPase activity of Arf6 in the respective reaction. However, when GTP was added to ACAP1 alone, GTP hydrolysis was significantly enhanced. Therefore, the high level of GTP hydrolysis verified in the reaction containing Arf6, ACAP1 and GTP cannot be due to the result of the specific ACAP1-stimulated GTPase activity of Arf6.

The reactions between Arl13b and ASAP1, ASAP3 or ACAP1 (Figure 4.4) were conducted in the same way as the positive control. None of the purified proteins contained phosphate and a similar increment due to spontaneous GTP hydrolysis was observed when GTP was added. However, in the case of Arl13b, namely Arl13b$^{1-225}$, the increment was slightly higher than the one observed in the spontaneous GTP hydrolysis control, which is expected to be a result of Arl13b intrinsic GTPase activity. The results obtained for ASAP1 and ASAP3 indicate that these Arf GAPs do not induce GTP hydrolysis activity of Arl13b, since no differences were found when the GTP hydrolysis rate of the two forms of Arl13b alone and in the presence of ASAP1 or ASAP3 were compared. Furthermore, if ASAP1 would function as a GAP of Arl13b, a lower GTP hydrolysis rate in the presence of the [R497K]ASAP1 GAP activity deficient mutant should be observed. Concerning ACAP1, since the same purified protein tested in the positive control was used here, an enhancement of GTP hydrolysis in several orders of magnitude was observed when GTP was added to ACAP1 alone. Therefore, the high level of GTP hydrolysis verified in the reaction containing Arl13b, ACAP1 and GTP cannot be due to the action of ACAP1 GAP activity on Arl13b. Overall, these results indicate that ASAP1 and ASAP3 do not function as Arl13b GAPs, whereas nothing can be concluded about ACAP1.

4.4. ACAP1 silencing enhances breast cancer cell migration and invasion

Our group has previously shown that Arl13b silencing in mouse fibroblasts leads to a decrease in the migratory capacity of these cells in wound healing and transwell migration assays (Casalou *et al.*, 2014). Moreover, in MCF7 and MDA-MB-231 breast cancer cells, Arl13b silencing also leads to impaired migration and invasion (Casalou, Faustino *et al.*, unpublished results). The role of ASAP1 and ASAP3 on cancer cell migration and invasion have also been described. The silencing of ASAP3 impairs cancer cell migration and invasion (Fang *et al.*, 2006; Ha *et al.*, 2008; Fan *et al.*, 2014), while the effects of ASAP1 silencing in these processes are contradictory (Furman *et al.*, 2002; Bharti *et al.*, 2007; Ha *et al.*, 2008; Lin *et al.*, 2008). For ACAP1, there are no studies describing a direct effect of this protein on migratory or invasion capacities of cancer cells. Therefore, I evaluated the effect of ACAP1 silencing by shRNA on migration and invasion of highly invasive breast cancer cells. For that, I performed transwell migration and invasion assays with MDA-MB-231 cells upon silencing of the corresponding gene.

I observed that ACAP1 silencing enhances breast cancer cell migration (Figure 4.5A and B) and invasion (Figure 4.5C and D), compared to cells transfected with the non-targeting (NT) shRNA control. These results support a direct involvement of ACAP1 in breast cancer progression, here described for the first time.

Interestingly, the silencing of ACAP1 also induced morphological changes on MDA-MB-231 cells (Supplementary Figure 8). The control MDA-MB-231 cells show, as expected, a typical elongated and stellate morphology (Cavo *et al.*, 2018). ACAP1 silenced cells appear to be rounder, in the case of cells silenced with shRNA #1, or more stretched, with more prominent protrusions and with larger focal sites, in the case of cells treated with shRNAs #2 and #3.

Silencing of ACAP1 in MDA-MB-231 cells was confirmed by analysis of mRNA levels through RT-qPCR. I observed an average of 61,37% of silencing for shRNA #1, 61,33% for shRNA #2 and 50,16% for shRNA #3 (Supplementary Figure 9).

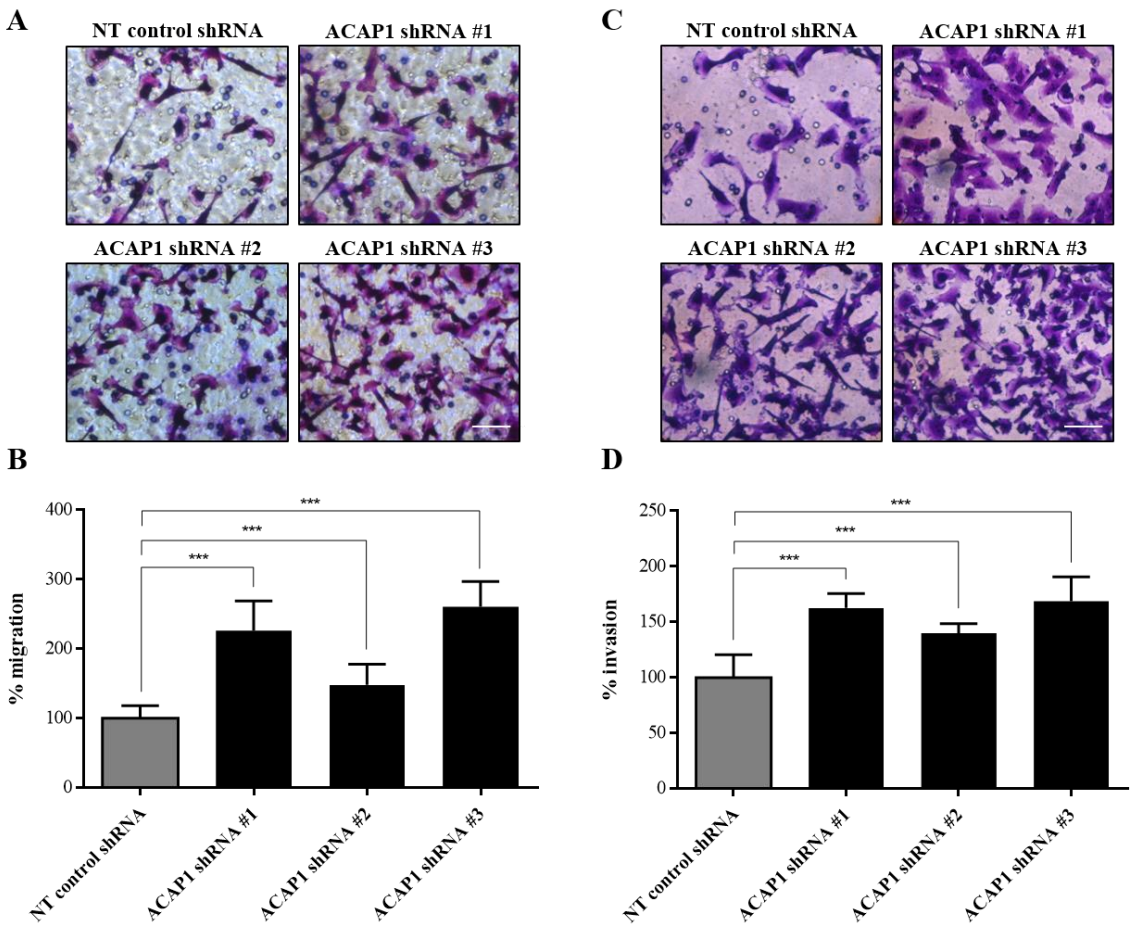

Figure 4.5. Cell migration and invasion of MDA-MB-231 breast cancer cells upon ACAP1 silencing. MDA-MB-231 cells treated with non-targeting (NT) control shRNA or shRNA targeting *ACAP1* were seeded into the upper chamber of a transwell **(A, B)** without or **(C, D)** with Matrigel. Medium containing 10% fetal bovine serum used as chemoattractant was added to the lower chamber. After **(A, B)** 6 or **(C, D)** 21 hours, cells that had migrated/invaded through the membrane were fixed and stained. **(A, C)** Representative images are shown. Cells from at least 10 randomly chosen fields were counted. For each condition, the **(B)** % of migration and **(D)** % of invasion were normalized to the control shRNA, in which migration/invasion was considered 100%. Experiments were repeated independently three times with duplicated transwells. Results are represented as mean ± SD of three independent experiments. *** $p \leq 0.0001$ (one-way ANOVA with Dunnett's multiple comparisons test). Scale bars: 100 µm.

4.5. *ARL13B, ASAP1, ASAP3* and *ACAP1* expression is associated with breast cancer invasiveness

Results from our laboratory have shown that Arl13b is upregulated in breast cancer patient-derived frozen tissues, when compared with the adjacent non-tumorigenic tissue, and that this correlates with tumor size and the late stages of invasion in breast cancer (Casalou, Faustino *et al.*, unpublished results). In agreement with these observations, we found that *ARL13B* expression is upregulated in highly invasive MDA-MB-231 breast cancer cells, comparing with poorly invasive MCF7 breast cancer cells and non-tumorigenic MCF10A breast cells (Figure 4.6A). Altogether, these data suggest that Arl13b expression is associated with breast tumor invasiveness and, consequently, breast tumor progression.

To verify if *ASAP1*, *ASAP3* and *ACAP1* expression also correlate with breast cancer invasiveness, I assessed their expression by analyzing mRNA levels through RT-qPCR in the same breast cell lines. Similar to what we observed for *ARL13B, ASAP1* (Figure 4.6B) and *ASAP3* (Figure 4.6C) are upregulated in invasive breast cancer cells, when compared with the expression levels in the non-tumorigenic breast cells. These results confirm the role of ASAP1 and ASAP3 in breast cancer progression, supporting previous studies (Onodera *et al.*, 2005; Mao *et al.*, 2017). Furthermore, I found that *ACAP1* is less expressed in highly invasive breast cancer cells when compared with non-

tumorigenic breast cells (Figure 4.6D). These results not only confirm the direct involvement of ACAP1 in breast cancer progression, but also corroborate the data on the effects of ACAP1 silencing on cancer cell migration and invasion, in which lower levels of ACAP1 lead to an enhancement of these processes.

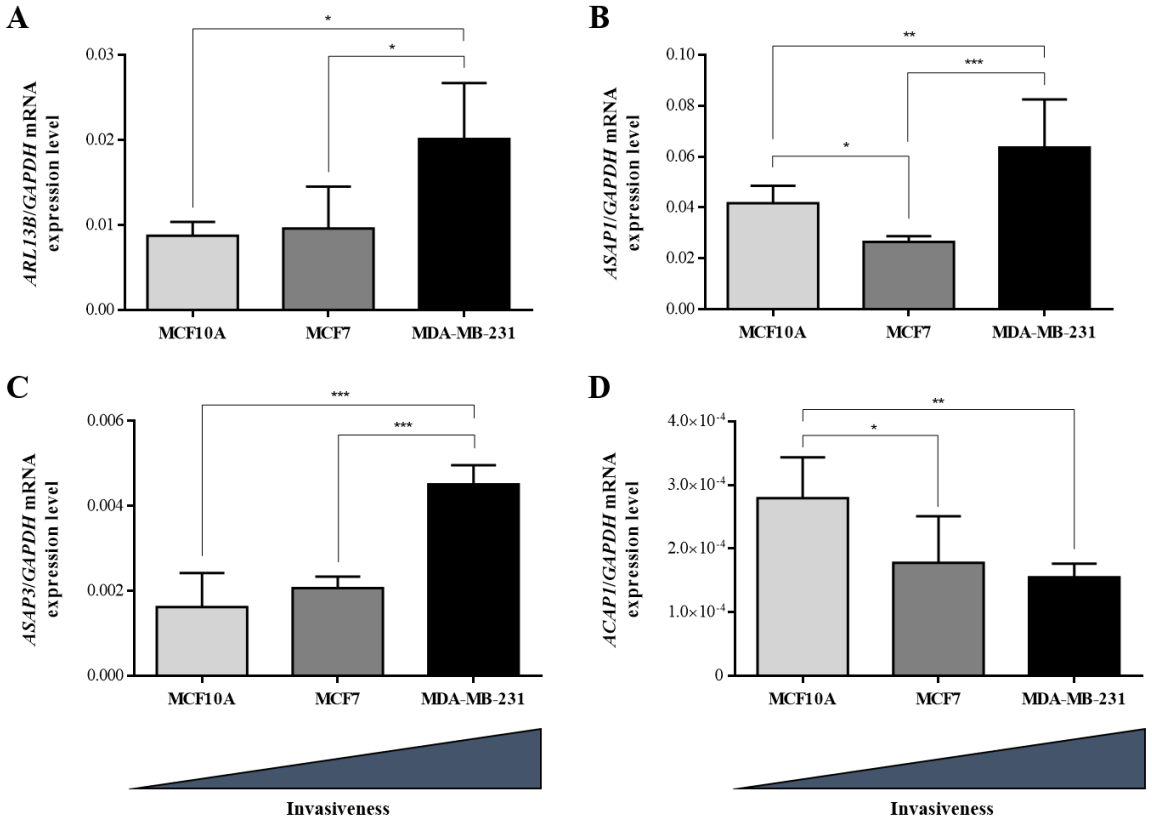

Figure 4.6. Arl13b, ASAP1, ASAP3 and ACAP1 mRNA levels in non-tumorigenic and tumorigenic breast cell lines. Transcript levels were quantified from cDNA obtained from non-tumorigenic MCF10A breast cells, poorly invasive MCF7 and highly invasive MDA-MB-231 breast cancer cells by RT-qPCR. The expression of each gene was normalized to the expression of *GAPDH*, used as a housekeeping gene. Results represent relative ratios between mRNA expression levels of **(A)** *ARL13B*, **(B)** *ASAP1*, **(C)** *ASAP3* or **(D)** *ACAP1* and *GAPDH* and are represented as mean ± SD of three independent experiments. *p≤0.05; **p≤0.01; ***p≤0.0001 (one-way ANOVA with Tukey's multiple comparisons test). **(A)** Courtesy of Cristina Casalou.

5. Discussion and conclusions

Membrane trafficking and actin cytoskeleton remodeling represent key regulators of many processes essential for the metastatic process, such as cell polarity, migration, invasion and growth, and are often disrupted in and by metastatic tumor cells. Therefore, understanding the mechanisms by which membrane traffic proteins and actin cytoskeleton modulators regulate these processes may provide a means for targeting these proteins, delaying or impairing cancer cell migration and invasion and consequently tumor progression.

Previous results from our group indicate that the small GTPase Arl13b plays an important role in breast tumor progression by positively regulating breast cancer cell migration, invasion and metastatic dissemination (Casalou, Faustino *et al.*, unpublished results). Interestingly, it was recently reported that some of these Arl13b functions extend to gastric cancer (Shao *et al.*, 2017) and medulloblastoma (Bay *et al.*, 2018). Accordingly, according to The Human Protein Atlas, Arl13b is widely expressed in most normal human tissues and its expression is enhanced in several tumorigenic tissues. These findings suggest that Arl13b and its activity regulators, GEFs and GAPs, could be targeted to impair tumor

progression, as it has been suggested for other proteins from the Arf family (Ohashi *et al.*, 2012; Dani *et al.*, 2013; Yamauchi *et al.*, 2017), as well as for the corresponding regulators (Vigil *et al.*, 2010). Therefore, I aimed to identify Arf GAPs that could promote the inactive conformation of Arl13b and contribute to unravel the mechanisms by which it regulates cell migration and invasion of cancer cells. As an *in vitro* model, MDA-MB-231 breast cancer cells were used. MDA-MB-231 is an epithelial, highly invasive and poorly differentiated triple-negative breast cancer cell line, characterized by an enrichment for markers associated with EMT, providing a suitable model for metastatic dissemination (Chavez *et al.*, 2010).

I started by assessing the interaction between Arl13b and selected Arf GAPs using total protein extracts obtained from MDA-MB-231 breast cancer cells loaded with either GTPγS or GDP. I observed that Arl13b interacts with ASAP1, ASAP3 and ACAP1 and that the interaction is enhanced when GTP-bound Arl13b is used, compared to GDP-loaded Arl13b. However, no interaction with GIT1 was detected. These results suggest that ASAP1, ASAP3 and ACAP1 but not GIT1 could function as Arl13b GAPs, promoting its inactive conformation, since the interaction occurs in a GTP-dependent manner.

To function as GAPs of Arl13b, ASAP1, ASAP3 and ACAP1 must interact directly, even if temporarily, with this protein. The co-immunoprecipitation assays using cell extracts do not allow to infer if the binding detected is direct or mediated by other proteins. Thus, I carried out *in vitro* pull-down assays with purified FLAG-tagged Arf GAPs and GST-tagged Arl13b$^{1-225}$ in the presence of GTPγS to investigate if the interactions between Arl13b and the Arf GAPs are direct (data not shown). For this, I used three different approaches: immunoprecipitation of FLAG-tagged Arf GAPs using an anti-FLAG resin, immunoprecipitation of FLAG-tagged Arf GAPs using Protein G Sepharose beads and an anti-FLAG antibody or immunoprecipitation of GST-tagged Arl13b$^{1-225}$ using anti-GST beads. In none of the three approaches it was possible to immunoprecipitate the target proteins and, subsequently, it was not possible to conclude if the interactions between Arl13b and the Arf GAPs are direct. These results may be associated with technical problems, such as alterations in protein conformation during the purification process. Also, the buffer used for pull-down assays may be inappropriate for these specific proteins fold properly. In both cases, the tag sequence would be inaccessible to the respective antibody. These issues should be solved, for instance, by using specific protein antibodies and optimizing the buffer composition.

To further explore the interactions detected by co-immunoprecipitation assays with total protein extracts, the subcellular co-localization of the Arf GAPs with F-actin and Arl13b was assessed. The co-localization between ASAP1, ASAP3 or ACAP1 and F-actin, as well as Arl13b, was detected mainly in structures associated with cell invasion or with cell migration at the cell periphery, such as lamellipodia, filopodia, PRs, CDRs and stress fibers. The first studies on ASAP1 showed that this protein localizes in the cytoplasm and at the cell periphery, specifically associated with the plasma membrane, in MEFs, monkey fibroblasts and HeLa cells (Brown *et al.*, 1998). In MEFs and HeLa cells stimulated with growth factors, the co-localization of ASAP1 with actin occurs at membrane ruffles (Kam *et al.*, 2000; Luo *et al.*, 2007; Chen *et al.*, 2016). Additionally, in MDA-MB-231 cells, ASAP1 associates with actin in invadopodia (Onodera *et al.*, 2005; Bharti *et al.*, 2007). In agreement with the published data, I detected ASAP1 in actin-rich protrusive structures near the plasma membrane and at structures resembling invadopodia, since they appear as small dot-like clusters with a core of actin localized near the nucleus (Gimona *et al.*, 2008), in MDA-MB-231 cells. Moreover, the association of ASAP1 with Arl13b was detected at the plasma membrane, namely in PRs and in structures that resemble invadopodia. To confirm if these structures are invadopodia, it would be necessary to assess the co-localization of F-actin with other actin-associated proteins, such as cortactin, cofilin, the actin nucleator complex Arp2/3 or the invadopodia scaffold protein Tks5 (Murphy and Courtneidge, 2011; Berginski *et al.*, 2014). Altogether, these results indicate that ASAP1 subcellular localization is conserved between different cell types, and

more importantly, supports its role in cell migration and invasion, strongly suggesting that ASAP1 acts together with Arl13b in the regulation of these processes.

More recently, it has been described that NMIIA activity is regulated by ASAP1 (Chen *et al.*, 2016) and, in addition, our group has identified this myosin as an Arl13b effector (Casalou *et al.*, 2014). Since I found that Arl13b interacts with ASAP1 in PRs at the cell periphery, a new link between Arl13b, ASAP1 and NMIIA can be hypothesized, strongly suggesting that they function together in the regulation of cell migration. The observation that ASAP1 binds preferentially to the GTP-bound form of Arl13b, and since ASAP1 did not promote the GTPase activity of Arl13b *in vitro*, it is likely that ASAP1, like NMIIA, acts as an Arl13b effector. In fact, it has been described that Arf GAPs can function as effectors of Arf proteins, besides their functions as activity modulators (Donaldson and Jackson, 2011). The observation that the interaction between Arl13b and the GAP activity deficient mutant [R497K]ASAP1 is enhanced when Arl13b is loaded with GTP supports this hypothesis. Additionally, [R497K]ASAP1 colocalizes with Arl13b in the same structures than the wildtype form, including structures that resemble invadopodia. Indeed, is has been described that ASAP1 GAP activity might not be necessary for some of ASAP1 specific functions, namely invadopodia formation (Ha *et al.*, 2008).

Finally, the observation that *ARL13B* and *ASAP1* expression increases with cancer cell invasiveness in breast cell lines is in agreement with results showing that high expression levels of Arl13b and ASAP1 in breast tumors are correlated with enhanced cell invasion and metastasis (Onodera *et al.*, 2005; Casalou, Faustino *et al*., unpublished results). Accordingly, it would be expected that ASAP1 silencing decreases cancer cell migration and invasion, as with Arl13b silencing. However, the reported effects of ASAP1 silencing on these processes have been contradictory. Thus, the role of ASAP1 in cell migration and invasion may differ between cell types and experimental conditions applied in these assays. Another possible explanation for these contradictory results is the fact that different oncogenes can bind to the C-terminal region of ASAP1, which could influence cell migration and invasion in different ways.

ASAP3 has an important role in actin stress fiber formation and it also associates with CDRs in MDA-MB-231 cells (Ha *et al.*, 2008). In the same cell line, I confirmed the co-localization between ASAP3 and actin in actin stress fibers. The co-localization with Arl13b in CDRs is also in agreement with previous results from our group describing that Arl13b is required for CDR formation in fibroblasts (Casalou *et al.*, 2014). These results suggest that Arl13b and ASAP3 act together in CDRs, providing a structural basis to generate force for cell migration. Although no studies describe an interaction between ASAP3 and NMII, recent data shows that ASAP3 silencing reduces NMII phosphorylation (Luo *et al.*, 2017). These observations are consistent with an effect of ASAP3 on NMII, which remains to be explored. Thus, it can be proposed that Arl13b, ASAP3 and NMII function together in the regulation of cell migration through CDRs.

Like for ASAP1, I observed that ASAP3 interacts with Arl13b in a GTP-dependent manner and does not promote the GTPase activity of Arl13b *in vitro*. Furthermore, the expression of *ARL13B* and *ASAP3* is enhanced in invasive cancer cells, supporting the reports showing that both proteins are highly expressed in human breast cancer samples (Mao *et al.*, 2017; Casalou, Faustino *et al*., unpublished results). Furthermore, the silencing of Arl13b or ASAP3 impairs breast cancer cell migration and invasion (Ha *et al.*, 2008; Casalou, Faustino *et al*., unpublished results). Altogether, these findings suggest that ASAP3 functions as an Arl13b effector.

From all Arf GAPs selected for this study, ACAP1 is the least studied and its direct role in tumor progression is not known. In MDA-MB-231 cells, I observed that ACAP1 associates with stress fibers in protrusive structures near the plasma membrane, in agreement with its known functions in actin remodeling and cell movement (Inoue and Randazzo, 2007). Interestingly, ACAP silencing promoted morphological alterations on MDA-MB-231 cells that could be partially explained by its role on actin cytoskeleton remodeling. In fact, it was reported that ACAP1 overexpression inhibits the formation of

membrane protrusions (Jackson *et al.*, 2000) and reduces the size of FAs (Chen *et al.*, 2014). Upon ACAP1 silencing, I observed the opposite. More importantly, in the same cell line, the co-localization between this Arf GAP and Arl13b was found in filopodia and PRs, suggesting that both proteins function together in cancer cell migration.

Contrary for what was observed for ASAP1 and ASAP3, the results of the *in vitro* GTPase activity of ACAP1 on Arl13b were not conclusive. The GTPase activity of ACAP1 alone in the presence of GTP was several times enhanced comparing to the absence of GTP. A possible explanation for this is the presence of a contaminant protein with GTPase activity not excluded during the purification process. In fact, the analysis of purified ACAP1 indicates the presence of two bands near the 75 kDa marker band. Therefore, the high level of GTP hydrolysis verified in the reaction between ACAP1 and Arf6 or Arl13b cannot be assumed as a result of the specific ACAP1-stimulated Arf6 or Arl13b GTPase activity, respectively. A new purification process is required to guarantee the absence of contaminants that could influence the GTP hydrolysis.

The opposite effects of Arl13b and ACAP1 silencing on breast cancer cell migration and invasion and their inverse expression correlation with breast cancer cell invasiveness support an antagonistic effect for these proteins. These data show that ACAP1 regulates the migratory capacity and invasion of breast cancer cells and, more importantly, suggest that ACAP1 is a promising candidate as a GAP of Arl13b, even considering that the results of *in vitro* GTPase activity assay were not conclusive.

Since the interaction between Arl13b and ACAP1 occurs in a GTP-dependent manner, ACAP1 could also function as an Arl13b effector. This hypothesis is less likely because, in that case, as verified for ASAP1 and ASAP3, ACAP1 silencing should have the same effects as Arl13b silencing in cancer cell migration and invasion and their both expression levels should positively correlate with cancer cell invasiveness.

Future studies on ACAP1 should investigate the reason for this contradictory effect on cell migration and invasion in different cancer cell lines, by performing rescue experiments, determining if ACAP1 overexpression inhibits metastasis *in vivo* (opposing the effect of Arl13b overexpression) and confirming if ACAP1 has a lower expression in human tumors compared to the normal tissue, contrary to what we verified for Arl13b.

Lastly, it was described that GIT1 associates with paxillin in FAs in rat embryo fibroblasts and hamster ovary cells, appearing as punctate supramolecular complexes localized in the cytoplasm (Manabe *et al.*, 2002). In HeLa cervical cancer cells, I confirmed that GIT1 does not co-localize with F-actin and that it can be found, indeed, in punctate cytoplasmic aggregates. To confirm if these structures are FAs, it would be necessary to use specific markers for those structures, namely paxillin and vinculin (Geiger *et al.*, 2001). More importantly, in the same cell line, GIT1 does not co-localize with Arl13b, in agreement with the co-immunoprecipitation results. However, since GIT1 co-immunoprecipitation with Arl13b was tested in MDA-MB-231 cells, the subcellular localization of this Arf GAP should be assessed in the same cell line. This analysis was done in HeLa cells since the transfection of MDA-MB-231 cells was only efficient using an electroporation-based transfection method and it was not possible to use the equipment with GIT1 construct due to material constraints.

Concerning the GTPase activity analysis, several biochemical assays have been described in the literature. The measurement of GTP levels decrease or GDP increment are alternative to the quantification of free Pi in solution (Mondal *et al.*, 2015). Some authors claim that chromogenic methods that measure Pi are poorly sensitive. Additionally, Pi is a common contaminant in various buffers causing high backgrounds. However, the assays I performed did not entail these technical problems. First, I verified that all samples and buffers used were completely free of phosphate. Second, the GTPase activity was clearly increased in reactions containing ACAP1 and GTP, showing a considerable sensitivity of the method. The most common approach used for decades in GTPase activity assays is the use of radio-labeled GTP, namely [α-^{32}P]GTP. Despite these methods involve specific procedures in the

manipulation of materials and reagents, as well as in waste treatment, they have a high robustness. Therefore, a method using radio-labeled GTP should be considered to confirm the results for ASAP1 and ASAP3 and to clarify if ACAP1 is a GAP of Arl13b.

Regarding the protein purification, the full-length Arl13b has often been described as insoluble in bacterial lysates (Hori *et al.*, 2008; Ivanova *et al.*, 2017), probably due to the hydrophobic properties of its coiled-coil domains (Burkhard *et al.*, 2001). Thus, we chose to express Arl13b$^{1-225}$ truncated form in bacteria since it contains mostly the G-domain, which is essential for GTPase activity (Goitre *et al.*, 2014). Even so, its purification process resulted in very low amounts of purified protein. We then decided to purify the full-length Arl13b in mammalian cells, not only to avoid the insolubility verified in bacteria, but also to provide better conditions in terms of folding and post-translational modifications that could be important for the interaction of Arl13b with the Arf GAPs, as well as for its function. The amount of purified Arl13b and Arf GAPs used in the assays was the maximum indicated by the manufacturers. Instead, a titration of both proteins should be done to find the optimal concentration for the experimental conditions adopted, using a positive control. This procedure was not performed since the purification process of both forms of Arl13b was not efficient, resulting in low amounts of purified protein. In addition, the presence of contaminant proteins and/or the possible degradation overestimated Arl13b concentration, as it is possible to observe in the analysis of the purified proteins. For these reasons, Arl13b purification process must be optimized further. Nevertheless, the detection of an intrinsic GTPase activity for the two forms of Arl13b indicates that both forms were active.

With this study, novel insights on the identity of Arl13b-binding partners were acquired. The results obtained indicate that ASAP1 and ASAP3 are Arl13b effectors, also suggesting ACAP1 as a potential Arf GAP of Arl13b. These new findings contribute to understand how Arl13b regulates cancer cell migration, invasion and metastasis, and raise new hypotheses for how this protein is inactivated. However, a validation of these novel targets is required, namely by using *in vivo* models. Further studies considering the already identified or new candidate proteins, such as effectors, GEFs and GAPs, could contribute to unravel the molecular mechanisms by which Arl13b regulates tumor progression and find new targets that can be used to develop anti-cancer therapies.

References

Abercrombie, M., Heaysman, J. E. M., and Pegrum, S. M. (1970). The locomotion of fibroblasts in culture: II. "Ruffling". *Experimental cell research*, **60**: 437-444.

Andreev, J., Simon, J.-P., Sabatini, D. D., Kam, J., Plowman, G., Randazzo, P. A., and Schlessinger, J. (1999). Identification of a New Pyk2 Target Protein with Arf-GAP Activity. *Molecular and Cellular Biology*, **19**(3): 2338-2350.

Barral, D. C., Garg, S., Casalou, C., Watts, G. F. M., Sandoval, J. L., Ramalho, J. S., Hsu, V. W., and Brenner, M. B. (2012). Arl13b regulates endocytic recycling traffic. *PNAS*, **109**(52): 21354-21359.

Bay, S. N., Long, A. B., and Caspary, T. (2018). Disruption of the ciliary GTPase Arl13b suppresses Sonic hedgehog overactivation and inhibits medulloblastoma formation. *PNAS*, **115**(7): 1570-1575.

Berginski, M. E., Creed, S. J., Cochran, S., Roadcap, D. W., Bear, J. E., and Gomez, S. M. (2014). Automated analysis of invadopodia dynamics in live cells. *PeerJ*, **2**: e462.

Bharti, S., Inoue, H., Bharti, K., Hirsch, D. S., Nie, Z., Yoon, H.-Y., Artym, V., Yamada, K. M., Mueller, S. C., Barr, V. A., and Randazzo, P. A. (2007). Src-Dependent Phosphorylation of ASAP1 Regulates Podosomes. *Molecular and Cellular Biology*, **27**(23): 8271-8283.

Bos, J. L., Rehmann, H., and Wittinghofer, A. (2007). GEFs and GAPs: Critical Elements in the Control of Small G Proteins. *Cell*, **129**(5): 865-877.

Bravo-Cordero, J. J., Hodgson, L., and Condeelis, J. (2012). Directed cell invasion and migration during metastasis. *Current Opinion in Cell Biology*, **24**(2): 277-283.

Brown, M. T., Andrade, J., Radhakrishna, H., Donaldson, J. G., Cooper, J. A., and Randazzo, P. A. (1998). ASAP1, a Phospholipid-Dependent Arf GTPase-Activating Protein That Associates with and Is Phosphorylated by Src. *Molecular and Cellular Biology*, **18**(12): 7038-7051.

Buccione, R., Orth, J. D., and McNiven M. A. (2004). Foot and mouth: podosomes, invadopodia and circular dorsal ruffles. *Nature Reviews Molecular Cell Biology*, **5**(8): 647-657.

Buffart, T. E., Coffa, J., Hermsen, M. A. J. A., Carvalho, B., Van der Sijp, J. R. M., Ylstra, B., Pals, G., Schouten, J. P., and Meijer, G. A. (2005). DNA copy number changes at 8q11-24 in metastasized colorectal cancer. *Cellular Oncology*, **27**(1): 57-65.

Burkhard, P., Stetefeld, J. and Strelkov, S. V. (2001). Coiled coils: a highly versatile protein folding motif. *Trends in Cell Biology*, **11**(2): 82-88.

Cantagrel, V., Silhavy, J. L., Bielas, S. L., Swistun, D., Marsh, S. E., Bertrand, J. Y., *et al.* (2008). Mutations in the Cilia Gene *ARL13B* Lead to the Classical Form of Joubert Syndrome. *American Journal of Human Genetics*, **83**(2): 170-179.

Casalou, C., Faustino, A., and Barral, D. C. (2016). Arf proteins in cancer cell migration. *Small GTPases*, **7**(4): 270-282.

Casalou, C., Seixas, C., Portelinha, A., Pintado, P., Barros, M., Ramalho, J. S., Lopes, S. S., and Barral, D. C. (2014). Arl13b and the non-muscle myosin heavy chain IIA are required for circular dorsal ruffle formation and cell migration. *Journal of Cell Science*, **127**(12): 2709-2722.

Caspary, T., Larkins, C. E., and Anderson, K. V. (2007). The Graded Response to Sonic Hedgehog Depends on Cilia Architecture. *Developmental Cell*, **12**(5): 767-778.

Cavo, M., Caria, M., Pulsoni, I., Beltrame, F., Fato, M., and Scaglione, S. (2018). A new cell-laden 3D Alginate-Matrigel hydrogel resembles human breast cancer cell malignant morphology, spread and invasion capability observed "*in vivo*". *Scientific Reports*, **8**(5333): 1-12.

Chan, S.-H., Huang, W.-C., Chang, J.-W., Chang, K.-J., Kuo, W.-H., Wang, M.-Y., Lin, K.-Y., Uen, Y.-H., Hou, M.-F., Lin, C.-M., Jang, T.-H., Tu, C.-W., Lee, Y.-R., Lee, Y.-H., Tien, M.-T., and Wang, L.-H. (2014). MicroRNA-149 targets GIT1 to suppress integrin signaling and breast cancer metastasis. *Oncogene*, **33**(36): 4496-4507.

Chang, J.-S., Su, C.-Y., Yu, W.-H., Lee, W.-J., Liu, Y.-P., Lai, T.-C., Jan, Y.-H., Yang, Y.-F., Shen, C.-N., Shew, J.-Y., Lu, J., Yang, C.-J., Huang, M.-S., Lu, P.-J., Lin, Y.-F., Kuo, M.-L., Hua, K.-T., and Hsiao, M. (2015). GIT1 promotes lung cancer cell metastasis through modulating Rac1/Cdc42 activity and is associated with poor prognosis. *Oncotarget*, **6**(34): 36278-36291.

Chavez, K. J., Garimella, S. V., and Lipkowitz, S. (2010). Triple negative breast cancer cell lines: One tool in the search for better treatment of triple negative breast cancer. *Breast Disease*, **32**(1-2): 35-48.

Chen, J., Yang, P., Yang, J., Wen, Z., Zhang, B., and Zheng, X. (2015). GIT1 is a novel prognostic biomarker and facilitates tumor progression via activating ERK/MMP9 signaling in hepatocellular carcinoma. *OncoTargets and Therapy*, **8**: 3731-3742.

Chen, P.-W., Jian, X., Heissler, S. M., Le, K., Luo, R., Jenkins, L. M., Nagy, A., Moss, J., Sellers, J. R., and Randazzo, P. A. (2016). The Arf GTPase-activating Protein, ASAP1, Binds Nonmuscle Myosin 2A to Control Remodeling of the Actomyosin Network. *Journal of Biological Chemistry*, **291**(14): 7517-7526.

Chen, P.-W., Luo, R., Jian, X., and Randazzo, P. A. (2014). The Arf6 GTPase-activating Proteins ARAP2 and ACAP1 Define Distinct Endosomal Compartments That Regulate Integrin α5β1 Traffic. *Journal of Biological Chemistry*, **289**(44): 30237-30248.

Cherfils, J., and Zeghouf, M. (2013). Regulation of Small GTPases by GEFs, GAPs, and GDIs. *Physiological Reviews*, **93**(1): 269-309.

D'Souza-Schorey, C., and Chavrier, P. (2006). ARF proteins: roles in membrane traffic and beyond. *Nature Reviews Molecular Cell Biology*, **7**(5): 347-358.

Dani, N., Barbosa, A. J. M., Del Rio, A., and Di Girolamo, M. (2013). ADP-Ribosylated Proteins as Old and New Drug Targets for Anticancer Therapy: The Example of ARF6. *Current Pharmaceutical Design*, **19**(4): 624-633.

De Curtis, I. (2001). Cell migration: GAPs between membrane traffic and the cytoskeleton. *EMBO Reports*, **2**(4): 277-281.

Donaldson, J. G., and Jackson, C. L. (2011). ARF family G proteins and their regulators: roles in membrane transport, development and disease. *Nature Reviews Molecular Cell Biology*, **12**(6): 362-375.

Dong, Y., Chang, C., Liu, J., and Qiang, J. (2017). Targeting of GIT1 by miR-149* in breast cancer suppresses cell proliferation and metastasis in vitro and tumor growth in vivo. *OncoTargets and Therapy*, **10**: 5873-5882.

Earp, M., Tyrer, J. P., Winham, S. J., Lin, H. Y., Chornokur, G., Dennis, J., *et al.* (2018). Variants in genes encoding small GTPases and association with epithelial ovarian cancer susceptibility. *PLoS One*, **13**(7): e0197561.

East, M. P., and Kahn, R. A. (2011). Models for the functions of Arf GAPs. *Seminars in Cell and Developmental Biology*, **22**(1): 3-9.

Eddy, R. J., Weidmann, M. D., Sharma, V. P., and Condeelis, J. S. (2017). Tumor Cell Invadopodia: Invasive Protrusions that Orchestrate Metastasis. *Trends in Cell Biology*, **27**(8): 595-607.

Ehlers, J. P., Worley, L., Onken, M. D., and Harbour, J. W. (2005). DDEF1 is Located in an Amplified Region of Chromosome 8q and Is Overexpressed in Uveal Melanoma. *Clinical Cancer Research*, **11**(10): 3609-3613.

Fan, C., Tian, Y., Miao, Y., Lin, X., Zhang, X., Jiang, G., Luan, L., and Wang, E. (2014). ASAP3 expression in non-small cell lung cancer: association with cancer development and patients' clinical outcome. *Tumor Biology*, **35**(2): 1489-1494.

Fang, Z., Miao, Y., Ding, X., Deng, H., Liu, S., Wang, F., Zhou, R., Watson, C., Fu, C., Hu, Q., Lillard, J. W., Powell, M., Chen, Y., Forte, J. G., and Yao, X. (2006). Proteomic Identification and Functional Characterization of a Novel ARF6 GTPase-activating Protein, ACAP4. *Molecular & Cellular Proteomics*, **5**(8): 1437-1449.

Fife, C. M., McCarroll, J. A., and Kavallaris, M. (2014). Movers and shakers: Cell cytoskeleton in cancer metastasis. *British Journal of Pharmacology*, **171**(24): 5507-5523.

Furman, C., Short, S. M., Subramanian, R. R., Zetter, B. R., and Roberts, T. M. (2002). DEF-1/ASAP1 Is a GTPase-activating Protein (GAP) for ARF1 That Enhances Cell Motility through a GAP-dependent Mechanism. *Journal of Biological Chemistry*, **277**(10): 7962-7969.

Gardel, M. L., Schneider, I. C., Aratyn-Schaus, Y., and Waterman, C. M. (2010). Mechanical Integration of Actin and Adhesion Dynamics in Cell Migration. *Annual Review of Cell and Developmental Biology*, **26**(1): 315-333.

Garrido, P., Osorio, F. G., Morán, J., Cabello, E., Alonso, A., Freije, J. M. P., and González, C. (2015). Loss of GLUT4 Induces Metabolic Reprogramming and Impairs Viability of Breast Cancer Cells. *Journal of Cellular Physiology*, **230**(1): 191-198.

Geiger, B., Bershadsky, A., Pankov, R., and Yamada, K. M. (2001). Transmembrane extracellular matrix-cytoskeleton crosstalk. *Nature Reviews Molecular Cell Biology*, **2**(11): 793-805.

Gillingham, A. K., and Munro, S. (2007). The Small G Proteins of the Arf Family and Their Regulators. *Annual Review of Cell and Developmental Biology*, **23**(1): 579-611.

Gimona, M., Buccione, R., Courtneidge, S. A., and Linder, S. (2008). Assembly and biological role of podosomes and invadopodia. *Current Opinion in Cell Biology*, **20**(2): 235-241.

Goitre, L., Trapani, E., Trabalzini, L., and Retta, S. F. (2014). The Ras Superfamily of Small GTPases: The Unlocked Secrets. *Methods in Molecular Biology*, **1120**: 1-18.

Gu, Z., Noss, E. H., Hsu, V. W., and Brenner, M. B. (2011). Integrins traffic rapidly via circular dorsal ruffles and macropinocytosis during stimulated cell migration. *Journal of Cell Biology*, **193**(1): 61-70.

Ha, V. L., Bharti, S., Inoue, H., Vass, W. C., Campa, F., Nie, Z., De Gramont, A., Ward, Y., and Randazzo, P. A. (2008). ASAP3 Is a Focal Adhesion-associated Arf GAP That Functions in Cell Migration and Invasion. *Journal of Biological Chemistry*, **283**(22): 14915-14926.

Ha, V. L., Luo, R., Nie, Z., and Randazzo, P. A. (2008). Contribution of AZAP-Type Arf GAPs to Cancer Cell Migration and Invasion. *Advances in Cancer Research*, **101**: 1-28.

Hanahan, D., and Weinberg, R. A. (2011). Hallmarks of Cancer: The Next Generation. *Cell*, **144**(5): 646-674.

Hanke-Gogokhia, C., Wu, Z., Sharif, A., Yazigi, H., Frederick, J. M., and Baehr, W. (2017). The guanine nucleotide exchange factor, Arf-like protein 13b, is essential for assembly of the mouse photoreceptor transition zone and outer segment. *Journal of Biological Chemistry*, **292**(52): 21442-21456.

Hashimoto, S., Onodera, Y., Hashimoto, A., Tanaka, M., Hamaguchi, M., Yamada, A., and Sabe, H. (2004). Requirement for Arf6 in breast cancer invasive activities. *PNAS*, **101**(17): 6647-6652.

Herrmann, C. (2003). Ras-effector interactions: after one decade. *Current Opinion in Structural Biology*, **13**(1): 122-129.

Hoffman, J. D., Graff, R. E., Emami, N. C., Tai, C. G., Passarelli, M. N., Hu, D., Huntsman, S., Hadley, D., Leong, L., Majumdar, A., Zaitlen, N., Ziv, E., and Witte, J. S. (2017). *Cis*-eQTL-based trans-ethnic meta-analysis reveals novel genes associated with breast cancer risk. *PLoS Genetics*, **13**(3): e1006690.

Hongu, T., Yamauchi, Y., Funakoshi, Y., Katagiri, N., Ohbayashi, N., and Kanaho, Y. (2016). Pathological functions of the small GTPase Arf6 in cancer progression: Tumor angiogenesis and metastasis. *Small GTPases*, **7**(2): 47-53.

Hoon, J.-L., Wong, W.-K., and Koh, C.-G. (2012). Functions and Regulation of Circular Dorsal Ruffles. *Molecular and Cellular Biology*, **32**(21): 4246-4257.

Hori, Y., Kobayashi, T., Kikko, Y., Kontani, K., and Katada, T. (2008). Domain architecture of the atypical Arf-family GTPase Arl13b involved in cilia formation. *Biochemical and Biophysical Research Communications*, **373**(1): 119-124.

Huang, W.-C., Chan, S.-H., Jang, T.-H., Chang, J.-W., Ko, Y.-C., Yen, T.-C., Chiang, S.-L., Chiang, W.-F., Shieh, T.-Y., Liao, C.-T., Juang, J.-L., Wang, H.-C., Cheng, A.-J., Lu, Y.-C., and Wang, L.-H. (2014). MiRNA-491-5p and GIT1 Serve as Modulators and Biomarkers for Oral Squamous Cell Carcinoma Invasion and Metastasis. *Cancer Research*, **74**(3): 751-764.

Inoue, H., and Randazzo, P. A. (2007). Arf GAPs and Their Interacting Proteins. *Traffic*, **8**(11): 1465-1475.

Inoue, H., Ha, V. L., Prekeris, R., Randazzo, P. A. (2008) Arf GTPase-activating Protein ASAP1 Interacts with Rab11 Effector FIP3 and Regulates Pericentrosomal Localization of Transferrin Receptor-positive Recycling Endosome. *Molecular Biology of the Cell*, **19**(10): 4224-4237.

Itoh, T., and Hasegawa, J. (2013). Mechanistic insights into the regulation of circular dorsal ruffle formation. *Journal of Biochemistry*, **153**(1): 21-29.

Ivanova, A. A., Caspary, T., Seyfried, N. T., Duong, D. M., West, A. B., Liu, Z., and Kahn, R. A. (2017). Biochemical characterization of purified mammalian ARL13B protein indicates that it is an atypical GTPase and ARL3 guanine nucleotide exchange factor (GEF). *Journal of Biological Chemistry*, **292**(26): 11091-11108.

Jackson, T. R., Brown, F. D., Nie, Z., Miura, K., Foroni, L., Sun, J., Hsu, V. W., Donaldson, J. G., and Randazzo, P. A. (2000). ACAPs Are Arf6 GTPase-activating Proteins That Function in the Cell Periphery. *Journal of Cell Biology*, **151**(3): 627-638.

Jiao, X., Wood, L. D., Lindman, M., Jones, S., Buckhaults, P., Polyak, K., Sukumar, S., Carter, H., Kim, D., Karchin, R., Sjöblom, T. (2012). Somatic Mutations in the Notch, NF-κB, PIK3CA, and Hedgehog Pathways in Human Breast Cancers. *Genes, Chromosomes and Cancer*, **51**(5): 480-489.

Kam, J. L., Miura, K., Jackson, T. R., Gruschus, J., Roller, P., Stauffer, S., Clark, J., Aneja, R., and Randazzo, P. A. (2000). Phosphoinositide-dependent Activation of the ADP-ribosylation Factor GTPase-activating Protein ASAP1. Evidence for the pleckstrin homology domain functioning as an allosteric site. *Journal of Biological Chemistry*, **275**(13): 9653-9663.

Kahn, R. A., Bruford, E., Inoue, H., Logsdon, J. M., Nie, Z., Premont, R. T., Randazzo, P. A., Satake, M., Theibert, A. B., Zapp, M. L., and Cassel, D. (2008). Consensus nomenclature for the human ArfGAP domain-containing proteins. *Journal of Cell Biology*, **182**(6): 1039-1044.

Kjos, I., Vestre, K., Guadagno, N. A., Distefano, M. B., and Progida, C. (2018). Rab and Arf proteins at the crossroad between membrane transport and cytoskeleton dynamics. *Biochimica et Biophysica Acta - Molecular Cell Research*, **1865**(10): 1397-1409.

Kondo, A., Hashimoto, S., Yano, H., Nagayama, K., Mazaki, Y., and Sabe, H. (2000). A New Paxillin-binding Protein, PAG3/Papα/KIAA0400, Bearing an ADP-Ribosylation Factor GTPase-activating Protein Activity, Is Involved in Paxillin Recruitment to Focal Adhesions and Cell Migration. *Molecular Biology of the Cell*, **11**(4): 1315-1327.

Kuo, J. C. (2013). Mechanotransduction at focal adhesions: integrating cytoskeletal mechanics in migrating cells. *Journal of Cellular and Molecular Medicine*, **17**(6): 704-712.

Larkins, C. E., Aviles, G. D. G., East, M. P., Kahn, R. A., and Caspary, T. (2011). Arl13b regulates ciliogenesis and the dynamic localization of Shh signaling proteins. *Molecular Biology of the Cell*, **22**(23): 4694-4703.

Le Clainche, C., and Carlier, M.-F. (2008). Regulation of Actin Assembly Associated With Protrusion and Adhesion in Cell Migration. *Physiological Reviews*, **88**(2): 489-513.

Letort, G., Ennomani, H., Gressin, L., Théry, M., and Blanchoin, L. (2015). Dynamic reorganization of the actin cytoskeleton. *F1000Research*, **4**: 1-11.

Li, J., Ballif, B. A., Powelka, A. M., Dai, J., Gygi, S. P., and Hsu, V. W. (2005). Phosphorylation of ACAP1 by Akt Regulates the Stimulation-Dependent Recycling of Integrin β1 to Control Cell Migration. *Developmental Cell*, **9**(5): 663-673.

Li, J., Peters, P. J., Bai, M., Dai, J., Bos, E., Kirchhausen, T., Kandror, K. V., and Hsu, V. W. (2007). An ACAP1-containing clathrin coat complex for endocytic recycling. *Journal of Cell Biology*, **178**(3): 453-464.

Li, J., Wang, Q., Wen, R., Liang, J., Zhong, X., Yang, W., Su, D., and Tang, J. (2015). MiR-138 inhibits cell proliferation and reverses epithelial-mesenchymal transition in non-small cell lung cancer cells by targeting GIT1 and SEMA4C. *Journal of Cellular and Molecular Medicine*, **19**(12): 2793-2805.

Li, Y., Wei, Q., Zhang, Y., Ling, K., and Hu, J. (2010). The small GTPases ARL-13 and ARL-3 coordinate intraflagellar transport and ciliogenesis. *Journal of Cell Biology*, **189**(6): 1039-1051.

Lin, D., Watahiki, A., Bayani, J., Zhang, F., Liu, L., Ling, V., Sadar, M. D., English, J., Fazli, L., So, A., Gout, P. W., Gleave, M., Squire, J. A., and Wang, Y.-Z. (2008). ASAP1, a Gene at 8q24, is Associated with Prostate Cancer Metastasis. *Cancer Research*, **68**(11): 4352-4359.

Linder, S. (2007). The matrix corroded: podosomes and invadopodia in extracellular matrix degradation. *Trends in Cell Biology*, **17**(3): 107-117.

Liu, Y., Loijens, J. C., Martin, K. H., Karginov, A. V., and Parsons, J. T. (2002) The Association of ASAP1, an ADP Ribosylation Factor-GTPase Activating Protein, with Focal Adhesion Kinase Contributes to the Process of Focal Adhesion Assembly. *Molecular Biology of the Cell*, **13**(6): 2147-2156.

Lu, X., Wan, F., Zhang, H., Shi, G., and Ye, D. (2015). ITGA2B and ITGA8 are predictive of prognosis in clear cell renal cell carcinoma patients. *Tumor Biology*, **37**(1): 253-262.

Luo, R., Ahvazi, B., Amariei, D., Shroder, D., Burrola, B., Losert, W., and Randazzo, P. A. (2007). Kinetic analysis of GTP hydrolysis catalysed by the Arf1-GTP-ASAP1 complex. *Biochemical Journal*, **402**(3): 439-447.

Luo, R., Reed, C. E., Sload, J. A., Wordeman, L., Randazzo, P. A., and Chen, P.-W. (2017). Arf GAPs and molecular motors. *Small GTPases*, **21**: 1-14.

Manabe, R., Kovalenko, M., Webb, D. J., and Horwitz, A. R. (2002). GIT1 functions in a motile, multi-molecular signaling complex that regulates protrusive activity and cell migration. *Journal of Cell Science*, **115**(7): 1497-1510.

Mao, X., Fan, C., Yu, X., Chen, B., and Jin, F. (2017). DDEFL1 correlated with Rho GTPases activity in breast cancer. *Oncotarget*, **8**(68): 112487-112497.

Mattila, P. K., and Lappalainen, P. (2008). Filopodia: molecular architecture and cellular functions. *Nature Reviews Molecular Cell Biology*, **9**(6): 446-454.

Mayor, R., and Etienne-Manneville, S. (2016). The front and rear of collective cell migration. *Nature Reviews Molecular Cell Biology*, **17**(2): 97-109.

Messina, S. (2018). Small GTPase RAS in multiple sclerosis - exploring the role of RAS GTPase in the etiology of multiple sclerosis. *Small GTPases*, **18**: 1-8.

Miura, Y., Hongu, T., Yamauchi, Y., Funakoshi, Y., Katagiri, N., Ohbayashi, N., and Kanaho, Y. (2016). ACAP3 regulates neurite outgrowth through its GAP activity specific to Arf6 in mouse hippocampal neurons. *Biochemical Journal*, **473**(17): 2591-2602.

Mondal, S., Hsiao, K., and Goueli, S. A. (2015). A Homogenous Bioluminescent System for Measuring GTPase, GTPase Activating Protein, and Guanine Nucleotide Exchange Factor Activities. *ASSAY and Drug Development Technologies*, **13**(8): 444-455.

Monteiro, P., Rossé, C., Castro-Castro, A., Irondelle, M., Lagoutte, E., Paul-Gilloteaux, P., Desnos, C., Formstecher, E., Darchen, F., Perrais, D., Gautreau, A., Hertzog, M., and Chavrier, P. (2013). Endosomal WASH and exocyst complexes control exocytosis of MT1-MMP at invadopodia. *Journal of Cell Biology*, **203**(6): 1063-1079.

Morishige, M., Hashimoto, S., Ogawa, E., Toda, Y., Kotani, H., Hirose, M., Wei, S., Hashimoto, A., Yamada, A., Yano, H., Mazaki, Y., Kodama, H., Nio, Y., Manabe, T., Wada, H., Kobayashi, H., and Sabe, H. (2008). GEP100 links epidermal growth factor receptor signalling to Arf6 activation to induce breast cancer invasion. *Nature Cell Biology*, **10**(1): 85-92.

Murphy, D. A., and Courtneidge, S. A. (2011). The 'ins' and 'outs' of podosomes and invadopodia: characteristics, formation and function. *Nature Reviews Molecular Cell Biology*, **12**(7): 413-426.

Nie, Z., Hirsch, D. S., and Randazzo, P. A. (2003). Arf and its many interactors. *Current Opinion in Cell Biology*, **15**(4): 396-404.

Ohashi, Y., Iijima, H., Yamaotsu, N., Yamazaki, K., Sato, S., Okamura, M., Sugimoto, K., Dan, S., Hirono, S., and Yamori, T. (2012). AMF-26, a Novel Inhibitor of the Golgi System, Targeting ADP-ribosylation Factor 1 (Arf1) with Potential for Cancer Therapy. *Journal of Biological Chemistry*, **287**(6): 3885-3897.

Okabe, H., Furukawa, Y., Kato, T., Hasegawa, S., Yamaoka, Y., and Nakamura, Y. (2004). Isolation of development and differentiation enhancing factor-like 1 (*DDEFL1*) as a drug target for hepatocellular carcinomas. *International Journal of Oncology*, **24**(1): 43-48.

Onodera, Y., Hashimoto, S., Hashimoto, A., Morishige, M., Mazaki, Y., Yamada, A., Ogawa, E., Adachi, M., Sakurai, T., Manabe, T., Wada, H., Matsuura, N., and Sabe, H. (2005). Expression of AMAP1, an ArfGAP, provides novel targets to inhibit breast cancer invasive activities. *EMBO Journal*, **24**(5): 963-973.

Pasqualato, S., Renault, L., and Cherfils, J. (2002). Arf, Arl, Arp and Sar proteins: a family of GTP-binding proteins with a structural device for 'front-back' communication. *EMBO Reports*, **3**(11): 1035-1041.

Peng, H., Dara, L., Li, T. W. H., Zheng, Y., Yang, H., Tomasi M. L., Tomasi, I., Giordano, P., Mato, J. M., Lu, S. C. (2013). Methionine Adenosyltransferase 2B-GIT1 Interplay Activates MEK1-ERK1/2 to Induce Growth in Human Liver and Colon Cancer. *Hepatology*, **57**(6): 2299-2313.

Porter, A. P., Papaioannou, A., and Malliri, A. (2016). Deregulation of Rho GTPases in cancer. *Small GTPases*, **7**(3): 123-138.

Premont, R. T., Perry, S. J., Schmalzigaug, R., Roseman, J. T., Xing, Y., Claing, A. (2004). The GIT/PIX complex: an oligomeric assembly of GIT family ARF GTPase-activating proteins and PIX family Rac1/Cdc42 guanine nucleotide exchange factors. *Cellular Signaling*, **16**(9): 1001-1011.

Rafiq, N. B. M., Lieu, Z. Z., Jiang, T., Yu, C. H., Matsudaira, P., Jones, G. E., and Bershadsky, A. D. (2017). Podosome assembly is controlled by the GTPase ARF1 and its nucleotide exchange factor ARNO. *Journal of Cell Biology*, **216**(1): 181-197.

Rafiullah, R., Long, A. B., Ivanova, A. A., Ali, H., Berkel, S., Mustafa, G., Paramasivam, N., Schlesner, M., Wiemann, S., Wade, R. C., Bolthauser, E., Blum, M., Kahn, R. A., Caspary, T., and Rappold, G. A. (2017). A novel homozygous *ARL13B* variant in patients with Joubert syndrome impairs its guanine nucleotide-exchange factor activity. *European Journal of Human Genetics*, **25**(12): 1324-1334.

Randazzo, P. A., and Hirsch, D. S. (2004). Arf GAPs: multifunctional proteins that regulate membrane traffic and actin remodelling. *Cellular Signalling*, **16**(4): 401-413.

Randazzo, P. A., Andrade, J., Miura, K., Brown, M. T., Long, Y.-Q., Stauffer, S., Roller, P., and Cooper, J. A. (2000). The Arf GTPase-activating protein ASAP1 regulates the actin cytoskeleton. *PNAS*, **97**(8): 4011-4016.

Randazzo, P. A., Inoue, H., and Bharti, S. (2007). Arf GAPs as regulators of the actin cytoskeleton. *Biology of the Cell*, **99**(10): 583-600.

Reymond, N., D'Água, B. B., and Ridley, A. J. (2013). Crossing the endothelial barrier during metastasis. *Nature Reviews Cancer*, **13**(12): 858-870.

Roy, K., Jerman, S., Jozsef, L., McNamara, T., Onyekaba, G., Sun, Z., and Marin, E. P. (2017). Palmitoylation of the ciliary GTPase ARL13b is necessary for its stability and its role in cilia formation. *Journal of Biological Chemistry*, **292**(43): 17703-17717.

Sambrook, J. and Russell, D. W. (2006). The Condensed Protocols From Molecular Cloning: A Laboratory Manual. Cold Spring Harbor Laboratory Press, New York. 1st edition. ISBN 0-87969-771-7.

Seixas, C., Choi, S. Y., Polgar, N., Umberger, N. L., East, M. P., Zuo, X., Moreiras, H., Ghossoub, R., Benmerah, A., Kahn, R. A., Fogelgren, B., Caspary, T., Lipschutz, J. H., and Barral, D. C. (2016). Arl13b and the exocyst interact synergistically in ciliogenesis. *Molecular Biology of the Cell*, **27**(2): 308-320.

Seixas, E., Barros, M., Seabra, M. C., and Barral, D. C. (2013). Rab and Arf proteins in Genetic Diseases. *Traffic*, **14**(8): 871-885.

Shao, J., Xu, L., Chen, L., Lu, Q., Xie, X., Shi, W., Xiong, H., Shi, C., Huang, X., Mei, J., Rao, H., Lu, H., Lu, N., and Luo, S. (2017). Arl13b Promotes Gastric Tumorigenesis by Regulating Smo Trafficking and Activation of the Hedgehog Signaling Pathway. *Cancer Research*, **77**(15): 4000-4013.

Shaughnessy, R., and Echard, A. (2018). Rab35 GTPase and cancer: Linking membrane trafficking to tumorigenesis. *Traffic*, **19**(4): 247-252.

Sheng, C., Qiu, J., Wang, Y., He, Z., Wang, H., Wang, Q., Huang, Y., Zhu, L., Shi, F., Chen, Y., Xiong, S., Xu, Z., and Ni, Q. (2018). Knockdown of Ran GTPase expression inhibits the proliferation and migration of breast cancer cells. *Molecular Medicine Reports*, **18**(1): 157-168.

Simanshu, D. K., Nissley, D. V., and McCormick, F. (2017). RAS Proteins and Their Regulators in Human Disease. *Cell*, **170**(1): 17-33.

Sirirattanakul, S., Wannakrairot, P., Tencomnao, T., and Santiyanont, R. (2015). Gene expression profile in breast cancer comprising predictive markers for metastatic risk. *Genetics and Molecular Research*, **14**(3): 10929-10936.

Small, J. V., Stradal, T., Vignal, E., and Rottner, K. (2002). The lamellipodium: where motility begins. *Trends in Cell Biology*, **12**(3): 112-120.

Sprang, S. R., and Coleman, D. E. (1998). Invasion of the Nucleotide Snatchers: Structural Insights into the Mechanism of G Protein GEFs. *Cell*, **95**(2): 155-158.

Sullivan, K. D., Nakagawa, A., Xue, D., and Espinosa, J. M. (2015). Human ACAP2 is a homolog of *C. elegans* CNT-1 that promotes apoptosis in cancer cells. *Cell Cycle*, **14**(12): 1771-1778.

Tao, W.-Y., Wang, C.-Y., Sun, Y.-H., Su, Y.-H., Pang, D., and Zhang, G.-Q. (2016). MicroRNA-34c Suppresses Breast Cancer Migration and Invasion by Targeting GIT1. *Journal of Cancer*, **7**(12): 1653-1662.

Taylor, M. A., Parvani, J. G., and Schiemann, W. P. (2010). The Pathophysiology of Epithelial-Mesenchymal Transition Induced by Transforming Growth Factor-β in Normal and Malignant Mammary Epithelial Cells. *Journal of Mammary Gland Biology and Neoplasia*, **15**(2): 169-190.

Thiery, J. P. (2002). Epithelial-mesenchymal transitions in tumour progression. *Nature Reviews Cancer*, **2**(6): 442-454.

Thomas, S., Cantagrel, V., Mariani, L., Serre, V., Lee, J. E., Elkhartoufi, N., De Lonlay, P., Desguerre, I., Munnich, A., Boddaert, N., Lyonnet, S., Vekemans, M., Lisgo, S. N., Caspary, T., Gleeson, J., and Attié-Bitach, T. (2015). Identification of a novel *ARL13B* variant in a Joubert syndrome-affected patient with retinal impairment and obesity. *European Journal of Human Genetics*, **23**(5): 621-627.

Tian, H., Qian, J., Ai, L., Li, Y., Su, W., Kong, X.-M., Xu, J., and Fang, J.-Y. (2017). Upregulation of ASAP3 contributes to colorectal carcinogenesis and indicates poor survival outcome. *Cancer Science*, **108**(8): 1544-1555.

Van Zijl, F., Krupitza, G., and Mikulits, W. (2011). Initial steps of metastasis: Cell invasion and endothelial transmigration. *Mutation Research/Reviews in Mutation Research*, **728**(1-2): 23-34.

Vetter, I. R., and Wittinghofer, A. (2001). The Guanine Nucleotide-Binding Switch in Three Dimensions. *Science*, **294**(5545): 1299-1304.

Vicente-Manzanares, M., Ma, X., Adelstein, R. S., and Horwitz, A. R. (2009). Non-muscle myosin II takes centre stage in cell adhesion and migration. *Nature Reviews Molecular Cell Biology*, **10**(11): 778-790.

Vigil, D., Cherfils, J., Rossman, K. L., and Der, C. J. (2010). Ras superfamily GEFs and GAPs: validated and tractable targets for cancer therapy? *Nature Reviews Cancer*, **10**(12): 842-857.

Vitale, N., Patton, W. A., Moss, J., Vaughan, M., Lefkowitz, R. J., and Premont, R. T. (2000). GIT Proteins, A Novel Family of Phosphatidylinositol 3,4,5-Trisphosphate-stimulated GTPase-activating Proteins for ARF6. *Journal of Biological Chemistry*, **275**(18): 13901-13906.

Wang, S., Hu, C., Wu, F., and He, S. (2017). Rab25 GTPase: Functional roles in cancer. *Oncotarget*, **8**(38): 64591-64599.

Wang, Y.-L. (1985). Exchange of Actin Subunits at the Leading Edge of Living Fibroblasts: Possible Role of Treadmilling. *Journal of Cell Biology*, **101**(2): 597-602.

Wennerberg, K., Rossman, K. L., and Der, C. J. (2005). The Ras superfamily at a glance. *Journal of Cell Science*, **118**(5): 843-846.

Yamaguchi, H., and Condeelis, J. (2007). Regulation of the actin cytoskeleton in cancer cell migration and invasion. *Biochimica et Biophysica Acta - Molecular Cell Research*, **1773**(5): 642-652.

Yamamoto-Furusho, J. K., Barnich, N., Xavier, R., Hisamatsu, T., and Podolsky, D. K. (2006). Centaurin β1 Down-regulates Nucleotide-binding Oligomerization Domains 1- and 2-dependent NF-κB Activation. *Journal of Biological Chemistry*, **281**(47): 36060-36070.

Yamauchi, Y., Miura, Y., and Kanaho, Y. (2017). Machineries regulating the activity of the small GTPase Arf6 in cancer cells are potential targets for developing innovative anti-cancer drugs. *Advances in Biological Regulation*, **63**: 115-121.

Zhang, B., Zhang, Y., Shacter, E., and Zheng, Y. (2005). Mechanism of the Guanine Nucleotide Exchange Reaction of Ras GTPase – Evidence for a GTP/GDP Displacement Model. *Biochemistry*, **44**(7): 2566-2576.

Zhou, W., Li, X., and Premont, R. T. (2016). Expanding functions of GIT Arf GTPase-activating proteins, PIX Rho guanine nucleotide exchange factors and GIT-PIX complexes. *Journal of Cell Science*, **129**(10): 1963-1974.

Supplementary data

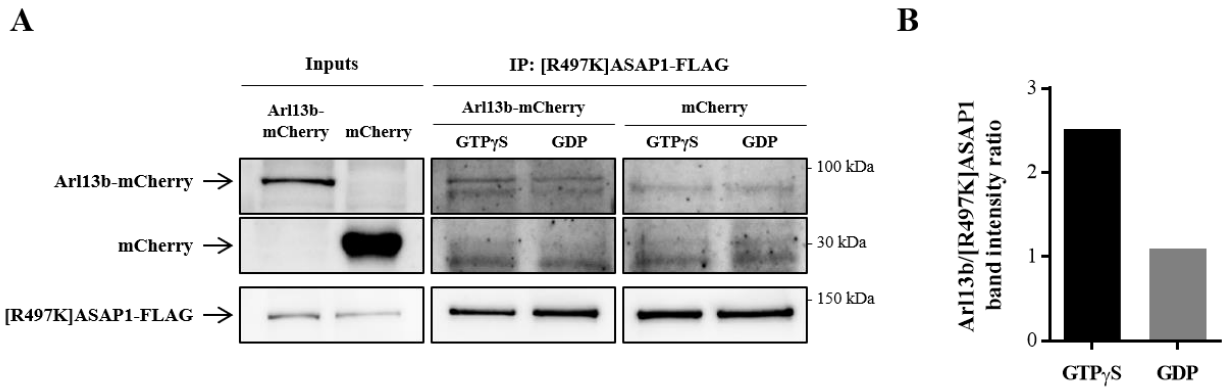

Supplementary Figure 1. Co-immunoprecipitation of [R497K]ASAP1 with Arl13b in MDA-MB-231 breast cancer cells. MDA-MB-231 cells stably overexpressing Arl13b-mCherry, or mCherry as a negative control, were transiently transfected with a plasmid encoding FLAG-tagged [R497K]ASAP1. **(A)** Protein extracts were incubated with an anti-FLAG antibody before immunoprecipitation with protein G sepharose beads in the presence of GTPγS or an excess of GDP. The immunoprecipitated products and total cell extracts were separated by SDS-PAGE. Immunoblotting was performed with an anti-mCherry antibody. [R497K]ASAP1 immunoprecipitation was confirmed by subsequently incubating the same blotting membrane with an anti-FLAG antibody. **(B)** Quantification of the bands intensity corresponding to Arl13b and [R497K]ASAP1 was performed using Image J. The ratios between the values obtained were calculated and the results normalized to the amount of immunoprecipitated proteins.

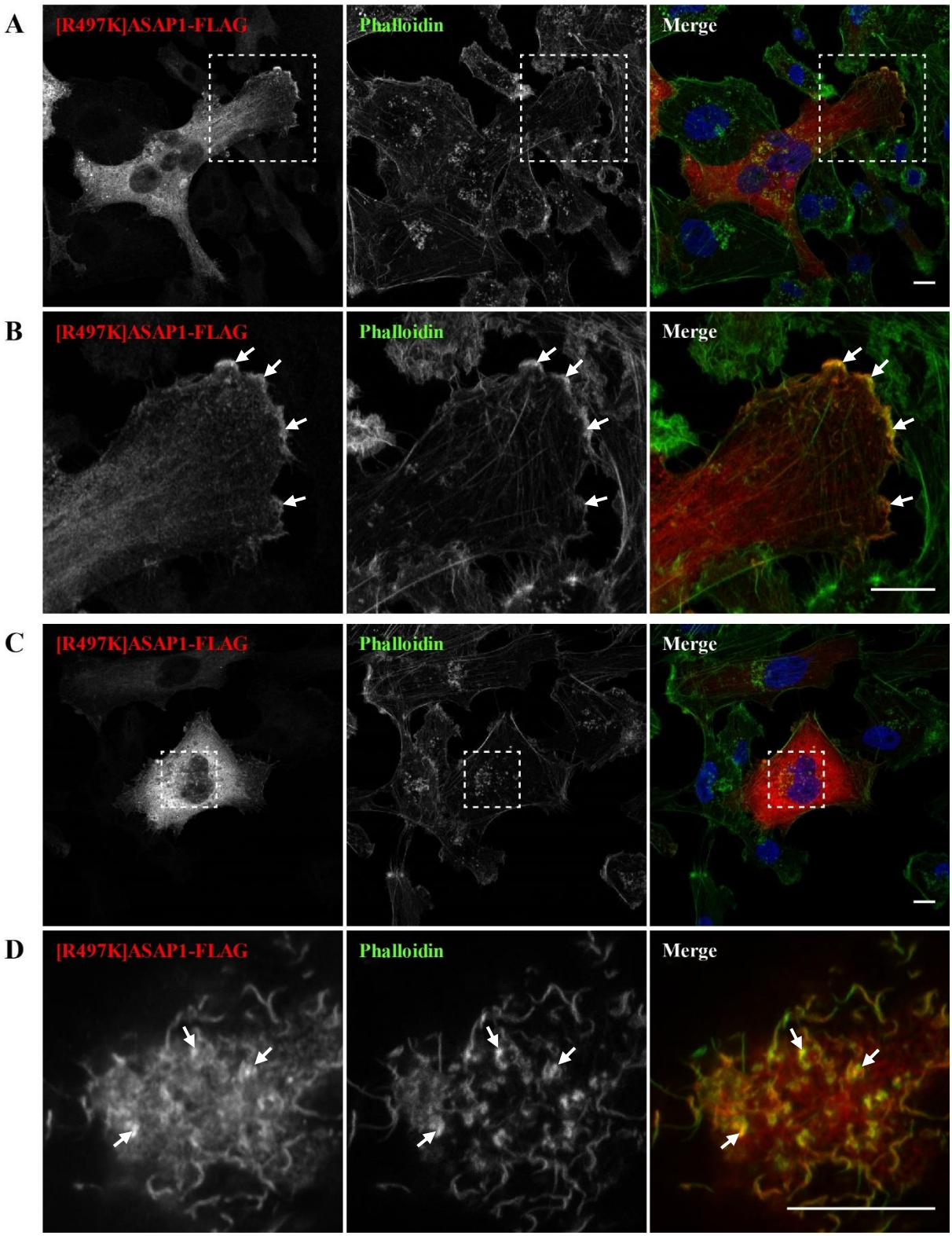

Supplementary Figure 2. Co-localization of [R497K]ASAP1 with F-actin in MDA-MB-231 breast cancer cells. MDA-MB-231 cells transiently overexpressing FLAG-tagged [R497K]ASAP were fixed and stained with anti-FLAG Cy3 and Alexa Fluor 568-conjugated phalloidin to label F-actin. DAPI was used to stain nuclei. [R497K]ASAP1 colocalizes with actin in the same structures than ASAP1 WT, **(A, B)** including protrusions near the plasma membrane, such as lamellipodia, **(C, D)** as well as in structures that resemble invadopodia. **(B)** and **(D)** correspond to zoomed images of the areas indicated by the boxes in **(A)** and **(C)**, respectively. All images correspond to representative Z stacks obtained by confocal microscopy. Scale bars: 10 µm.

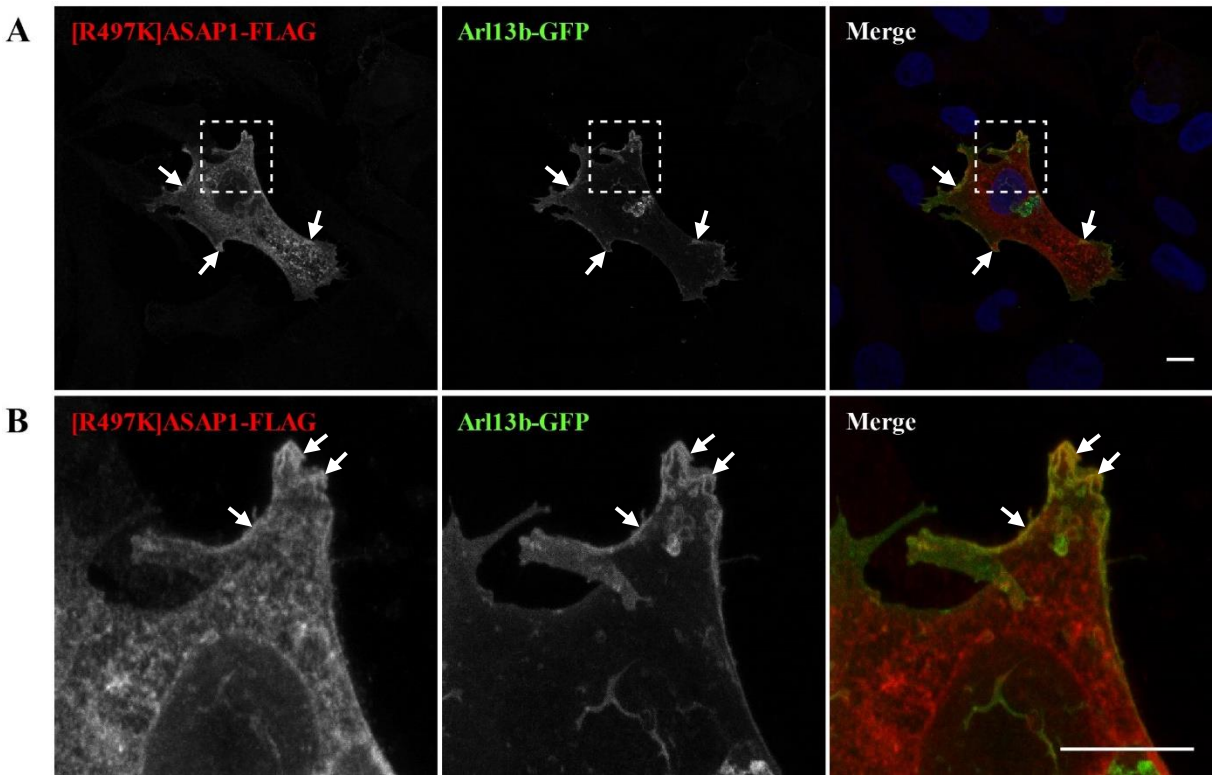

Supplementary Figure 3. Co-localization of [R497K]ASAP1 with Arl13b in MDA-MB-231 breast cancer cells. MDA-MB-231 cells transiently overexpressing FLAG-tagged [R497K]ASAP1 and GFP-tagged Arl13b were fixed and stained with anti-FLAG Cy3. DAPI was used to stain nuclei. **(A, B)** [R497K]ASAP1 colocalizes with Arl13b in the same locations than ASAP1 WT, namely at the plasma membrane and in PRs. **(B)** corresponds to the zoomed image of the area indicated by the box in **(A)**. All images correspond to representative Z stacks obtained by confocal microscopy. Scale bars: 10 µm.

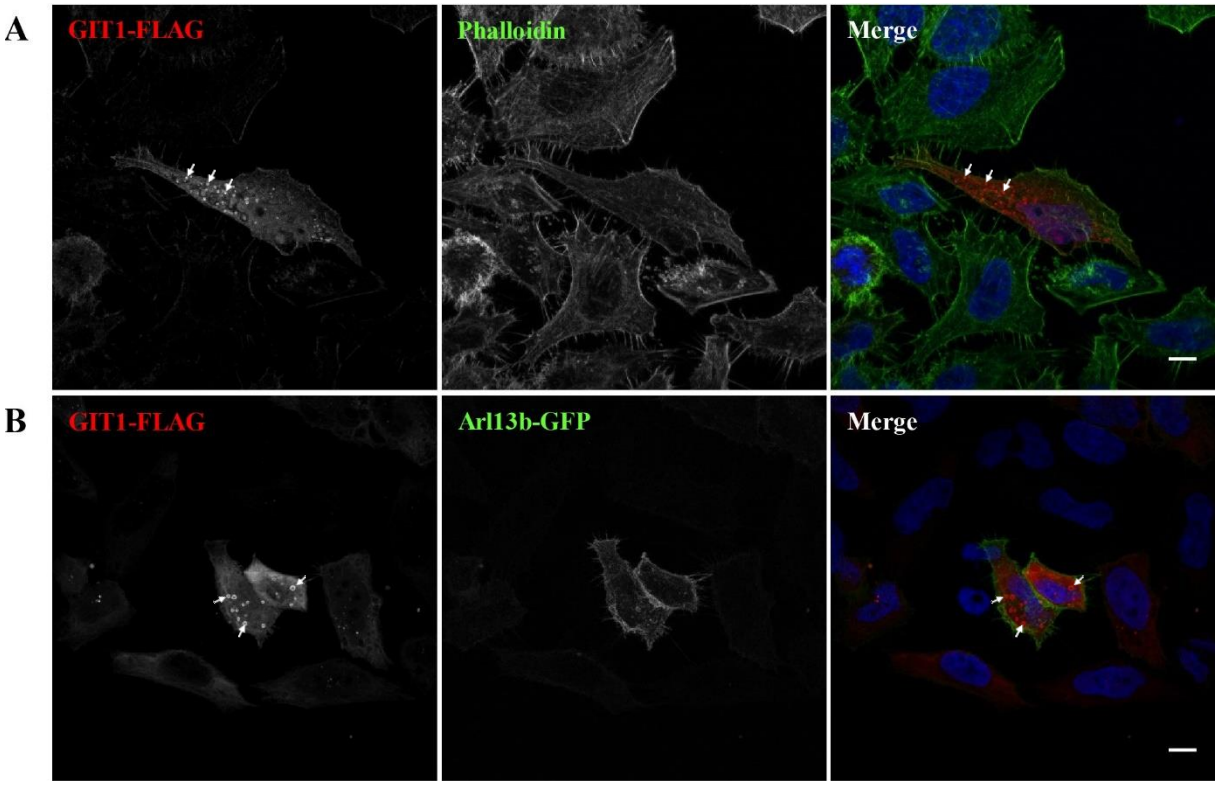

Supplementary Figure 4. Co-localization of GIT1 with F-actin or Arl13b in HeLa cells. (A) HeLa cells transiently overexpressing FLAG-tagged GIT1 were fixed and stained with anti-FLAG Cy3 and Alexa Fluor 568-conjugated phalloidin to label F-actin. **(B)** HeLa cells transiently overexpressing FLAG-tagged GIT1 and GFP-tagged Arl13b were fixed and stained with anti-FLAG Cy3. DAPI was used to stain nuclei. **(A, B)** GIT1 localizes to punctate cytoplasmic structures (indicated by the arrows), **(A)** but does not co-localize with actin **(B)** or Arl13b. All images correspond to representative Z stacks obtained by confocal microscopy. Scale bars: 10 µm.

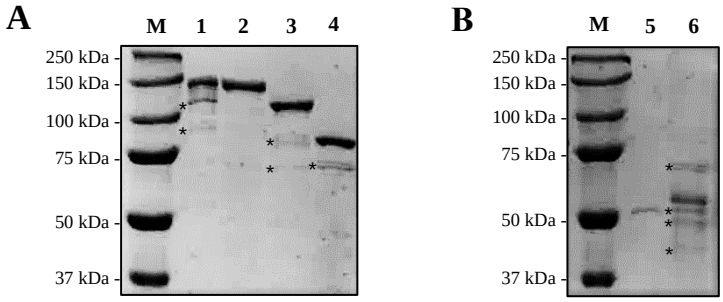

Supplementary Figure 5. Analysis of the purified proteins ASAP1, [R497K]ASAP1, ASAP3, ACAP1 and Arl13b. (A) FLAG-tagged ASAP1 WT (1), [R497K]ASAP1 (2), ASAP3 (3) and ACAP1 (4) were expressed in HEK293-E6 mammalian cells and purified using an anti-FLAG affinity column. **(B)** GST-tagged Arl13b$^{1-225}$ (5), with the approximate molecular weight of 50 kDa, was expressed in *E. coli* and purified using a GSTrap affinity column, while full length FLAG-tagged Arl13b (6) was expressed in HEK293-E6 mammalian cells and purified using an anti-FLAG affinity column. One µg of protein was loaded in each lane. All samples were resolved by SDS-PAGE and the gel was stained with Coomassie Blue. M, molecular weight marker. The asterisks (⋆) indicate contaminant proteins and/or degradation products.

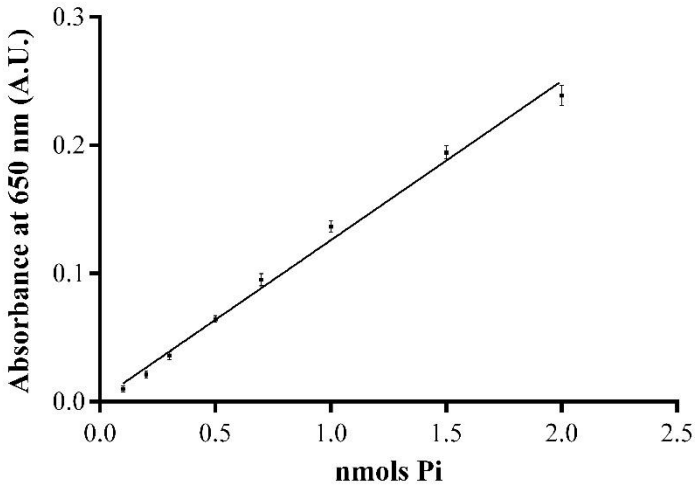

Supplementary Figure 6. Calibration curve for standard phosphate solution. Increasing concentrations of a phosphate standard solution were used. After an incubation at 37ºC for 20 minutes, CytoPhos reagent was added for 10 minutes at room temperature. The absorbance was read at 650 nm and is expressed in arbitrary units (A.U.). Results are displayed as mean ± SD of four independent experiments. The corresponding regression equation obtained was y = 0.1242x + 0.001772 with a coefficient of determination (R^2) of 0.9899.

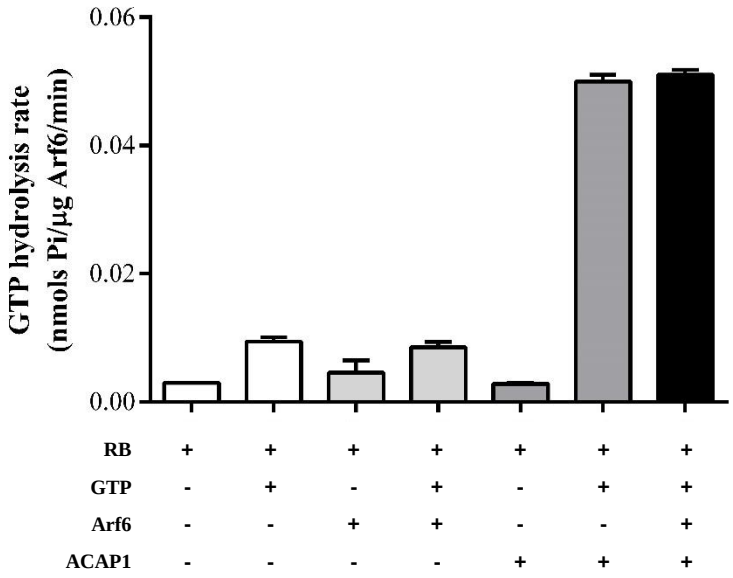

Supplementary Figure 7. Measurement of intrinsic and GAP-stimulated Arf6 activity *in vitro*. The reaction (in black) contained 4.5 µg of GTP-loaded Arf6 and 8 µg of ACAP1. Control reactions (in white or gray) contained only reaction buffer (RB), purified Arf6 in RB or purified ACAP1 in RB in the same amount used in the reaction, with or without GTP. All reactions were incubated at 37ºC for 20 minutes followed by the addition of CytoPhos reagent for 10 minutes at room temperature. The absorbance was read at 650 nm and the values were converted to GTP hydrolysis rate in nmols Pi/µg Arf6/min. Results are displayed as mean ± SD of at least two independent experiments.

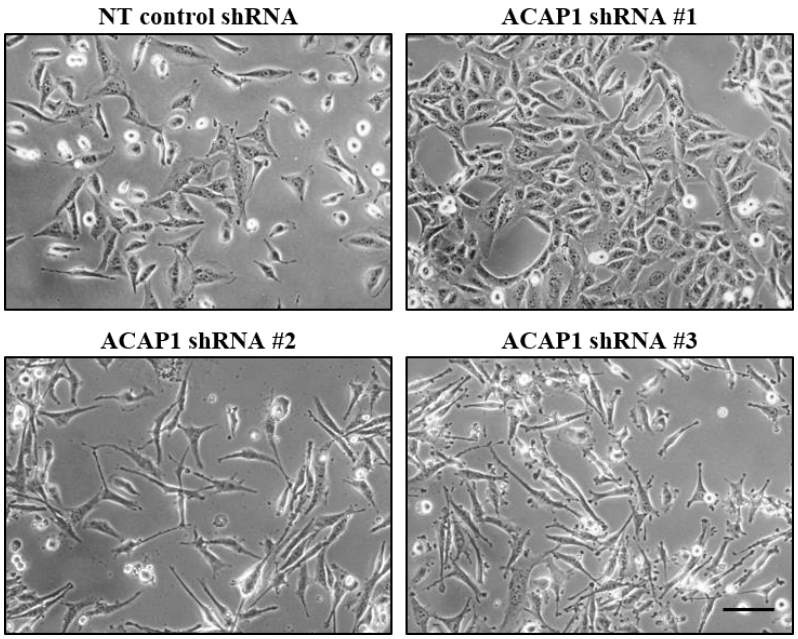

Supplementary Figure 8. Morphology of MDA-MB-231 breast cancer cells upon ACAP1 silencing. MDA-MB-231 cells were treated with non-targeting (NT) control shRNA or shRNA targeting *ACAP1*. The images were taken seven days after lentiviral infection. Scale bar: 100 µm.

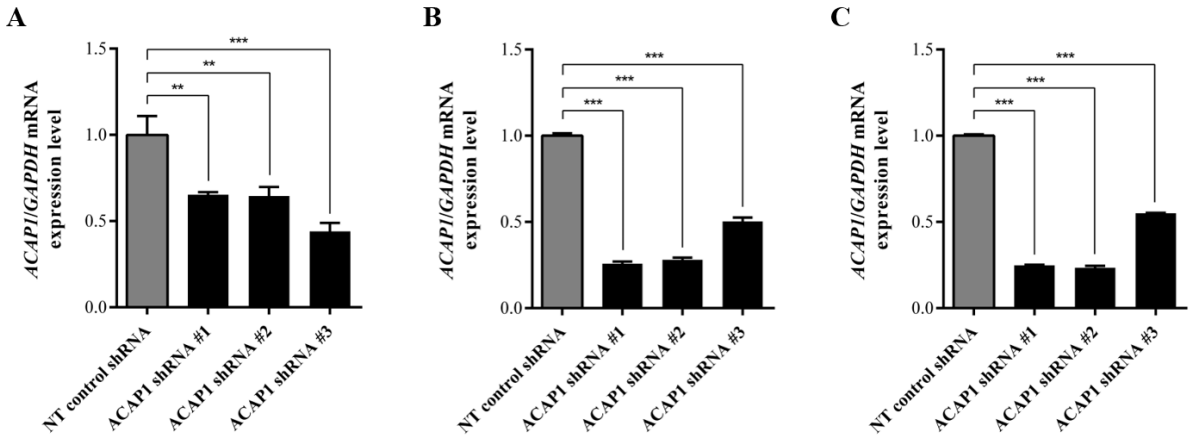

Supplementary Figure 9. Quantification of ACAP1 mRNA levels by RT-qPCR. Transcript levels were quantified from cDNA obtained from MDA-MB-231 cells treated with non-targeting (NT) control shRNA or shRNA targeting *ACAP1*, collected at the beginning of each independent transwell migration and invasion experiment **(A, B, C)**. ACAP1 silencing was confirmed by analysis of mRNA expression levels by RT-qPCR. The expression of *ACAP1* was normalized to the expression of *GAPDH*, used as a housekeeping gene. Results represent relative ratios between mRNA expression levels of *ACAP1* and *GAPDH* and are represented as mean ± SD of four replicas. **p≤0.01; ***p≤0.0001 (one-way ANOVA with Tukey's multiple comparisons test).